SIDE-SLIP ESTIMATION FOR ESP APPLICATIONS

by

Can Şahin

B.S., Mechanical Engineering, Boğaziçi University, 2006

Submitted to the Institute for Graduate Studies in
Science and Engineering in partial fulfillment of
the requirements for the degree of
Master of Science

Graduate Program in Mechanical Engineering
Boğaziçi University

2010

ACKNOWLEDGEMENTS

I would like to thank my advisor Prof. İ. Emre Köse for his guidance and endless support. His trust has encouraged me and his friendly attitude has enhanced my motivation on this study.

I would also like to thank Barış Efendioğlu from Tofaş for providing necessary data for this study.

My special thanks go to my family for their patience and understanding.

Finally, I would like to express my best feelings to all of my friends, who have shared their energy and valuable time with me.

ABSTRACT

SIDE-SLIP ESTIMATION FOR ESP APPLICATIONS

ESP (Electronic Stability Programme) applications require reliable data about vehicle state in order to operate correctly. One of these data is the vehicle side-slip angle.

In this study, a nominal and a robust side-slip estimator are designed using static multipliers. The design is based on the well-known Single Track Model. Then, the performances of the estimators are analyzed using a more complex nonlinear model. With the nonlinear model, more realistic results are obtained because this model resembles a real vehicle in many aspects.

After the construction of the nonlinear model and the Single Track Model, vehicle parameter values are set for these two models so that they behave similarly. Then, the sensitivity analysis is conducted to be able to determine the uncertain parameters, which are to be used during the side-slip estimator design. After the system is put in the LFT (linear fractional transformation) form, the nominal and the robust estimators are constructed using static multipliers. Finally, the obtained side-slip estimators are connected to the nonlinear model and the Single Track Model, and then results for different kinds of inputs and conditions are gathered and compared.

ÖZET

ESP UYGULAMALARI İÇİN YANAL KAYMA TAHMİNİ

ESP (Elektronik Stabilite Programı) uygulamaları, doğru çalışabilmek için araç durumu hakkında güvenilir verilere ihtiyaç duyarlar. Bu verilerden bir tanesi araç yanal kayma açısıdır.

Bu çalışmada, statik çarpanlar kullanılarak bir nominal ve bir de dayanıklı yanal kayma estimatörü tasarlanmıştır. Tasarım, iyi bilinen Tek İz Modeli üzerine kurulmuştur. Daha sonra, estimatörlerin performansları daha karmaşık ve lineer olmayan bir model kullanılarak analiz edilmiştir. Lineer olmayan modelle daha gerçekçi sonuçlar elde edilmiştir çünkü bu model birçok açıdan gerçek bir araca benzemektedir.

Lineer olmayan modelin ve Tek İz Modeli'nin tamamlanmasından sonra, bu iki modelin benzer davranışlar göstermeleri için araç parametrelerinin değerleri bulunmuştur. Daha sonra, yanal kayma estimatörü tasarımı sırasında kullanılacak olan kesin olmayan parametrelerin tespiti için hassasiyet analizi yapılmıştır. Sistem, LFT (lineer fraksiyonel transformasyon) formuna sokulduktan sonra nominal estimatör ve dayanıklı estimatör statik çarpanlar kullanılarak bulunmuştur. Son olarak, elde edilen yanal kayma estimatörleri lineer olmayan modele ve Tek İz Modeli'ne bağlanmıştır. Farklı girdiler ve şartlar için sonuçlar elde edilip karşılaştırılmıştır.

TABLE OF CONTENTS

LIST OF FIGURES

LIST OF TABLES

LIST OF SYMBOLS/ABBREVIATIONS

$A1$, $A2$, $A3$, $A4$	Interaction points between the road and the wheels (They are also the projections of the wheel centers onto the road in wheel plane directions. They are not supposed to be on the wheels.)
$B1$, $B2$, $B3$, $B4$	Interaction points connecting the wheels and the wheel knuckles
$C1$, $C2$, $C3$, $C4$	Interaction points connecting the wheel knuckles and the sliding masses
C_I	Integral constant of the PI controller (It is a positive quantity.)
C_P	Proportional constant of the PI controller (It is a positive quantity.)
$D1$, $D2$, $D3$, $D4$	Interaction points connecting the sliding masses and the suspensions
d_{1L}, d_{2L}, d_{3L}, d_{4L}	Vertical positions of the interaction points, which connect the suspensions and the sprung mass, with respect to an arbitrary point, which has a constant height, when the vehicle is loaded (A positive value means that the interaction point is above the arbitrary point. An increase in the value means that the suspension is extending.)
d_{1U}, d_{2U}, d_{3U}, d_{4U}	Vertical positions of the interaction points, which connect the suspensions and the sprung mass, with respect to an arbitrary point, which has a constant height, when the vehicle is unloaded (A positive value means that the interaction point is above the arbitrary point. An increase in the value means that the suspension is extending.)

$disp_1$, $disp_2$, $disp_3$, $disp_4$	Vertical displacements of the interaction points, which connect the suspensions and the sprung mass, as the loading condition changes from unloaded to loaded (A positive value means that the interaction point is above the level achieved in the unloaded case.)
$E1$, $E2$, $E3$, $E4$	Interaction points connecting the suspensions and the sprung mass
F	Center of gravity of the fuel
$F_{Damper1}$, $F_{Damper2}$, $F_{Damper3}$, $F_{Damper4}$	Vertical forces on the dampers which are parts of the suspensions (A positive value means that the damper is extending.)
$F_{Spring1}$, $F_{Spring2}$, $F_{Spring3}$, $F_{Spring4}$	Vertical forces on the springs which are parts of the suspensions (A positive value means that the spring is in tension.)
$Fx_Fy_Fz_F$	Coordinate frame which is attached to the fuel
h_1, h_2, h_3, h_4	Heights of the interaction points, which connect the suspensions and the sprung mass, when the vehicle is unloaded
L	Center of gravity of the luggage
l	Distance between the front and rear interaction points which connect the suspensions and the sprung mass
$Lx_Ly_Lz_L$	Coordinate frame which is attached to the luggage
n_1, n_2, n_3, n_4	Lateral displacements of the interaction points, which connect the suspensions and the sprung mass, from sprung mass boundary (A positive value means that the interaction point is inside the sprung mass.)
O	Reference point which is on the road surface and fixed
$OXYZ$	Reference coordinate frame which is attached to the road
P	Reference point which is used to define the relative positions of the vehicle parts
$P1$, $P2$, $P3$, $P4$, $P5$	Center of gravities of the passengers
$P1x_{P1}y_{P1}z_{P1}$	Coordinate frame which is attached to the front left passenger

$P2x_{P2}y_{P2}z_{P2}$	Coordinate frame which is attached to the front right passenger
$P3x_{P3}y_{P3}z_{P3}$	Coordinate frame which is attached to the rear left passenger
$P4x_{P4}y_{P4}z_{P4}$	Coordinate frame which is attached to the rear middle passenger
$P5x_{P5}y_{P5}z_{P5}$	Coordinate frame which is attached to the rear right passenger
q_1, q_2, q_3, q_4	Steering ratios (They are positive quantities.)
r_1, r_2, r_3, r_4	Radii of the wheels when the vehicle is unloaded
$S1$, $S2$, $S3$, $S4$	Center of gravities of the suspensions
$S1x_{S1}y_{S1}z_{S1}$	Coordinate frame which is attached to the front left suspension
$S2x_{S2}y_{S2}z_{S2}$	Coordinate frame which is attached to the front right suspension
$S3x_{S3}y_{S3}z_{S3}$	Coordinate frame which is attached to the rear left suspension
$S4x_{S4}y_{S4}z_{S4}$	Coordinate frame which is attached to the rear right suspension
$SM1$, $SM2$, $SM3$, $SM4$	Center of gravities of the sliding masses
$SM1x_{SM1}y_{SM1}z_{SM1}$	Coordinate frame which is attached to the front left sliding mass
$SM2x_{SM2}y_{SM2}z_{SM2}$	Coordinate frame which is attached to the front right sliding mass
$SM3x_{SM3}y_{SM3}z_{SM3}$	Coordinate frame which is attached to the rear left sliding mass
$SM4x_{SM4}y_{SM4}z_{SM4}$	Coordinate frame which is attached to the rear right sliding mass
SML	Center of gravity of the loaded sprung mass
$SMLxyz$	Coordinate frame which is attached to the loaded sprung mass
SMU	Center of gravity of the unloaded sprung mass
$SMUx'y'z'$	Coordinate frame which is attached to the unloaded sprung mass
t	Width of the sprung mass

$T1$, $T2$, $T3$, $T4$	Instant contact points on the wheels, where the road and the wheels contact each other (They are also the projections of the wheel centers onto the road in wheel plane directions.)
W	Point which is exactly between the center of gravities of the front wheels when the vehicle is unloaded
$W1$, $W2$, $W3$, $W4$	Center of gravities of the wheels
$W1x_{W1}y_{W1}z_{W1}$	Coordinate frame which is attached to the front left wheel
$W2x_{W2}y_{W2}z_{W2}$	Coordinate frame which is attached to the front right wheel
$W3x_{W3}y_{W3}z_{W3}$	Coordinate frame which is attached to the rear left wheel
$W4x_{W4}y_{W4}z_{W4}$	Coordinate frame which is attached to the rear right wheel
$WK1$, $WK2$, $WK3$, $WK4$	Center of gravities of the wheel knuckles
$WK1x_1y_1z_1$	Coordinate frame which is attached to the front left wheel knuckle
$WK2x_2y_2z_2$	Coordinate frame which is attached to the front right wheel knuckle
$WK3x_3y_3z_3$	Coordinate frame which is attached to the rear left wheel knuckle
$WK4x_4y_4z_4$	Coordinate frame which is attached to the rear right wheel knuckle
β	Side-slip angle (It is measured with respect to a forward pointing axis. A positive value means that the velocity vector is on the left side of the vehicle when the vehicle is moving forward.)
δ_1, δ_2, δ_3, δ_4	Wheel steering angles (A positive value means that the wheel is turned to the left.)
δ_S	Steering wheel angle (A positive value means that the vehicle corners to the left.)
θ	Pitch angle (A positive value means that the sprung mass dives.)
ϕ	Roll angle (A positive value means that the sprung mass leans right.)
ψ	Yaw angle (A positive value means that the vehicle corners to the left.)

Ω_1, Ω_2, Ω_3, Ω_4	Angular speeds of wheel spins (A positive value means that the vehicle moves forward.)
ABS	Anti-lock Braking System
DVD	Digital Versatile Disc
EKF	Extended Kalman Filter
ESP	Electronic Stability Programme
Est	Estimated
Ext	External force
F	Fuel
IQC	Integral quadratic constraint
L	Luggage
LFT	Linear fractional transformation
LMI	Linear matrix inequality
LTI	Linear time-invariant
NLM	Nonlinear model
P1, P2, P3, P4, P5	Passengers
PI	Proportional integral
PID	Proportional integral derivative
R	Road
S1, S2, S3, S4	Suspensions
SM1, SM2, SM3, SM4	Sliding masses
SML	Loaded sprung mass
SMU	Unloaded sprung mass
STM	Single Track Model
W1, W2, W3, W4	Wheels
WK1, WK2, WK3, WK4	Wheel knuckles

1. INTRODUCTION

Nowadays, safety is a very dominant issue during vehicle design. Big investments are being made to protect both passengers and pedestrians. A lot of active and passive safety systems are still being discovered and improved to push the safety levels even higher. Airbag, ESP and ABS are some of the commonly known safety systems.

One of the most important facts about safety systems is that they work in collaboration with each other [1]. That is the reason why a minor change in one of these systems may lead to drastic changes in vehicle behavior finally. Therefore, the changes or improvements have to be made with great care during the design stage. In order to ensure that the systems work fine together, tests are conducted after the design of these systems. The main purpose of the tests is to simulate almost every condition and observe vehicle response. If the vehicle does not respond as desired in some conditions, then the safety systems are revised until the desired safety levels are achieved.

Safety systems mostly rely on information about the state of the vehicle [2]. The actions taken by the safety systems depend on this information. Therefore, the information has to be supplied to the safety systems correctly.

Among the data supplied to the safety systems, mostly used ones are the velocity, yaw rate, side-slip angle and lateral acceleration [3]. As stated before, it is very crucial that these signals are obtained and transmitted to the other systems without any mistake or error.

There are two main methods to obtain the information about the state of the vehicle. The first one is via direct measurement, which requires sensors. The second method is obtaining the information using some other states of the vehicle.

The first method requires the usage of sensors. The advantages are that the sensors are designed specially for the purpose and they output independent data. This

method has a few disadvantages on the other hand. The first disadvantage is the cost of the tools, which are used to measure the desired states. The cost is especially high for the side-slip sensor [4], making it impossible to be included in the production vehicles. Another disadvantage of using sensors is that the obtained data have the possibility to be noisy or erroneous [5]. This is strongly related with sensor quality. In most occasions, the quality and cost rise together. This means that a more expensive measurement tool is required to obtain better results.

The second method to obtain data is making estimations using some other measured data. This reduces the costs dramatically because the number of sensors used in a vehicle is decreased by this approach. However, estimation requires theoretical skills. If the design is not adequate for the purpose or there are mistakes in the design, the results are fatal. Therefore, it is very important to set the underlying theory right. Also, the operating conditions have to be well-determined. The main reason for this is that observers and estimators generally operate in limited conditions [6]. A lot of efforts are being spent to widen the operating conditions, which are related with vehicle state. In some articles such as [5], [7] and [8], it is noted that some designs are improved over time yielding to more accurate results for different operating conditions. The external factors are also taken into account in some researches. These studies are mainly focused on the change of road conditions such as changing friction coefficient [9] or changing slant of the road [8], [10].

An observer is designed to estimate the state of the vehicle at any time knowing the inputs and outputs of the real system. As the state of the vehicle is known, the required data are sent to systems, which then take the necessary actions. Estimation can be done by designing observers using linear [11] or quasi-linear techniques [12]. Nonlinear observers are also used widely for the purpose of improving the accuracy of the observer.

There are many different kinds of observers which rely on different models internally. The most commonly used one is the Road-Tire Friction Model, which is nonlinear, with a variety of assumptions and considerations on each study such as

[5], [7] and [9]. This is not surprising because the only interactions, which define the motion of the vehicle, are between tyres and road, if the comparatively small effects such as wind disturbance or air drag are neglected [11]. Therefore, it is concluded that tyre-road interaction is important while determining the motion of a vehicle and thus it is used widely as a model to be used in an observer.

The EKF approach is used for estimation purposes in some studies such as [13], [14] and [15]. However, using the EKF approach is not practical in some cases due to its computational complexity [5]; high performance electronic control units are required to solve the involved Ricatti equations in real time [7].

The side-slip angle is the angle between the velocity vector and the longitudinal direction of a vehicle. This shows the importance of side-slip angle. It gives information about the orientation of the vehicle with respect to its velocity. If the side-slip angle is large, the vehicle is probably spinning or the driver has lost control. Therefore, side-slip estimation is very important in a vehicle with safety systems. Also, side-slip angle is the most difficult parameter to measure, which leads to high costs of side-slip sensors. Because of these facts, it is concluded that the side-slip angle has great importance and somehow has to be obtained. Since placing a side-slip sensor to every production vehicle is not possible due to the cost, the only remaining method is estimating the side-slip angle.

The solutions for estimating the side-slip angle which are represented above, however, lack of robustness; and recent results allow to solve this problem in terms of robust estimators [16]. Also, the computational requirement of the designed robust estimator is minimal which turns out to be a great advantage. This makes the approach preferable because the estimator can easily be integrated into electronic control units with normal processing capabilities. Robust estimation using static multipliers, which includes solutions for LMIs via convex optimization, is used for estimator design in this text.

Before attempting to find a robust estimator using static multipliers, the uncer-

tainties in the plant of interest have to be taken out first. The system has to be put in the LFT form. This is done by starting with the state-space form of the plant. The parameters, which are thought to impose uncertainties to the system, are written with uncertain terms. Then, these uncertain terms are written as another plant. This makes it easier to deal with uncertainties. Finally, all of the uncertainties are collected in a plant, and the remaining original plant is thought to include no uncertainties.

To write the system in the linear LFT form however, the uncertain parameters have to be determined first. All of the parameters are thought to have some amount of uncertainty, but some of the parameters affect the system more than the others as their values vary. Here, it is important to determine the parameters, which change the behavior of the system or plant drastically. To do this, the sensitivity of the system to a change in each parameter has to be studied. The methodology in [17] is used for sensitivity analysis.

In this study, the aim is to design a robust estimator using static multipliers, which is then used with a nonlinear model to estimate the side-slip angle using the known yaw rate data. During the design stage however, the internal dynamics of the system have to be known. The internal dynamics of the nonlinear model are not known. For this reason, the robust estimator is designed using a linear model, which is the well-known "Single Track Model" in this case. At this stage, it is important that the two models behave similarly so that the estimator, which is designed based on the Single Track Model, performs as desired with the nonlinear model. Finally, the estimator is connected to the nonlinear model and its performance is measured. The details are discussed later on the text but it is beneficial to include a general scheme of the problem here. Figure 1.1 on page 5 serves for this purpose.

Firstly in the text, information about rules, guidelines and conventions, which are used throughout the text, is given.

Next, the nonlinear model and the Single Track Model are constructed. For each model, definitions are done first. Then, assumptions are stated. Next, equations of

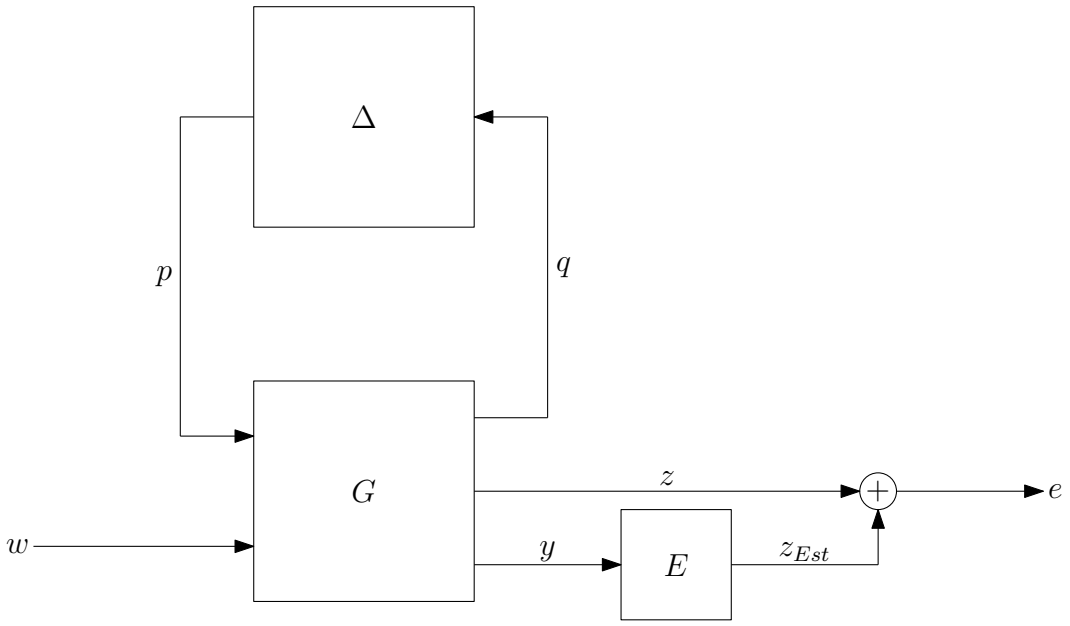

Figure 1.1. A general scheme of the robust estimation problem

motion are written. After writing the equations of motion, modeling in Simulink is discussed.

After the construction of the two models, vehicle parameter values are set for these two models. First, vehicle parameter values for the nonlinear model are determined according to known data, which are obtained using a dynamic simulation software called "MSC Adams/Car". Then, the nonlinear model is linearized and the vehicle parameter values for the Single Track Model are determined so that the two models behave similarly.

Next, estimators are designed using static multipliers. First, the sensitivity analyses of the models are done. Here, the parameters, which are thought to be uncertain, are determined. Then, these uncertainties are taken out of the plant. As the next step, a weighing function is added. By doing this, the performances of the estimators are increased, which is explained later in the text. The last step is constructing the estimators using static multipliers. These estimators are later used to estimate side-slip angle using yaw rate data.

After the estimators are designed, the nonlinear model and the Single Track

Model are simulated with the nominal and robust estimators connected. The graphs, which show the real and estimated values of the side-slip angles for various cases, are included. In addition, the results are compared.

Finally, conclusions are done according to the results, which are obtained previously.

2. GENERAL CONSIDERATIONS

Setting some rules, guidelines and conventions in the beginning is crucial. Rules, guidelines and conventions do not change in different parts of the study, which is a time saving fact. As another result, it becomes easier to follow the text. In this section, these rules, guidelines and conventions are discussed. It is very important to keep in mind that the discussions made in this section are always valid for the whole study.

The symbols are seen in the list of symbols/abbreviations. However, additional symbols have to be used in some parts of the study. In these cases, the symbols are defined within the part and these definitions are used in that part. In other words, if some additional definitions are made in a part, these definitions overwrite the ones in the list of symbols/abbreviations for that part.

Various coordinate frames are used in vehicle dynamics. Here, it is sufficient to discuss three of them; namely the "ISO", "SAE" and "MSC Adams/Car" coordinate frames. The common characteristic of these coordinate frames is that they all obey the right hand rule. Therefore, any transformation is done without any hassle if there are variables defined with respect to different coordinate frames. These three coordinate frames are seen in Figure 2.1 on page 8. The ISO coordinate frame is defined by the International Organization for Standardization. The x axis points forward. The y axis points to the left. The z axis points upward. The SAE coordinate frame is defined by the Society of Automotive Engineers. The x axis points forward. The y axis points to the right. The z axis points downward. The last coordinate frame is used in MSC Adams/Car, which is a mechanical system simulation software produced by MSC Software. The x axis points backward. The y axis points to the right. The z axis points upward.

If nothing is mentioned about the type of the coordinate frame, it is understood that it is an ISO coordinate frame. It is also beneficial to remind that all of the coordinate frames obey the right hand rule independent of their types. When the

Figure 2.1. Representation of the ISO, SAE and MSC Adams/Car coordinate frames respectively

name of a coordinate frame is known, its origin and the names of its axes are easily gathered. For example, the origin of the $Gxyz$ coordinate frame is point G. Its axes are named as "x", "y" and "z".

In this study, some conventions are used and declaring them here is necessary. These conventions are represented as the following:

- m_K stands for the mass of rigid body K.
- $I_{K/Gxyz}$ stands for the inertia tensor of rigid body K with respect to the $Gxyz$ coordinate frame.
- $I_{K/x}$, $I_{K/y}$, $I_{K/z}$, $I_{K/xy}$, $I_{K/xz}$ and $I_{K/yz}$ stand for the inertia components of rigid body K with respect to the $Gxyz$ coordinate frame.
- $T_{A/B}$ stands for the transformation matrix from the coordinate frame which has its origin at point A, to the coordinate frame which has its origin at point B.
- $\boldsymbol{p_{A/B}}$ stands for the position of point A with respect to point B.
- $\boldsymbol{p_A}$ stands for the position of point A with respect to the reference point which is fixed.
- $\boldsymbol{v_{A/B}}$ stands for the velocity of point A with respect to point B.
- $\boldsymbol{v_A}$ stands for the velocity of point A with respect to the reference point which is

fixed.

- $\boldsymbol{a_{A/B}}$ stands for the acceleration of point A with respect to point B.
- $\boldsymbol{a_A}$ stands for the acceleration of point A with respect to the reference point which is fixed.
- $\boldsymbol{\omega_K}$ stands for the angular velocity of rigid body K with respect to the reference coordinate frame which is fixed.
- $\boldsymbol{\alpha_K}$ stands for the angular acceleration of rigid body K with respect to the reference coordinate frame which is fixed.
- $\boldsymbol{F_{K/L}}$ stands for the force on rigid body K applied by rigid body L.
- $\boldsymbol{F_K}$ stands for the total force on rigid body K.
- $\boldsymbol{M_{K/L}}$ stands for the moment on rigid body K applied by rigid body L.
- $\boldsymbol{M_{K(A)}}$ stands for the total moment on rigid body K about point A.
- $\boldsymbol{W_K}$ stands for the weight of rigid body K.

As seen above, vectors are written in bold unlike matrices and tensors. As an additional information, the magnitude of a vector is represented with characters which are not bold. For example, $v_{A/B}$ stands for the magnitude of $\boldsymbol{v_{A/B}}$. Sometimes, initial conditions of the variables are used. The initial condition of a variable is represented with an "i" in the subscript. For example, $\boldsymbol{v_{A/Bi}}$ stands for the initial condition of $\boldsymbol{v_{A/B}}$.

In this study, the vehicle model is constructed so that it is divided into four quarters. For some variables, it is necessary to include the information about their quarters. In these situations, numbers are used to represent the quarters. "1", "2", "3" and "4" stand for the front left, front right, rear left and rear right quarters, respectively. A similar situation exists for passengers. "1", "2", "3", "4" and "5" stand for the front left, front right, rear left, rear middle and rear right passengers, respectively.

If nothing is mentioned about the unit of a variable, it is N, kg, m, s, rad or a combination of these according to the type of the variable.

In Simulink, color codes are assigned for different types of signals. Color of the constant signals (signals that do not change during simulation) is cyan. If the color of a signal is magenta, it means that the signal is an input. The signals belonging to the transformation matrices are represented with gray. Signals belonging to the front left, front right, rear left and rear right quarters are represented with red, green, blue and yellow, respectively. The remaining signals are colored black. There is another fact which has to be kept in mind while working with the models in Simulink: Sometimes, signals belonging to the four quarters are combined. In these situations, numbers on the subscripts (1, 2, 3 and 4) are no longer meaningful. These numbers are replaced with "Q", meaning that the signal includes information about all of the quarters of the vehicle.

3. NONLINEAR MODEL

In this section, a vehicle model, which is later used to test the performance of the estimator, is made. The vehicle model shows nonlinear characteristics and it has 11 degrees of freedom. A lot of tests are conducted in this study, this is why this model is essential. There are two primary goals which have to be achieved during the design of the model. The first one is about how the model behaves. It is very important that the model behaves like a real vehicle. This means that, for various inputs, the outputs of the simulations done using the model have to be similar to the outputs of the real simulations. The second goal is about the running speeds of the simulations using the model. The simulations conducted with the model have to run as fast as possible; they have to last less than real time. This decreases the time spent during simulations. Because a lot of tests are conducted, this turns out to be an important fact.

To accomplish the first goal, the model has to be as complex as possible. As the complexity of the model increases, the results of the simulations with the model become more similar to the ones obtained via real simulations. On the other hand, the model has to be as simple as possible to accomplish the second goal. The model is made simpler by decreasing the amount of calculations involved. This puts less effort on the processor and therefore reduces the running time, or increases the running speed of the simulation. Because both of the goals have great importance, the effort is spent to keep the simplicity (or the complexity) of the model in a level so that both of the goals are accomplished. This always has to be kept in mind during the design of the model.

In the multibody systems approach, several bodies are considered to exist in a model. This is the approach used to construct the nonlinear model. As the model consists of bodies, these bodies have to be discussed first. This can be thought as dividing the vehicle into parts which are reasonable in the dynamic aspect. It is a common approach to separate the suspended part of the vehicle and call it the “sprung mass”. This is the upper part of the vehicle which includes the chassis, power train,

interior, exterior etc. Loads such as passengers, luggage and fuel are also considered to be parts of the sprung mass. The remaining part is called the "unsprung mass". This mass includes wheels and some parts of the suspensions. Obviously, the suspensions are modeled so that they connect the sprung and unsprung masses to each other. Since the vehicle has four wheels, there are four suspensions between the sprung and unsprung masses.

When there are two masses (the sprung and unsprung masses) connected to each other with four suspensions, the solution of the equations of motion is challenging because the number of equations is less than the number of unknowns. This problem is solved by separating the unsprung mass into four parts: Front left, front right, rear left and rear right unsprung masses. By doing this, the number of equations is increased due to the increase in the number of parts involved in the nonlinear model. As a result, it becomes easy to solve the equations of motion to obtain the unknowns. This is an approach used in the past, which is called the "Quarter Model Approach" [18], [19]. The representation of this approach is seen in Figure 3.1. This figure is included here only for the purpose of giving an idea about the Quarter Model Approach. It is studied in detail later on the text.

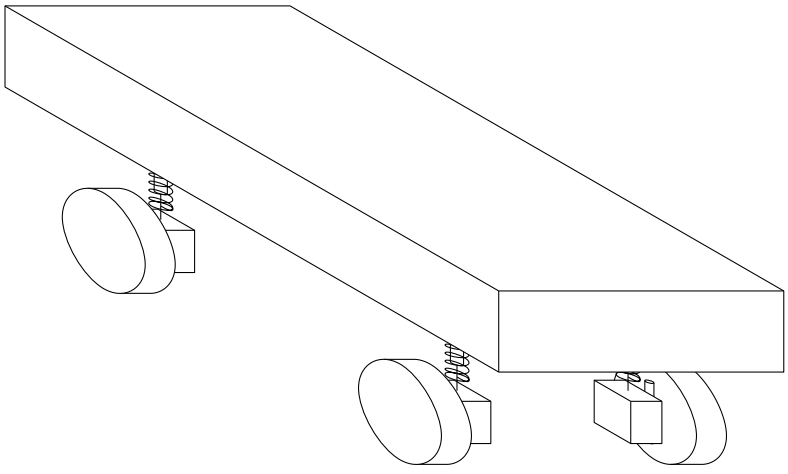

Figure 3.1. The representation of the Quarter Model Approach

Since the sprung mass includes many parts of the vehicle such as the engine or the chassis, it is the heaviest part. Also, all of the additional loads (passengers, luggage and fuel) are considered to be parts of the sprung mass. Since the sprung mass can be loaded, it is beneficial to make two definitions such as "unloaded" and "loaded" sprung

mass, which makes it easy to distinguish between the unloaded and the loaded case. The unloaded sprung mass includes only the parts belonging to the vehicle, hence the specifications of the unloaded sprung mass do not change. On the other hand, the specifications of the loaded sprung mass change according to the loading conditions. So it is necessary to always indicate the loading condition when a loaded sprung mass is considered.

There are different ways of modeling suspensions in a dynamic vehicle model. Each method is appropriate for a case; which means that each method is compatible for different modeling conditions. Five most commonly used methods are called "Lumped Mass Model", "Equivalent Roll Stiffness Model", "Swing Arm Model", "Linkage Model" and "Concept Suspension Approach" [18]. As stated before, the unsprung mass is separated into four parts. Because of that, the most appropriate method among those is the Lumped Mass Model. In the Lumped Mass Model, the camber angles of the wheels are directly related to the roll angle of the sprung mass, which means that the wheels roll together with the sprung mass. However, setting the camber angles of the wheels equal to zero simplifies the tyre model, the details of which are explained later. Because of that, the Lumped Mass Model is modified according to the needs. This modified version is explained as the following: Suspensions are always vertical, which means that they do not roll and pitch. The unsprung masses also do not perform these two rotations. This results in zero camber angles of the wheels as desired.

In vehicles, suspensions are connected to the body from several points, the number of which varies according to the vehicle and the type of the suspensions. In modeling however, these points have to be less in number because every connection point introduces additional forces and moments to the model. These additional forces and moments increase the number of unknowns, making the equations of motion unsolvable. This is why the suspensions have to be connected to the sprung and unsprung masses from a number of connecting points as small as possible. In this model, suspensions are connected to the sprung and unsprung masses from one point.

It is stated that the unsprung mass is divided into four parts according to the

Quarter Model Approach. Each quarter of the unsprung mass is also divided into parts which are wheels, wheel knuckles and sliding masses. This is seen in Figure 3.2, where the rear left quarter of the unsprung mass is not shown. Separation makes it easier to visualize and handle the dynamics involved. The wheel knuckles exist to represent the steering of the wheels. As the driver steers, the wheel knuckles turn as well as the wheels. In other words, the wheel knuckles rotate about the vertical axis with respect to the sliding masses. In each quarter of the unsprung mass, there are various parts other than wheels. These parts are represented by means of the sliding masses.

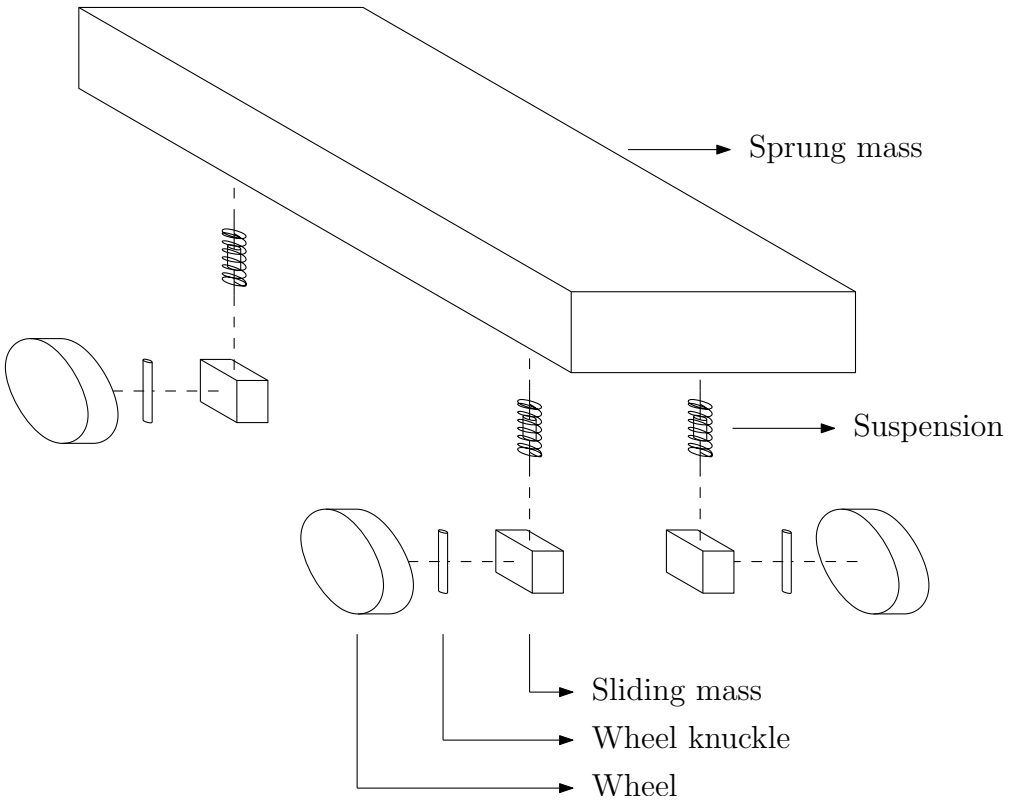

Figure 3.2. The expanded view of the nonlinear model (The rear left quarter of the unsprung mass is not shown.)

As the general considerations about the nonlinear model are discussed briefly, a more detailed analysis of the parts and interaction points has to be done, which provides a better understanding of the model.

Parts involved in the vehicle model are the wheels, wheel knuckles, sliding masses, suspensions and the sprung mass. These parts are also seen in Figure 3.2. It is good to have a look at Table 3.1 on page 16 to see some features of the parts involved in

the vehicle model. In this table, it has to be noted that the last seven parts are the loads which are put on the unloaded sprung mass. After loading the sprung mass, it is called the "loaded sprung mass".

There are many points used in the nonlinear model. However, some of them have to be studied in order to understand how the model is constructed. These are called the "interaction points". These points are actually frictionless joints which connect parts to each other. Therefore, the forces and moments between parts are applied via the interaction points. This fact reveals the importance of these points. The front view of the model is seen in Figure 3.3 where the interaction points of the front left quarter are also shown.

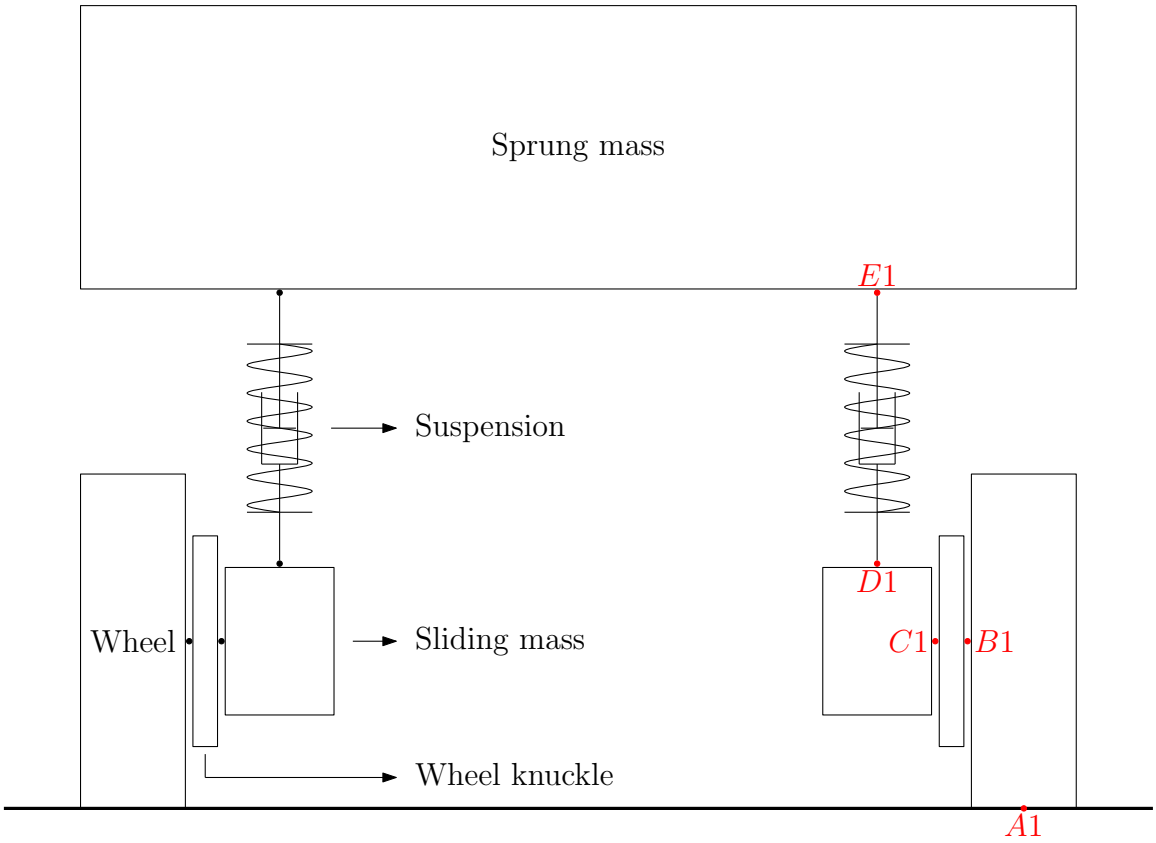

Figure 3.3. The front view of the nonlinear model

Looking at Figure 3.3, it is seen that point $A1$ is the interaction point between the road and the front left wheel. Point $B1$ connects the front left wheel and the front left wheel knuckle to each other. This point actually represents a joint which provides the rotation of the parts with respect to each other. Point $B1$ represents a revolute

Table 3.1. Some features of the parts involved in the nonlinear model

Name	Abbreviation	Center of Gravity	Coordinate Frame Attached to the Part with the Origin on the Center of Gravity
Front left wheel	W1	$W1$	$W1x_{W1}y_{W1}z_{W1}$
Front right wheel	W2	$W2$	$W2x_{W2}y_{W2}z_{W2}$
Rear left wheel	W3	$W3$	$W3x_{W3}y_{W3}z_{W3}$
Rear right wheel	W4	$W4$	$W4x_{W4}y_{W4}z_{W4}$
Front left wheel knuckle	WK1	$WK1$	$WK1x_1y_1z_1$
Front right wheel knuckle	WK2	$WK2$	$WK2x_2y_2z_2$
Rear left wheel knuckle	WK3	$WK3$	$WK3x_3y_3z_3$
Rear right wheel knuckle	WK4	$WK4$	$WK4x_4y_4z_4$
Front left sliding mass	SM1	$SM1$	$SM1x_{SM1}y_{SM1}z_{SM1}$
Front right sliding mass	SM2	$SM2$	$SM2x_{SM2}y_{SM2}z_{SM2}$
Rear left sliding mass	SM3	$SM3$	$SM3x_{SM3}y_{SM3}z_{SM3}$
Rear right sliding mass	SM4	$SM4$	$SM4x_{SM4}y_{SM4}z_{SM4}$
Front left suspension	S1	$S1$	$S1x_{S1}y_{S1}z_{S1}$
Front right suspension	S2	$S2$	$S2x_{S2}y_{S2}z_{S2}$
Rear left suspension	S3	$S3$	$S3x_{S3}y_{S3}z_{S3}$
Rear right suspension	S4	$S4$	$S4x_{S4}y_{S4}z_{S4}$
Unloaded sprung mass	SMU	SMU	$SMUx'y'z'$
Loaded sprung mass	SML	SML	$SMLxyz$
Front left passenger	P1	$P1$	$P1x_{P1}y_{P1}z_{P1}$
Front right passenger	P2	$P2$	$P2x_{P2}y_{P2}z_{P2}$
Rear left passenger	P3	$P3$	$P3x_{P3}y_{P3}z_{P3}$
Rear middle passenger	P4	$P4$	$P4x_{P4}y_{P4}z_{P4}$
Rear right passenger	P5	$P5$	$P5x_{P5}y_{P5}z_{P5}$
Luggage	L	L	$Lx_Ly_Lz_L$
Fuel	F	F	$Fx_Fy_Fz_F$

joint because the front left wheel can spin with respect to the front left wheel knuckle. Point $C1$, which is between the front left wheel knuckle and the front left sliding mass, also represents a revolute joint. It provides the rotation of the front left wheel knuckle with respect to the front left sliding mass. The front left sliding mass and the front left suspension are rigidly connected to each other, which means that they neither rotate nor translate with respect to each other. This fixed joint is represented with point $D1$. Finally, point $E1$ is where the front left suspension is mounted to the sprung mass. This is a joint as well. This joint prevents any translation of the parts with respect to each other. It also prevents the relative rotation of the parts about the vertical axis. As the result, this is a universal joint. These explanations about the interaction points are also valid for the other quarters with the appropriate changes in the names of the points.

Types of joints also reveal the prevented motions of each part. Accordingly, an analysis can be made to find the degrees of freedom of the nonlinear model. Here, it may also be helpful to refer to the assumptions which are discussed later. No translational or rotational motion of the sprung mass is prevented which means that it has six degrees of freedom. Suspensions translate in horizontal directions and rotate about vertical axes, but these motions are completely defined if the motion of the sprung mass is known. Therefore, suspensions do not add any degrees of freedom. This is also the case for the sliding masses because the sliding masses and the suspensions are rigidly connected to each other. While the vehicle is cornering, rotation of the wheel knuckles and the sliding masses about the vertical axes differ. Since all of the rotations of the wheel knuckles are dependent on the steering wheel, knowing the position of the steering wheel is enough to gather the motions of the wheel knuckles; bringing only one additional degree of freedom. The wheels move similar to the wheel knuckles, except that they also spin. This adds four degrees of freedom to the model. Finally, adding up the degrees of freedom, it is concluded that the model has 11 degrees of freedom.

One of the most important features of this model is that it involves nonlinearities. Adding nonlinearities to a model increases the simulation time or, in other words, lowers the performance. But, as an advantage, the behavior of the model becomes

more similar to a real vehicle. In a real vehicle, there are a lot of parts which show nonlinear characteristics. In a model however, nonlinearities have to be less because the performance of the model has to be kept in a high level. Interaction of the vehicle with the road is a very dominant fact to define the motion of the vehicle. Therefore, relations between the road and the wheels are modeled nonlinearly. In addition, springs and dampers, being parts of the suspensions, also play important role in defining the motion of the vehicle. This is why their nonlinear characteristics are also included in the model. The details of these nonlinearities are discussed in Section 3.3.4.

As stated before, the unsprung mass is divided into four parts, each representing a quarter. Most of the time, the properties of the quarters are the same. In these cases, statements are only made for the front left quarter, and it is stated that results for the other quarters can easily be obtained by modifying the statements appropriately. This makes it easier to follow and understand the text.

This section is divided into four parts. In the first part, the definitions used in this section are explained. In the second part, assumptions are discussed. Next, all of the equations, which belong to the nonlinear model, are presented. Finally, modeling in Simulink is discussed.

3.1. Definitions

All of the definitions, which are used in the nonlinear model, are included in the list of symbols/abbreviations, so they are not discussed here again. However, to provide a better understanding of the model, some of the variables are represented with figures in this section.

Understanding the interaction points is important since they define the relative motion of the parts with respect to each other. The interaction points of the front left quarter of the vehicle, namely points $A1$, $B1$, $C1$, $D1$ and $E1$, are shown in Figure 3.3 on page 15. The structures of the other quarters are exactly the same, so there is no need to show the interaction points belonging to the other quarters.

It is also beneficial to represent l, t, n_1, n_2, n_3 and n_4 using a figure. To see them clearly, the sprung mass is viewed from the bottom. This is seen in Figure 3.4.

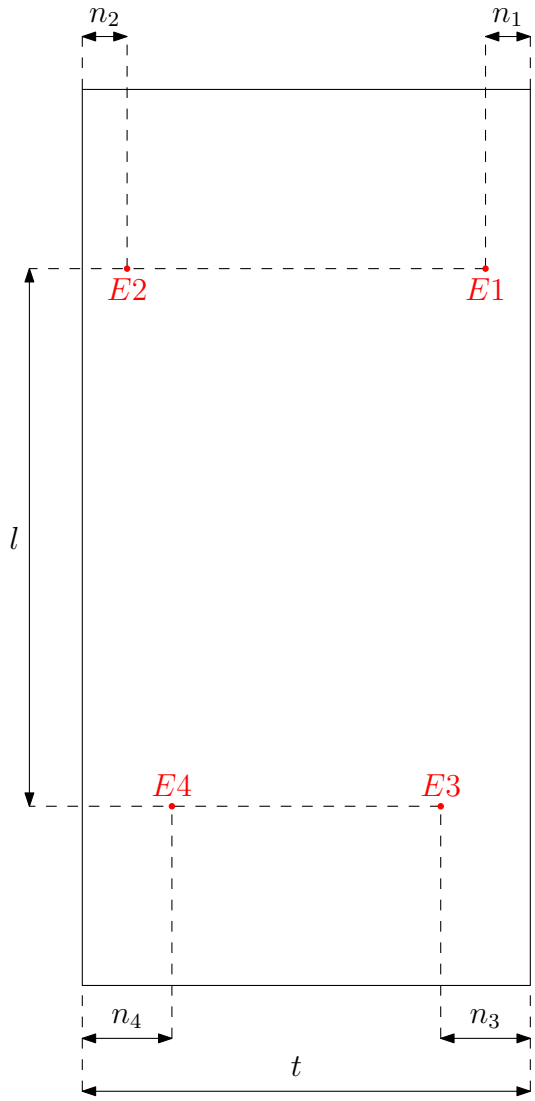

Figure 3.4. The bottom view of the sprung mass

Next, angles and rotation rates are visualized. This is easily done if the rotational motions are treated separately. First, the rotation about the longitudinal axis, which is called "roll", is represented as seen in Figure 3.5 on page 20.

The rotation about the lateral axis, which is called "pitch", is represented in Figure 3.6 on page 21.

The rotation about the vertical axis, which is called "yaw", is represented in Figure 3.7 on page 21.

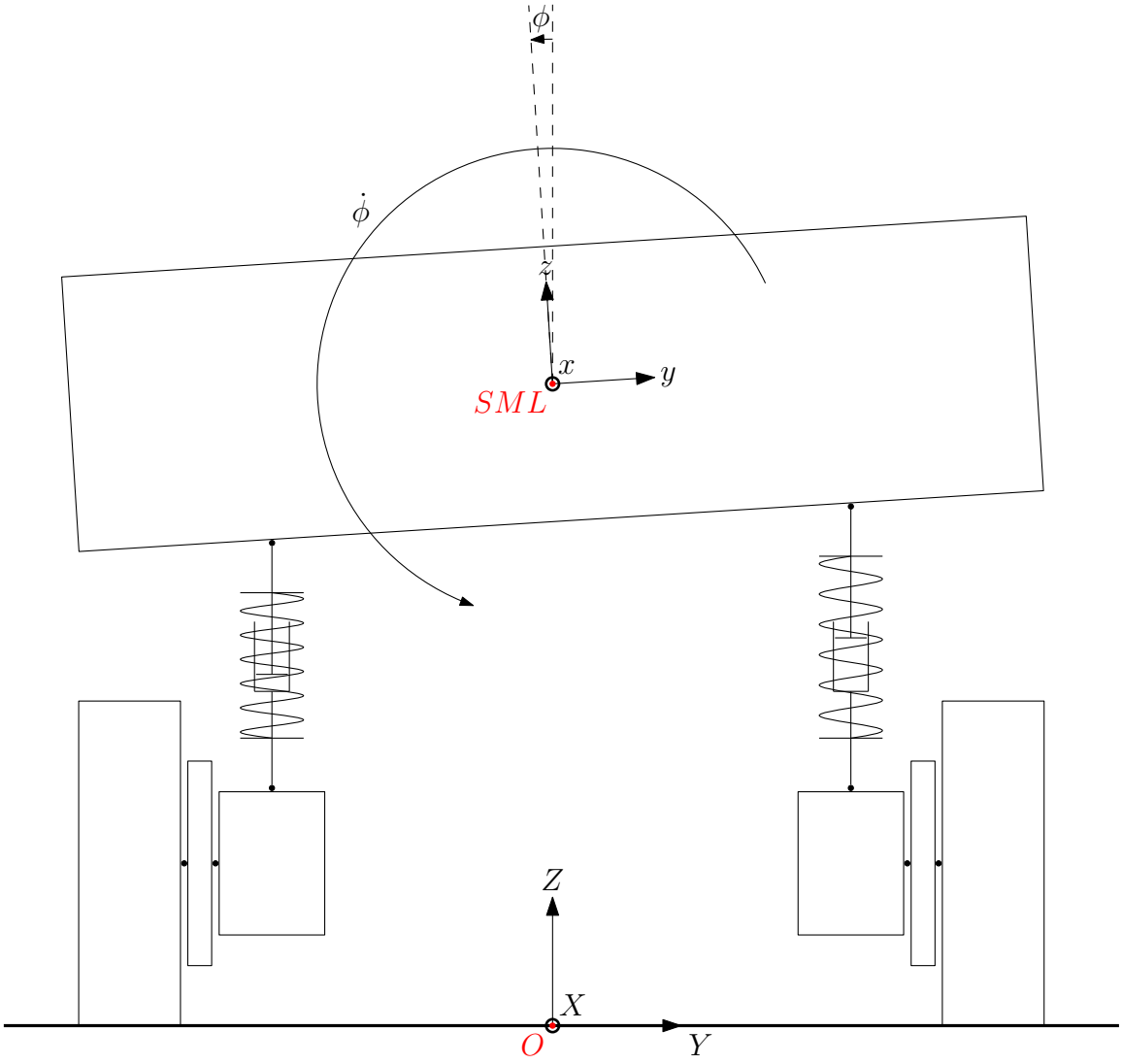

Figure 3.5. The front view of the nonlinear model while performing roll (Roll angle and roll rate are shown in positive directions.)

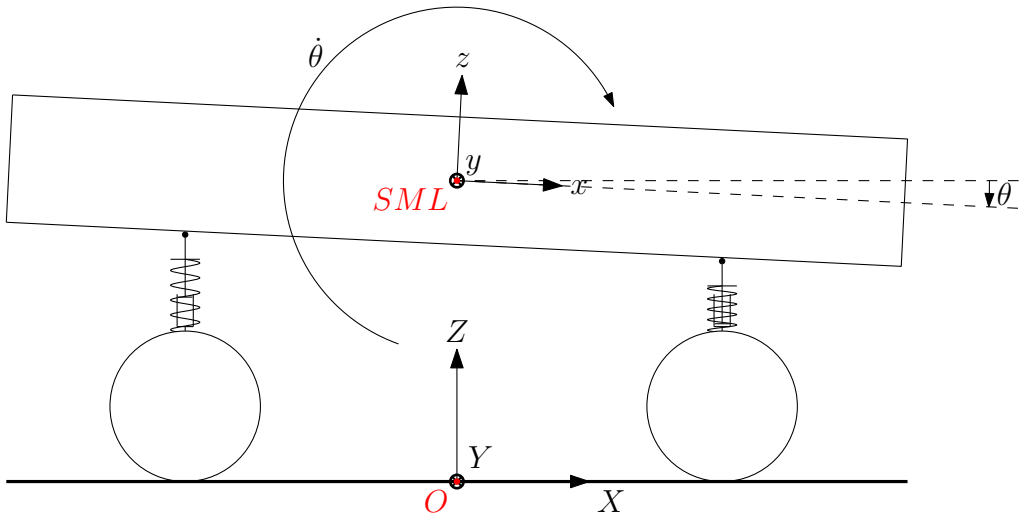

Figure 3.6. The side view of the nonlinear model while performing pitch (Pitch angle and pitch rate are shown in positive directions.)

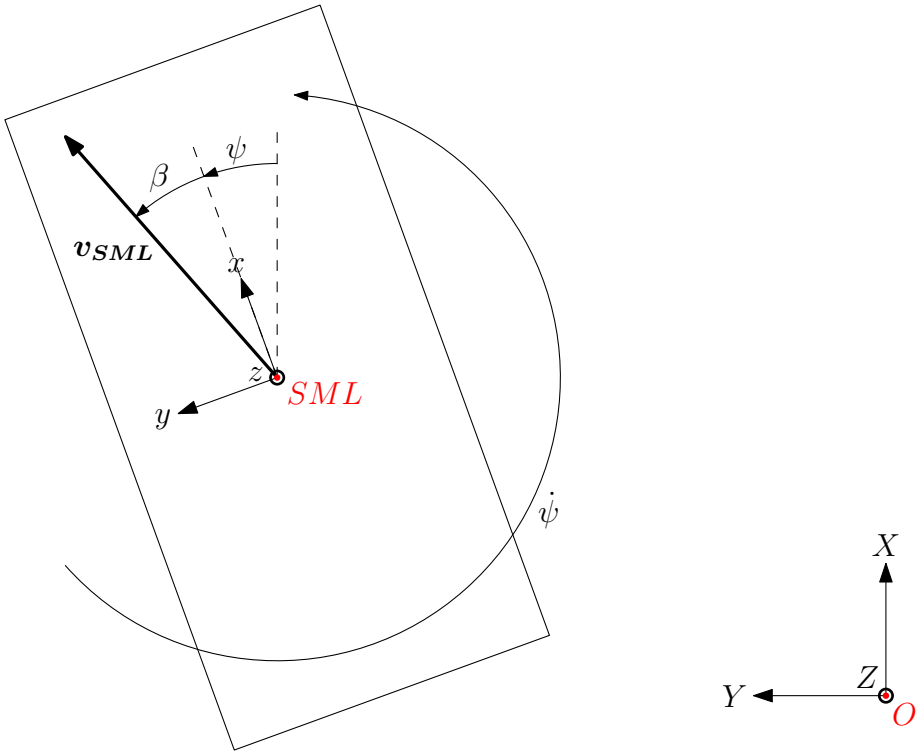

Figure 3.7. The top view of the nonlinear model while performing yaw (Angles and yaw rate are shown in positive directions.)

3.2. Assumptions

Simplifying the nonlinear model leads to faster simulations which is a desired fact. To make the model simpler, some assumptions have to be made. Assumptions have to be declared clearly and carefully because each assumption has effects on the model. While making the model simpler, assumptions also change the behavior of the model. Therefore all of them have to be consistent. If the assumptions somehow change the model behavior in different ways, the model fails because of inconsistencies. To avoid this, assumptions are discussed one by one and related assumptions are grouped together.

Interaction points for the front left quarter of the vehicle are seen in Figure 3.3 on page 15. When the force and moment balance equations of the parts are discussed, interaction points and center of gravities of the parts are used. The positions of these points have role in simplifying the force and moment balance equations. To make some of the moments equal to zero, it is assumed that related interaction points and center of gravities are coincident. This simplifies some of the moment balance equations because the distances between the force application points (interaction points) and center of gravities become to zero.

Assumption 3.1. Points $W1$ and $B1$ are coincident. This assumption is also valid for the other quarters of the vehicle.

Assumption 3.2. Points $WK1$ and $B1$ are coincident. This assumption is also valid for the other quarters of the vehicle.

Assumption 3.3. Points $WK1$ and $C1$ are coincident. This assumption is also valid for the other quarters of the vehicle.

Assumption 3.4. Points $SM1$ and $C1$ are coincident. This assumption is also valid for the other quarters of the vehicle.

Assumption 3.5. Points $SM1$ and $D1$ are coincident. This assumption is also valid for the other quarters of the vehicle.

Assumptions about the masses and inertias of the parts help to reduce the com-

putational load.

Assumption 3.6. Wheels are axisymmetrical about their spinning axes.

Assumption 3.7. Wheel knuckles do not have mass.

Assumption 3.8. Sliding masses do not have inertia.

Assumption 3.9. Suspensions do not have mass.

Some movements of the parts are restricted. This is done mainly to simplify force and moment balance equations. As a side effect, some kinematic relation equations are also simplified.

Assumption 3.10. Wheels do not translate vertically.

Assumption 3.11. Wheels do not roll.

Assumption 3.12. Wheel knuckles do not roll and pitch.

Assumption 3.13. Sliding masses do not roll and pitch.

Assumption 3.14. Suspensions do not roll and pitch.

The following assumption about the suspensions simplifies the moment balance equations as well as the kinematic relation equations.

Assumption 3.15. Center of gravities of the suspensions are always exactly in the middle of the interaction points.

Computation of the drag force on the vehicle is a challenging task, so this force is assumed not to exist.

Assumption 3.16. There is no drag force on the vehicle.

Determining the characteristics of the external force makes its calculation easier.

Assumption 3.17. External force is always applied on the center of gravity of the sprung mass.

Assumption 3.18. External force is always parallel to the road and it always points forward.

The equations of the tyre model are complex, increasing the computational load. By investigating the nature of the tyre model, it is concluded that doing some simplification is possible via elementary considerations.

Assumption 3.19. The road is flat and even.

Assumption 3.20. The speed of the vehicle is constant.

Assumption 3.21. Wheels spin freely, meaning that no driving or braking torque is applied on the wheels.

In the unloaded case of the vehicle, some of its properties ease the calculations.

Assumption 3.22. Vehicle is completely symmetric in the left-right sense when unloaded.

Assumption 3.23. Sprung mass is horizontal when unloaded; meaning that the x' and y' axes are horizontal whereas the z' axis is vertical.

Information about the initial state of the vehicle motion has to be included too.

Assumption 3.24. Initially, vehicle moves straight along X axis.

Assumption 3.25. Initially, points O and SML are vertically aligned.

3.3. Equations

The equations belonging to the nonlinear model are shown in this section. Since all of them are used while preparing the model, each equation has to be derived carefully. They should be consistent and, of course, correct. In addition, it is very important to use the assumptions properly because if there is any inconsistency between assumptions, the whole model fails.

Before starting to write the equations however, there are some facts which have to be explained. These facts are widely used, so mentioning them here is necessary.

For the front left quarter of the vehicle; it can be easily said that points $W1$, $B1$, $WK1$, $C1$, $SM1$ and $D1$ are coincident, considering Assumptions 3.1, 3.2, 3.3, 3.4 and

3.5. Obviously, this is true for the other quarters as well, with the appropriate changes in the names of the points. This fact is used many times while deriving the equations.

The equations involving vectors have to be written in the component form. At this point, the selection of the appropriate coordinate frame arises as an issue. While selecting the coordinate frame, two main goals have to be achieved. Most of the time, the simplicity of an equation is directly related to the selected coordinate frame. Therefore, the coordinate frame has to be selected so that the equation has the possible simplest form. Since different coordinate frames are used for different equations, transformations are necessary. The coordinate frames have to be selected so that the number of transformations is as small as possible. For example, while writing most of the equations for the front left quarter, the $WK1x_1y_1z_1$ coordinate frame is used. Firstly, it is appropriate to be used in the equations related with the front left wheel as explained in Section 3.3.4.2. Secondly, according to Assumption 3.12, x_1 and y_1 axes are always horizontal; and z_1 axis is always vertical. This makes the $WK1x_1y_1z_1$ coordinate frame suitable for the equations of the front left quarter in some cases. Finally, the use of this coordinate frame reduces the number of transformations. Another example is the $SMUx'y'z'$ coordinate frame. This coordinate frame is especially used where the positions are considered because all of the positions are provided in terms of the x', y' and z' components.

For the sake of simplicity, the equations are grouped. This is done by thinking of the steps which are followed while preparing a real vehicle for simulation. Firstly, the vehicle is stationary and unloaded. This is the case for the first part. In the second part, the stationary vehicle is loaded. Next, the initial conditions of the movement of the vehicle are discussed. Finally, the fourth part is devoted to the case in which the vehicle moves.

3.3.1. Stationary and Unloaded Vehicle

Here, the effort is spent mainly to find the vertical forces on the suspensions and, accordingly, to determine the vertical positions of points $E1$, $E2$, $E3$ and $E4$.

First of all, the positions of points $E1$, $E2$, $E3$ and $E4$ with respect to point SMU have to be found. This work is not shown here because it involves only vector addition; but it is necessary to remind that Assumption 3.22 is used.

Since the vehicle is at rest, the accelerations of points $W1$ and $SM1$ are zero. By using the suitable equations from Section 3.3.4, it is concluded that

$$\boldsymbol{F_{SMU/S1} = F_{W1/R} + W_{W1} + W_{SM1}}. \tag{3.1}$$

According to the tyre model, which is explained in Section 3.3.4.1, the horizontal components of the forces on the wheels from the road are zero when the vehicle is stationary. Using this with Assumption 3.14 and the suitable equations from Section 3.3.4,

$$\boldsymbol{M_{SMU/S1} = -M_{W1/WK1}}. \tag{3.2}$$

It should be noted that these equations are valid for the front left quarter of the vehicle. The equations related to the other quarters can be found easily by changing the subscripts.

Using Assumptions 3.22, 3.23, Equations (3.1), (3.2) and the suitable equations from Section 3.3.4,

$$F_{W1/R_{z'}} = \frac{p_{E1/SMU_{x'}} g\left(m_{W1} + m_{SM1}\right) - p_{E3/SMU_{x'}} g\left(m_{W1} + m_{SM1} + \frac{m_{SMU}}{2}\right)}{p_{E1/SMU_{x'}} - p_{E3/SMU_{x'}}}, \tag{3.3}$$

$$F_{W3/R_{z'}} = \left(m_{W1} + m_{W3} + m_{SM1} + m_{SM3} + \frac{m_{SMU}}{2}\right) g - F_{W1/R_{z'}}. \tag{3.4}$$

Using Equations (3.1) and (3.78),

$$F_{S1/SMU_{z'}} = m_{W1} g + m_{SM1} g - F_{W1/R_{z'}}, \tag{3.5}$$

$$F_{S3/SMU_{z'}} = m_{W3} g + m_{SM3} g - F_{W3/R_{z'}}. \tag{3.6}$$

Since the vehicle is stationary, the forces generated by the dampers are zero. By using Equation (3.77),

$$d_{1U} = {f_{Spring1}}^{-1}\left(F_{S1/SMU_{z'}}\right), \tag{3.7}$$

$$d_{3U} = {f_{Spring3}}^{-1}\left(F_{S3/SMU_{z'}}\right). \tag{3.8}$$

As the result of symmetry,

$$d_{2U} = d_{1U}, \tag{3.9}$$

$$d_{4U} = d_{3U}. \tag{3.10}$$

When Equations (3.3), (3.4), (3.5), (3.6), (3.7), (3.8), (3.9) and (3.10) are used, all of the results belonging to the stationary unloaded case are obtained.

3.3.2. Stationary and Loaded Vehicle

In the nonlinear model, the loads are passengers, luggage and fuel. Combining these loads, many loading conditions are obtained. Some variables change according to the loading condition. In this section, these variables are obtained.

Obviously, masses, inertias and positions change as the loading condition change; which means that they have to be found. However, obtaining them involves elementary concepts, so the work is not represented here.

The roll and pitch angles, and the vertical position of the center of gravity of the loaded sprung mass change according to the loading condition.

Using the facts in Section A.4.2.3,

$$\begin{bmatrix} p_{E1/SML_X} \\ p_{E1/SML_Y} \\ p_{E1/SML_Z} \end{bmatrix} = \begin{bmatrix} \cos\theta_i & 0 & \sin\theta_i \\ 0 & 1 & 0 \\ -\sin\theta_i & 0 & \cos\theta_i \end{bmatrix} \begin{bmatrix} 1 & 0 & 0 \\ 0 & \cos\phi_i & -\sin\phi_i \\ 0 & \sin\phi_i & \cos\phi_i \end{bmatrix} \begin{bmatrix} p_{E1/SML_x} \\ p_{E1/SML_y} \\ p_{E1/SML_z} \end{bmatrix}. \quad (3.11)$$

It should be noted that this equation is valid for the front left quarter of the vehicle. The equations related to the other quarters can be found easily by changing the subscripts.

Since the vehicle is stationary, the forces generated by the dampers are zero. Also, Equation (3.77) is valid here, which follows

$$f_{Spring1}{}^{-1}\left(F_{S1/SML_Z}\right) - d_{1U} + h_1 - p_{E1/SML_Z} - p_{SMLiZ} = 0. \quad (3.12)$$

It should be noted that this equation is valid for the front left quarter of the vehicle. The equations related to the other quarters can be found easily by changing the subscripts.

According to the tyre model, which is explained in Section 3.3.4.1, the horizontal components of the forces on the wheels from the road are zero when the vehicle is stationary. Using this,

$$F_{S1/SML_Z} + F_{S2/SML_Z} + F_{S3/SML_Z} + F_{S4/SML_Z} + m_{SML}g = 0. \quad (3.13)$$

Equations (3.42), (3.44) and (3.45) are also valid here. Using these equations with the discussion about the tyre model, which is stated above, yields

$$p_{E1/SML_X}F_{S1/SML_Z} + p_{E2/SML_X}F_{S2/SML_Z} + p_{E3/SML_X}F_{S3/SML_Z} + p_{E4/SML_X}F_{S4/SML_Z} = 0, \quad (3.14)$$

$$p_{E1/SML_Y}F_{S1/SML_Z} + p_{E2/SML_Y}F_{S2/SML_Z} + p_{E3/SML_Y}F_{S3/SML_Z} + p_{E4/SML_Y}F_{S4/SML_Z} = 0. \quad (3.15)$$

Equations (3.11), (3.12), (3.13), (3.14) and (3.15) are solved together to obtain ϕ_i, θ_i and p_{SMLi_Z}.

Additionally, the following two equations are also used in order to provide the initial conditions of the nonlinear model. As the result of Assumption 3.25 and the facts in Section A.4.2.3,

$$\begin{bmatrix} p_{SMLi_x} \\ p_{SMLi_y} \\ p_{SMLi_z} \end{bmatrix} = \begin{bmatrix} 1 & 0 & 0 \\ 0 & \cos\phi_i & \sin\phi_i \\ 0 & -\sin\phi_i & \cos\phi_i \end{bmatrix} \begin{bmatrix} \cos\theta_i & 0 & -\sin\theta_i \\ 0 & 1 & 0 \\ \sin\theta_i & 0 & \cos\theta_i \end{bmatrix} \begin{bmatrix} 0 \\ 0 \\ p_{SMLi_Z} \end{bmatrix}. \tag{3.16}$$

Assumption 3.24 states that

$$\psi_i = 0. \tag{3.17}$$

3.3.3. Moving Vehicle, Initial Conditions

By looking at Assumption 3.24, it is easily concluded that

$$\begin{bmatrix} v_{SMLi_x} \\ v_{SMLi_y} \\ v_{SMLi_z} \end{bmatrix} = \begin{bmatrix} 1 & 0 & 0 \\ 0 & \cos\phi_i & \sin\phi_i \\ 0 & -\sin\phi_i & \cos\phi_i \end{bmatrix} \begin{bmatrix} \cos\theta_i & 0 & -\sin\theta_i \\ 0 & 1 & 0 \\ \sin\theta_i & 0 & \cos\theta_i \end{bmatrix} \begin{bmatrix} v_{SMLi_X} \\ 0 \\ 0 \end{bmatrix}. \tag{3.18}$$

Considering this assumption, it can be said that the vehicle does not perform any maneuvers, leading to

$$\delta_{Si} = 0, \tag{3.19}$$

$$\dot{\delta}_{Si} = 0, \tag{3.20}$$

$$\ddot{\delta}_{Si} = 0. \tag{3.21}$$

Again, if the vehicle does not perform any maneuvers,

$$\begin{bmatrix} \omega_{SMLi_x} \\ \omega_{SMLi_y} \\ \omega_{SMLi_z} \end{bmatrix} = \begin{bmatrix} 0 \\ 0 \\ 0 \end{bmatrix}. \tag{3.22}$$

The equations in this section are used in order to provide the initial conditions of the nonlinear model.

3.3.4. Moving Vehicle

The case, in which the vehicle moves, includes complex equations. In addition to the complexity, the number of equations is too many. The equations and the relations between them have to be represented so that they can be followed and understood easily. Therefore, the equations are grouped. Grouping is done according to the parts of the vehicle because the equations are derived part by part. This also makes it easier to locate the equations when required.

In this section, most of the equations are written to represent the intermediate derivation steps. Therefore, all of the equation are not used in the end while preparing the nonlinear model. Even though the equations are represented later, it is mandatory to declare which equations are used finally while preparing the nonlinear model. Some of the finally used equations are written only for the front left quarter of the vehicle. They are Equations (3.27), (3.28), (3.29), (3.30), (3.31), (3.32), (3.35), (3.42), (3.44), (3.45), (3.46), (3.47), (3.53), (3.60), (3.61), (3.64), (3.69), (3.70), (3.71), (3.77), (3.79), (3.80), (3.86), (3.87), (3.88), (3.100), (3.101), (3.102), (3.103), (3.104), (3.105), (3.106), (3.107), (3.108), (3.109), (3.110), (3.111), (3.112), (3.113), (3.114), (3.115), (3.116), (3.117), (3.131), (3.133), (3.135), (3.136), (3.138), (3.140), (3.141) and (3.142). The equations for other quarters of the vehicle can easily be obtained by changing the subscripts in these equations. The obtained equations for all of the quarters and Equations (3.81), (3.82), (3.83), (3.84), (3.85), (3.89), (3.90), (3.91), (3.92), (3.93), (3.95), (3.97), (3.98), (3.99), (3.118), (3.122), (3.123), (3.124), (3.125), (3.126), (3.127),

(3.128), (3.129), (3.130), (3.132), (3.134), (3.137), (3.139) and (3.143) completely define the motion of the vehicle.

3.3.4.1. Road and Wheels (Magic Formula Tyre Model). Considering Assumption 3.16, it is concluded that the only forces and moments applied on the vehicle are the ones from the road, except the external force. The external force, of which the details are discussed later, is used to keep the speed of the vehicle constant. Since the vehicle is mainly affected by the forces and moments from the road, these forces and moments are highly important for the discussion of the vehicle motion.

The dynamics of tyre forces and moments are complex. However, in the literature, many methods are developed to deal with that complexity. Some models rely on experimental data, whereas others try to solve the problem using the physical structure of the tyre. These approaches differ from each other in some aspects. The first aspect is the complexity. More complex models are generally used for analysis concerning only tyre properties. Simpler models, on the other hand, are suitable to be used in simulations because these models do not slow down the simulations due to their simple structures. The second aspect is the accuracy. The accuracy is not always related with the complexity of the model, especially under certain conditions. Some models return good results in certain conditions even if they are not complex. Therefore, the tyre model should be chosen carefully according to the conditions and nature of the problem [20].

The well-known "Magic Formula" is used as the tyre model in this study. Magic Formula is a semi-empirical model, which means that the tyre parameters are obtained trying to fit the curves of the experimental results. Due to the opportunity to make endless numbers of experiment, the results of the model are said to be very similar to the experimental results. That is why Magic Formula is very suitable for use in simulations. Also, tyre data are generally provided in terms of Magic Formula parameters. As a result, there is no alternative to Magic Formula to be used in the vehicle model.

Magic Formula calculates the steady-state forces and moments [20]. At first glance, this can be considered as a fact which makes Magic Formula inappropriate for dynamic simulations. This is not the case though, because the simulation sends the information to Magic Formula in samples. Each sample of signal can be thought of as a steady-state input, so the results of Magic Formula can be used in the model. In this text, Magic Formula is not discussed in deep detail, but only its characteristics, which are important for the constructed model, are explained.

Magic Formula tries to find appropriate tyre parameters, ensuring that the generated curves are similar to the experimental curves. A standard curve and elementary parameters are seen in Figure 3.8.

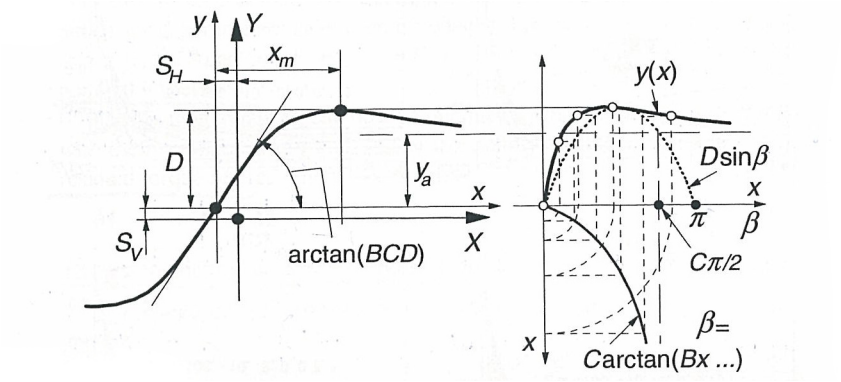

Figure 3.8. A standard Magic Formula curve with elementary parameters [20]

As stated before, Assumptions 3.19, 3.20 and 3.21 are made to simplify the Magic Formula equations. These assumptions lead to the fact that the longitudinal slip constants of the tyres are zero. This also means that the tyres do not slip relative to the road along the wheel longitudinal axes. As a result of this, no forces are generated along the wheel longitudinal axes. This extremely simplifies the Magic Formula equations because calculation of one of the force components becomes unnecessary, reducing the calculation load. Introducing Assumption 3.11, it is also concluded that there are no cambers on wheels. Accordingly, the use of the extended equations of Magic Formula becomes unnecessary, simplifying the equations even more.

Magic Formula is improved over time and, thus, there are various versions of Magic Formula equations. Knowing the version of the equations is important because

the tyre parameters are provided accordingly. The equations in [20] are version 2004 and they are used in this study. Considering the assumptions and neglecting toe and camber effects, the number of equations is reduced and the remaining equations are simplified. The final equations are seen in Section B.

Even though Magic Formula is appropriate to be used in simulations, integrating it to the model via its equations slows down the simulation in a significant amount. Using lookup tables instead, is the solution for this problem. Equations in Section B are used to generate lookup tables. The generated lookup tables are placed into the appropriate places in the model. These lookup tables basically receive wheel longitudinal and lateral components of the contact point velocities and the vertical components of the forces on wheels. They return the forces and moments which are applied on the wheels by the road.

As stated before, the equations in [20] are used to construct the lookup tables. The definitions used in [20] show slight differences, so it is necessary to briefly introduce them here. V_{cx} stands for the wheel longitudinal component of the contact point velocity and its positive direction is forward. V_{cy} stands for the wheel lateral component of the contact point velocity and its positive direction is to the right. F_x stands for the wheel longitudinal component of the force on the wheel from the road and its positive direction is forward. F_y stands for the wheel lateral component of the force on the wheel from the road and its positive direction is to the right. F_z stands for the vertical component of the force on the wheel from the road and its positive direction is upward. M_x stands for the wheel longitudinal component of the moment on the wheel from the road and its positive direction is forward. M_y stands for the wheel lateral component of the moment on the wheel from the road and its positive direction is to the right. M_z stands for the vertical component of the moment on the wheel from the road and its positive direction is downward.

Now that the definitions are done according to [20], the equations can be written.

Using Assumptions 3.19, 3.20 and 3.21, it is concluded that

$$F_x = 0. \tag{3.23}$$

The other equations are written as the following:

$$F_y = f_{MF\_Force\_Lateral1}\left(V_{cx}, V_{cy}, F_z\right) \tag{3.24}$$

$$M_x = f_{MF\_Moment\_Roll1}\left(V_{cx}, V_{cy}, F_z\right) \tag{3.25}$$

$$M_z = f_{MF\_Moment\_Yaw1}\left(V_{cx}, V_{cy}, F_z\right) \tag{3.26}$$

Here, it should be noted that M_y is not found because it is not used by any other equation in the model.

In [20], a coordinate frame, which makes all of the rotations as the wheel except spinning, is used. Among the coordinate frames used in the nonlinear model, the $WK1x_1y_1z_1$ coordinate frame is the appropriate one. Therefore, while doing the variable transformations, this coordinate frame is used. The details of the transformations are not included here. After the transformations, Equations (3.23), (3.24), (3.25) and (3.26) become to

$$F_{W1/R_{x_1}} = 0, \tag{3.27}$$

$$F_{W1/R_{y_1}} = -f_{MF\_Force\_Lateral1}\left(v_{A1_{x_1}}, -v_{A1_{y_1}}, F_{W1/R_{z_1}}\right), \tag{3.28}$$

$$M_{W1/R_{x_1}} = f_{MF\_Moment\_Roll1}\left(v_{A1_{x_1}}, -v_{A1_{y_1}}, F_{W1/R_{z_1}}\right), \tag{3.29}$$

$$M_{W1/R_{z_1}} = -f_{MF\_Moment\_Yaw1}\left(v_{A1_{x_1}}, -v_{A1_{y_1}}, F_{W1/R_{z_1}}\right). \tag{3.30}$$

It should be noted that all of the equations shown in this section are valid for the front left quarter of the vehicle. The equations related to the other quarters can be found easily by changing the subscripts.

3.3.4.2. Wheels. Using Equation (A.59a), the force balance equations of the front left wheel are written as

$$F_{W1/WK1_{x_1}} = m_{W1} a_{W1_{x_1}} - F_{W1/R_{x_1}}, \tag{3.31}$$

$$F_{W1/WK1_{y_1}} = m_{W1} a_{W1_{y_1}} - F_{W1/R_{y_1}}, \tag{3.32}$$

$$F_{W1/WK1_{z_1}} = m_{W1} a_{W1_{z_1}} - F_{W1/R_{z_1}} + m_{W1} g. \tag{3.33}$$

Using Assumption 3.10, it is concluded that

$$a_{W1_{z_1}} = 0. \tag{3.34}$$

Using Equations (3.33) and (3.34) yields

$$F_{W1/R_{z_1}} = m_{W1} g - F_{W1/WK1_{z_1}}. \tag{3.35}$$

Writing the moment balance equations of the front left wheel is more challenging. As stated before, points $W1$ and $B1$ are coincident. Using this fact,

$$\boldsymbol{M_{W1(W1)}} = \boldsymbol{M_{W1/R}} + \boldsymbol{M_{W1/WK1}} + \left(\boldsymbol{p_{A1/W1}} \times \boldsymbol{F_{W1/R}}\right). \tag{3.36}$$

Using Assumption 3.11 and the definition of point $A1$, it can be said that points $A1$ and $W1$ are vertically aligned; resulting in

$$\boldsymbol{p_{A1/W1}} = -r_1 \boldsymbol{k_1}. \tag{3.37}$$

Using Equations (3.36) and (3.37) yields

$$\begin{bmatrix} M_{W1(W1)_{x_1}} \\ M_{W1(W1)_{y_1}} \\ M_{W1(W1)_{z_1}} \end{bmatrix} = \begin{bmatrix} M_{W1/R_{x_1}} + M_{W1/WK1_{x_1}} + r_1 F_{W1/R_{y_1}} \\ M_{W1/R_{y_1}} + M_{W1/WK1_{y_1}} - r_1 F_{W1/R_{x_1}} \\ M_{W1/R_{z_1}} + M_{W1/WK1_{z_1}} \end{bmatrix}. \tag{3.38}$$

When Assumption 3.6 is considered, it is seen that the second part of Section A.4.2.5 can be used for the wheels. If the fact that points $W1$ and $WK1$ are coincident and Assumption 3.12 are considered, $WK1x_1y_1z_1$ is selected as the coordinate frame which does not spin. As the result,

$$\begin{bmatrix} M_{W1(W1)_{x_1}} \\ M_{W1(W1)_{y_1}} \\ M_{W1(W1)_{z_1}} \end{bmatrix} = \begin{bmatrix} I_{W1/x_1}\dot{\omega}_{W1_{x_1}} + \left(I_{W1/z_1} - I_{W1/y_1}\right)\omega_{W1_{y_1}}\omega_{W1_{z_1}} - I_{W1/z_1}\omega_{W1_{z_1}}\Omega_1 \\ I_{W1/y_1}\dot{\omega}_{W1_{y_1}} + \left(I_{W1/x_1} - I_{W1/z_1}\right)\omega_{W1_{x_1}}\omega_{W1_{z_1}} \\ I_{W1/z_1}\dot{\omega}_{W1_{z_1}} + \left(I_{W1/y_1} - I_{W1/x_1}\right)\omega_{W1_{x_1}}\omega_{W1_{y_1}} + I_{W1/x_1}\omega_{W1_{x_1}}\Omega_1 \end{bmatrix}. \tag{3.39}$$

Assumption 3.11 results in

$$\boldsymbol{\omega_{W1}} = \Omega_1 \boldsymbol{j_1} + \left(\dot{\psi} + \dot{\delta}_1\right)\boldsymbol{k_1}. \tag{3.40}$$

Using Equations (3.39) and (3.40) yields

$$\begin{bmatrix} M_{W1(W1)_{x_1}} \\ M_{W1(W1)_{y_1}} \\ M_{W1(W1)_{z_1}} \end{bmatrix} = \begin{bmatrix} -I_{W1/y_1}\Omega_1\left(\dot{\psi} + \dot{\delta}_1\right) \\ I_{W1/y_1}\dot{\Omega}_1 \\ I_{W1/z_1}\left(\ddot{\psi} + \ddot{\delta}_1\right) \end{bmatrix}. \tag{3.41}$$

Putting Equations (3.38) and (3.41) together,

$$M_{W1/WK1_{x_1}} = -I_{W1/y_1}\Omega_1\left(\dot{\psi} + \dot{\delta}_1\right) - M_{W1/R_{x_1}} - r_1 F_{W1/R_{y_1}}, \tag{3.42}$$

$$M_{W1/WK1_{y_1}} = I_{W1/y_1}\dot{\Omega}_1 - M_{W1/R_{y_1}} + r_1 F_{W1/R_{x_1}}, \tag{3.43}$$

$$M_{W1/WK1_{z_1}} = I_{W1/z_1}\left(\ddot{\psi} + \ddot{\delta}_1\right) - M_{W1/R_{z_1}}. \tag{3.44}$$

Using Assumption 3.21, Equation (3.43) is superseded by

$$M_{W1/WK1_{y_1}} = 0. \tag{3.45}$$

As stated before, points $A1$ and $W1$ are vertically aligned; resulting in

$$v_{A1_{x_1}} = v_{W1_{x_1}}, \tag{3.46}$$

$$v_{A1_{y_1}} = v_{W1_{y_1}}. \tag{3.47}$$

By using definitions,

$$p_{W1_{z_1}} = r_1. \tag{3.48}$$

Modifying Equation (A.41) according to the definitions of points,

$$\boldsymbol{v_{T1}} = \boldsymbol{v_{W1}} + \boldsymbol{\omega_{W1}} \times \boldsymbol{p_{T1/W1}}. \tag{3.49}$$

Using Assumption 3.11 and the definition of point $T1$, it can be said that points $W1$ and $T1$ are vertically aligned; resulting in

$$\boldsymbol{p_{T1/W1}} = -r_1 \boldsymbol{k_1}. \tag{3.50}$$

Using Equations (3.40), (3.49) and (3.50), it is concluded that

$$\begin{bmatrix} v_{T1_{x_1}} \\ v_{T1_{y_1}} \\ v_{T1_{z_1}} \end{bmatrix} = \begin{bmatrix} v_{W1_{x_1}} \\ v_{W1_{y_1}} \\ v_{W1_{z_1}} \end{bmatrix} + \begin{bmatrix} -r_1\Omega_1 \\ 0 \\ 0 \end{bmatrix}. \tag{3.51}$$

Assumptions 3.19, 3.20 and 3.21 lead to

$$v_{T1_{x_1}} = 0. \tag{3.52}$$

Using Equations (3.51) and (3.52),

$$\Omega_1 = \frac{v_{W1_{x_1}}}{r_1}. \tag{3.53}$$

It should be noted that all of the equations shown in this section are valid for the front left quarter of the vehicle. The equations related to the other quarters can be found easily by changing the subscripts.

3.3.4.3. Wheels and Wheel Knuckles. Front left wheel and front left wheel knuckle interact with each other via point $B1$, and the related force and moment equations are as the following:

$$\boldsymbol{F_{W1/WK1}} = -\boldsymbol{F_{WK1/W1}} \tag{3.54}$$

$$\boldsymbol{M_{W1/WK1}} = -\boldsymbol{M_{WK1/W1}} \tag{3.55}$$

It should be noted that these equations are valid for the front left quarter of the vehicle. The equations related to the other quarters can be found easily by changing the subscripts.

3.3.4.4. Wheel Knuckles. As the result of Assumption 3.7, Equation (A.62) is used to write the force balance equation of the front left wheel knuckle as the following:

$$\boldsymbol{F_{WK1/W1}} + \boldsymbol{F_{WK1/SM1}} = 0 \tag{3.56}$$

Reconsidering Assumption 3.7 and the facts in Section A.4.1.1, it is concluded that Equation (A.67) can be used to write the moment balance equation of the front left wheel knuckle. As stated before, points $B1$, $WK1$ and $C1$ are coincident, simplifying

the moment balance equation as

$$\boldsymbol{M_{WK1/W1}} + \boldsymbol{M_{WK1/SM1}} = 0. \tag{3.57}$$

It should be noted that all of the equations shown in this section are valid for the front left quarter of the vehicle. The equations related to the other quarters can be found easily by changing the subscripts.

3.3.4.5. Wheel Knuckles and Sliding Masses. Front left wheel knuckle and front left sliding mass interact with each other via point $C1$, and the related force and moment equations are as the following:

$$\boldsymbol{F_{WK1/SM1}} = -\boldsymbol{F_{SM1/WK1}} \tag{3.58}$$

$$\boldsymbol{M_{WK1/SM1}} = -\boldsymbol{M_{SM1/WK1}} \tag{3.59}$$

It should be noted that these equations are valid for the front left quarter of the vehicle. The equations related to the other quarters can be found easily by changing the subscripts.

3.3.4.6. Sliding Masses. Using Equation (A.59a), the force balance equations of the front left sliding mass are written as

$$F_{SM1/S1_{x_1}} = m_{SM1} a_{SM1_{x_1}} - F_{SM1/WK1_{x_1}}, \tag{3.60}$$

$$F_{SM1/S1_{y_1}} = m_{SM1} a_{SM1_{y_1}} - F_{SM1/WK1_{y_1}}, \tag{3.61}$$

$$F_{SM1/S1_{z_1}} = m_{SM1} a_{SM1_{z_1}} - F_{SM1/WK1_{z_1}} + m_{SM1} g. \tag{3.62}$$

Using Assumption 3.10 and the fact that points $W1$ and $SM1$ are coincident, it is concluded that

$$a_{SM1_{z_1}} = 0. \tag{3.63}$$

Using Equations (3.62) and (3.63) yields

$$F_{SM1/WK1_{z_1}} = m_{SM1}g - F_{SM1/S1_{z_1}}. \tag{3.64}$$

Considering Assumption 3.8, it is concluded that Equation (A.67) can be used to write the moment balance equation of the front left sliding mass. As stated before, points $C1$, $SM1$ and $D1$ are coincident, simplifying the moment balance equation as

$$\boldsymbol{M_{SM1/WK1}} + \boldsymbol{M_{SM1/S1}} = 0. \tag{3.65}$$

It should be noted that all of the equations shown in this section are valid for the front left quarter of the vehicle. The equations related to the other quarters can be found easily by changing the subscripts.

3.3.4.7. Sliding Masses and Suspensions. Front left sliding mass and front left suspension interact with each other via point $D1$, and the related force and moment equations are as the following:

$$\boldsymbol{F_{SM1/S1}} = -\boldsymbol{F_{S1/SM1}} \tag{3.66}$$

$$\boldsymbol{M_{SM1/S1}} = -\boldsymbol{M_{S1/SM1}} \tag{3.67}$$

It should be noted that these equations are valid for the front left quarter of the vehicle. The equations related to the other quarters can be found easily by changing the subscripts.

3.3.4.8. Suspensions. As the result of Assumption 3.9, Equation (A.62) is used to write the force balance equation of the front left suspension as the following:

$$\boldsymbol{F_{S1/SM1}} + \boldsymbol{F_{S1/SML}} = 0 \tag{3.68}$$

Reconsidering Assumption 3.9 and the facts in Section A.4.1.1, it is concluded that Equation (A.67) can be used to write the moment balance equation of the front left suspension. With the addition of Assumption 3.14, the moment balance equation is written as

$$\begin{bmatrix} M_{S1/SML_{x_1}} \\ M_{S1/SML_{y_1}} \\ M_{S1/SML_{z_1}} \end{bmatrix} = - \begin{bmatrix} M_{S1/SM1_{x_1}} \\ M_{S1/SM1_{y_1}} \\ M_{S1/SM1_{z_1}} \end{bmatrix} - \begin{bmatrix} -p_{D1/S1_{z_1}} F_{S1/SM1_{y_1}} \\ p_{D1/S1_{z_1}} F_{S1/SM1_{x_1}} \\ 0 \end{bmatrix} - \begin{bmatrix} -p_{E1/S1_{z_1}} F_{S1/SML_{y_1}} \\ p_{E1/S1_{z_1}} F_{S1/SML_{x_1}} \\ 0 \end{bmatrix}. \tag{3.69}$$

As stated before, points $W1$ and $D1$ are coincident. Using this fact with Assumptions 3.14, 3.15 and Equation (3.48) yields

$$p_{D1/S1_{z_1}} = \frac{r_1 - p_{E1_{z_1}}}{2}, \tag{3.70}$$

$$p_{E1/S1_{z_1}} = \frac{p_{E1_{z_1}} - r_1}{2}. \tag{3.71}$$

In the nonlinear model, each suspension is made up of a spring and a damper. Springs and dampers are connected in parallel just like in a real vehicle. Here, the forces generated by the springs and dampers are studied separately. Then, these forces are summed up. By definitions,

$$disp_1 = p_{E1_Z} - h_1, \tag{3.72}$$

$$disp_1 = d_{1L} - d_{1U}, \tag{3.73}$$

$$F_{Spring1} = f_{Spring1}\left(d_{1L}\right). \tag{3.74}$$

Putting Equations (3.72), (3.73) and (3.74) together yields

$$F_{Spring1} = f_{Spring1}\left(d_{1U} + p_{E1_Z} - h_1\right). \tag{3.75}$$

Again by definitions,

$$F_{Damper1} = f_{Damper1}\left(v_{E1_Z}\right). \tag{3.76}$$

Adding Equations (3.75) and (3.76),

$$F_{S1/SML_{z_1}} = f_{Spring1}\left(d_{1U} + p_{E1_{z_1}} - h_1\right) + f_{Damper1}\left(v_{E1_{z_1}}\right). \tag{3.77}$$

It should be noted that all of the equations shown in this section are valid for the front left quarter of the vehicle. The equations related to the other quarters can be found easily by changing the subscripts.

3.3.4.9. Suspensions and Sprung Mass. Front left suspension and sprung mass interact with each other via point $E1$, and the related force equation is as the following:

$$\boldsymbol{F_{S1/SML}} = -\boldsymbol{F_{SML/S1}} \tag{3.78}$$

This equation is written in z_1 components as

$$F_{SML/S1_{z_1}} = -F_{S1/SML_{z_1}}. \tag{3.79}$$

The related moment equation is as the following:

$$\begin{bmatrix} M_{SML/S1_{x_1}} \\ M_{SML/S1_{y_1}} \\ M_{SML/S1_{z_1}} \end{bmatrix} = - \begin{bmatrix} M_{S1/SML_{x_1}} \\ M_{S1/SML_{y_1}} \\ M_{S1/SML_{z_1}} \end{bmatrix} \tag{3.80}$$

It should be noted that all of the equations shown in this section are valid for the front left quarter of the vehicle. The equations related to the other quarters can

be found easily by changing the subscripts.

3.3.4.10. Sprung Mass. The total force applied on the sprung mass is written as

$$\begin{bmatrix} F_{SML_x} \\ F_{SML_y} \\ F_{SML_z} \end{bmatrix} = \begin{bmatrix} F_{SML/S1_x} \\ F_{SML/S1_y} \\ F_{SML/S1_z} \end{bmatrix} + \begin{bmatrix} F_{SML/S2_x} \\ F_{SML/S2_y} \\ F_{SML/S2_z} \end{bmatrix} + \begin{bmatrix} F_{SML/S3_x} \\ F_{SML/S3_y} \\ F_{SML/S3_z} \end{bmatrix} + \begin{bmatrix} F_{SML/S4_x} \\ F_{SML/S4_y} \\ F_{SML/S4_z} \end{bmatrix} + \begin{bmatrix} F_{SML/Ext_x} \\ F_{SML/Ext_y} \\ F_{SML/Ext_z} \end{bmatrix} + \begin{bmatrix} W_{SML_x} \\ W_{SML_y} \\ W_{SML_z} \end{bmatrix}. \tag{3.81}$$

By looking at Equation (A.59a), the force balance equation of the sprung mass is written as

$$\begin{bmatrix} a_{SML_x} \\ a_{SML_y} \\ a_{SML_z} \end{bmatrix} = \frac{1}{m_{SML}} \begin{bmatrix} F_{SML_x} \\ F_{SML_y} \\ F_{SML_z} \end{bmatrix}. \tag{3.82}$$

Or, alternatively,

$$\begin{bmatrix} \dot{v}_{SML_x} \\ \dot{v}_{SML_y} \\ \dot{v}_{SML_z} \end{bmatrix} = \frac{1}{m_{SML}} \begin{bmatrix} F_{SML_x} \\ F_{SML_y} \\ F_{SML_z} \end{bmatrix} - \begin{bmatrix} \omega_{SML_x} \\ \omega_{SML_y} \\ \omega_{SML_z} \end{bmatrix} \times \begin{bmatrix} v_{SML_x} \\ v_{SML_y} \\ v_{SML_z} \end{bmatrix} \tag{3.83}$$

by looking at Equation (A.61).

As the result of Assumption 3.17, the external force does not have any effect on the total moment applied on the sprung mass. Accordingly, the total moment applied

on the sprung mass is written as

$$\begin{bmatrix} M_{SML(SML)_x} \\ M_{SML(SML)_y} \\ M_{SML(SML)_z} \end{bmatrix} = \begin{bmatrix} M_{SML/S1_x} \\ M_{SML/S1_y} \\ M_{SML/S1_z} \end{bmatrix} + \begin{bmatrix} M_{SML/S2_x} \\ M_{SML/S2_y} \\ M_{SML/S2_z} \end{bmatrix} + \begin{bmatrix} M_{SML/S3_x} \\ M_{SML/S3_y} \\ M_{SML/S3_z} \end{bmatrix} + \begin{bmatrix} M_{SML/S4_x} \\ M_{SML/S4_y} \\ M_{SML/S4_z} \end{bmatrix}$$
$$+ \left(\begin{bmatrix} p_{E1/SML_x} \\ p_{E1/SML_y} \\ p_{E1/SML_z} \end{bmatrix} \times \begin{bmatrix} F_{SML/S1_x} \\ F_{SML/S1_y} \\ F_{SML/S1_z} \end{bmatrix} \right)$$
$$+ \left(\begin{bmatrix} p_{E2/SML_x} \\ p_{E2/SML_y} \\ p_{E2/SML_z} \end{bmatrix} \times \begin{bmatrix} F_{SML/S2_x} \\ F_{SML/S2_y} \\ F_{SML/S2_z} \end{bmatrix} \right)$$
$$+ \left(\begin{bmatrix} p_{E3/SML_x} \\ p_{E3/SML_y} \\ p_{E3/SML_z} \end{bmatrix} \times \begin{bmatrix} F_{SML/S3_x} \\ F_{SML/S3_y} \\ F_{SML/S3_z} \end{bmatrix} \right)$$
$$+ \left(\begin{bmatrix} p_{E4/SML_x} \\ p_{E4/SML_y} \\ p_{E4/SML_z} \end{bmatrix} \times \begin{bmatrix} F_{SML/S4_x} \\ F_{SML/S4_y} \\ F_{SML/S4_z} \end{bmatrix} \right). \tag{3.84}$$

By looking at Equation (A.66), the moment balance equation of the sprung mass is written as

$$\begin{bmatrix} \dot{\omega}_{SML_x} \\ \dot{\omega}_{SML_y} \\ \dot{\omega}_{SML_z} \end{bmatrix} = {I_{SML/SMLxyz}}^{-1} \left(\begin{bmatrix} M_{SML(SML)_x} \\ M_{SML(SML)_y} \\ M_{SML(SML)_z} \end{bmatrix} - \begin{bmatrix} \omega_{SML_x} \\ \omega_{SML_y} \\ \omega_{SML_z} \end{bmatrix} \times I_{SML/SMLxyz} \begin{bmatrix} \omega_{SML_x} \\ \omega_{SML_y} \\ \omega_{SML_z} \end{bmatrix} \right). \tag{3.85}$$

Position, velocity and acceleration of point $E1$ have to be found. By looking at Equation (A.38),

$$\begin{bmatrix} p_{E1_x} \\ p_{E1_y} \\ p_{E1_z} \end{bmatrix} = \begin{bmatrix} p_{SML_x} \\ p_{SML_y} \\ p_{SML_z} \end{bmatrix} + \begin{bmatrix} p_{E1/SML_x} \\ p_{E1/SML_y} \\ p_{E1/SML_z} \end{bmatrix}. \tag{3.86}$$

By looking at Equation (A.41),

$$\begin{bmatrix} v_{E1_x} \\ v_{E1_y} \\ v_{E1_z} \end{bmatrix} = \begin{bmatrix} v_{SML_x} \\ v_{SML_y} \\ v_{SML_z} \end{bmatrix} + \begin{bmatrix} \omega_{SML_x} \\ \omega_{SML_y} \\ \omega_{SML_z} \end{bmatrix} \times \begin{bmatrix} p_{E1/SML_x} \\ p_{E1/SML_y} \\ p_{E1/SML_z} \end{bmatrix}. \tag{3.87}$$

By looking at Equation (A.44),

$$\begin{aligned} \begin{bmatrix} a_{E1_x} \\ a_{E1_y} \\ a_{E1_z} \end{bmatrix} = & \begin{bmatrix} a_{SML_x} \\ a_{SML_y} \\ a_{SML_z} \end{bmatrix} + \begin{bmatrix} \alpha_{SML_x} \\ \alpha_{SML_y} \\ \alpha_{SML_z} \end{bmatrix} \times \begin{bmatrix} p_{E1/SML_x} \\ p_{E1/SML_y} \\ p_{E1/SML_z} \end{bmatrix} \\ & + \begin{bmatrix} \omega_{SML_x} \\ \omega_{SML_y} \\ \omega_{SML_z} \end{bmatrix} \times \left(\begin{bmatrix} \omega_{SML_x} \\ \omega_{SML_y} \\ \omega_{SML_z} \end{bmatrix} \times \begin{bmatrix} p_{E1/SML_x} \\ p_{E1/SML_y} \\ p_{E1/SML_z} \end{bmatrix} \right). \end{aligned} \tag{3.88}$$

It should be noted that positions, velocities and accelerations of points $E2$, $E3$ and $E4$ can be obtained by changing the subscripts in the last three equations.

Modification of Equations (A.14) and (A.15) results in

$$\begin{bmatrix} \dot{p}_{SML_x} \\ \dot{p}_{SML_y} \\ \dot{p}_{SML_z} \end{bmatrix} = \begin{bmatrix} v_{SML_x} \\ v_{SML_y} \\ v_{SML_z} \end{bmatrix} - \begin{bmatrix} \omega_{SML_x} \\ \omega_{SML_y} \\ \omega_{SML_z} \end{bmatrix} \times \begin{bmatrix} p_{SML_x} \\ p_{SML_y} \\ p_{SML_z} \end{bmatrix}. \tag{3.89}$$

Similarly,

$$\begin{bmatrix} \alpha_{SML_x} \\ \alpha_{SML_y} \\ \alpha_{SML_z} \end{bmatrix} = \begin{bmatrix} \dot{\omega}_{SML_x} \\ \dot{\omega}_{SML_y} \\ \dot{\omega}_{SML_z} \end{bmatrix}. \tag{3.90}$$

Modification of Equations (A.47) - (A.49) yields

$$\dot{\phi} = \omega_{SML_x} + \frac{\left(\omega_{SML_y} \sin\phi + \omega_{SML_z} \cos\phi\right) \sin\theta}{\cos\theta}, \tag{3.91}$$

$$\dot{\theta} = \omega_{SML_y} \cos\phi - \omega_{SML_z} \sin\phi, \tag{3.92}$$

$$\dot{\psi} = \frac{\omega_{SML_y} \sin\phi + \omega_{SML_z} \cos\phi}{\cos\theta}. \tag{3.93}$$

Changing the notation of Equation (A.46c) appropriately,

$$\boldsymbol{\omega_{SML}} = \left(\dot{\phi} - \dot{\psi}\sin\theta\right)\boldsymbol{i} + \left(\dot{\psi}\cos\theta\sin\phi + \dot{\theta}\cos\phi\right)\boldsymbol{j} + \left(\dot{\psi}\cos\theta\cos\phi - \dot{\theta}\sin\phi\right)\boldsymbol{k}. \tag{3.94}$$

Using Equations (3.90) and (3.94),

$$\ddot{\psi} = \frac{\alpha_{SML_y} \sin\phi + \alpha_{SML_z} \cos\phi + \dot{\theta}\dot{\psi}\sin\theta + \dot{\phi}\dot{\theta}}{\cos\theta}. \tag{3.95}$$

3.3.4.11. External Force. The external force is an imaginary force which is used to keep the vehicle speed constant. Keeping the vehicle speed constant is necessary to satisfy some of the assumptions. For this purpose, a PI controller is integrated into the model. A PID controller is not preferred because it involves derivation, which is undesirable for simulations. The PI controller basically takes the difference between the actual and reference speeds, and generates a force.

Considering Assumption 3.14, it can be said that the only rotation of the suspensions is yaw. Moreover, the yaw motion of the suspensions is the same as the yaw motion of the vehicle. Therefore, any of the coordinate frames attached to the suspensions can be used. Here, $S1x_{S1}y_{S1}z_{S1}$ coordinate frame is used. The use of Assumption 3.18 leads

$$F_{SML/Ext_{x_{S1}}} \neq 0, \tag{3.96}$$

$$F_{SML/Ext_{y_{S1}}} = 0, \tag{3.97}$$

$$F_{SML/Ext_{z_{S1}}} = 0. \tag{3.98}$$

By looking at Equation (3.96), it is understood that $F_{SML/Ext_{x_{S1}}}$ has to be found. Considering what a PI controller does, it is found as

$$F_{SML/Ext_{x_{S1}}} = C_P \left(v_{SMLi_X} - v_{SML_{x_{S1}}} \right) + C_I \int \left(v_{SMLi_X} - v_{SML_{x_{S1}}} \right) dt \tag{3.99}$$

where the actual and reference speeds are represented with $v_{SML_{x_{S1}}}$ and v_{SMLi_X} respectively.

3.3.4.12. Combination of Equations. In this section, the suitable equations belonging to different vehicle parts are combined. This is done to reduce the number of equations which are used while preparing the nonlinear model in the end.

Using Equations (3.54), (3.56) and (3.58),

$$F_{SM1/WK1_{x_1}} = -F_{W1/WK1_{x_1}}, \tag{3.100}$$

$$F_{SM1/WK1_{y_1}} = -F_{W1/WK1_{y_1}}, \tag{3.101}$$

$$F_{W1/WK1_{z_1}} = -F_{SM1/WK1_{z_1}}. \tag{3.102}$$

Using Equations (3.68) and (3.78),

$$F_{S1/SM1_{x_1}} = F_{SML/S1_{x_1}}, \tag{3.103}$$

$$F_{S1/SM1_{y_1}} = F_{SML/S1_{y_1}}. \tag{3.104}$$

Using Equations (3.66) and (3.68),

$$F_{S1/SML_{x_1}} = F_{SM1/S1_{x_1}}, \tag{3.105}$$

$$F_{S1/SML_{y_1}} = F_{SM1/S1_{y_1}}, \tag{3.106}$$

$$F_{SM1/S1_{z_1}} = F_{S1/SML_{z_1}}. \tag{3.107}$$

Using Equations (3.66), (3.68) and (3.78),

$$F_{SML/S1_{x_1}} = -F_{SM1/S1_{x_1}}, \tag{3.108}$$

$$F_{SML/S1_{y_1}} = -F_{SM1/S1_{y_1}}. \tag{3.109}$$

Using Equations (3.55), (3.57), (3.59), (3.65) and (3.67),

$$\begin{bmatrix} M_{S1/SM1_{x_1}} \\ M_{S1/SM1_{y_1}} \\ M_{S1/SM1_{z_1}} \end{bmatrix} = - \begin{bmatrix} M_{W1/WK1_{x_1}} \\ M_{W1/WK1_{y_1}} \\ M_{W1/WK1_{z_1}} \end{bmatrix}. \tag{3.110}$$

Using the fact that points $W1$ and $SM1$ are coincident,

$$a_{SM1_{x_1}} = a_{W1_{x_1}}, \tag{3.111}$$

$$a_{SM1_{y_1}} = a_{W1_{y_1}}. \tag{3.112}$$

Using Assumption 3.14 and the fact that points $W1$ and $D1$ are coincident,

$$v_{W1_{x_1}} = v_{E1_{x_1}}, \tag{3.113}$$

$$v_{W1_{y_1}} = v_{E1_{y_1}}, \tag{3.114}$$

$$a_{W1_{x_1}} = a_{E1_{x_1}}, \tag{3.115}$$

$$a_{W1_{y_1}} = a_{E1_{y_1}}. \tag{3.116}$$

It should be noted that all of the equations shown in this section are valid for the front left quarter of the vehicle. The equations related to the other quarters can be found easily by changing the subscripts.

3.3.4.13. Transformations. All of the equations about transformations are explained in this section. First, the transformation matrices are found, then vector transformations are done using the transformation matrices.

Using Assumptions 3.12 and 3.13,

$$T_{WK1/SM1} = \begin{bmatrix} \cos\delta_1 & -\sin\delta_1 & 0 \\ \sin\delta_1 & \cos\delta_1 & 0 \\ 0 & 0 & 1 \end{bmatrix}. \tag{3.117}$$

It should be noted that this equation is valid only for the front left quarter of the vehicle. The transformation matrices belonging to the other quarters can be obtained by changing the subscripts.

Considering Assumption 3.14,

$$T_{S1/SML} = \begin{bmatrix} 1 & 0 & 0 \\ 0 & \cos\phi & \sin\phi \\ 0 & -\sin\phi & \cos\phi \end{bmatrix} \begin{bmatrix} \cos\theta & 0 & -\sin\theta \\ 0 & 1 & 0 \\ \sin\theta & 0 & \cos\theta \end{bmatrix}, \tag{3.118}$$

$$T_{S2/SML} = T_{S1/SML}, \tag{3.119}$$

$$T_{S3/SML} = T_{S1/SML}, \tag{3.120}$$

$$T_{S4/SML} = T_{S1/SML}. \tag{3.121}$$

Remembering Equation (A.10),

$$T_{SML/S1} = {T_{S1/SML}}^T. \tag{3.122}$$

Since the front left sliding mass and the front left suspension make exactly the same rotation, $T_{SM1/S1}$ is an identity matrix; which follows

$$T_{WK1/SML} = T_{S1/SML} T_{WK1/SM1}. \tag{3.123}$$

Writing for the other quarters using Equations (3.119), (3.120) and (3.121),

$$T_{WK2/SML} = T_{S1/SML} T_{WK2/SM2}, \tag{3.124}$$

$$T_{WK3/SML} = T_{S1/SML} T_{WK3/SM3}, \tag{3.125}$$

$$T_{WK4/SML} = T_{S1/SML} T_{WK4/SM4}. \tag{3.126}$$

Remembering Equation (A.10) again,

$$T_{SML/WK1} = {T_{WK1/SML}}^T, \tag{3.127}$$

$$T_{SML/WK2} = {T_{WK2/SML}}^T, \tag{3.128}$$

$$T_{SML/WK3} = {T_{WK3/SML}}^T, \tag{3.129}$$

$$T_{SML/WK4} = {T_{WK4/SML}}^T. \tag{3.130}$$

Now that the transformation matrices are found, all of the required vector trans-

formations are written as

$$\begin{bmatrix} F_{SML/S1_x} \\ F_{SML/S1_y} \\ F_{SML/S1_z} \end{bmatrix} = T_{WK1/SML} \begin{bmatrix} F_{SML/S1_{x_1}} \\ F_{SML/S1_{y_1}} \\ F_{SML/S1_{z_1}} \end{bmatrix}, \tag{3.131}$$

$$\begin{bmatrix} F_{SML/Ext_x} \\ F_{SML/Ext_y} \\ F_{SML/Ext_z} \end{bmatrix} = T_{S1/SML} \begin{bmatrix} F_{SML/Ext_{x_{S1}}} \\ F_{SML/Ext_{y_{S1}}} \\ F_{SML/Ext_{z_{S1}}} \end{bmatrix}, \tag{3.132}$$

$$\begin{bmatrix} M_{SML/S1_x} \\ M_{SML/S1_y} \\ M_{SML/S1_z} \end{bmatrix} = T_{WK1/SML} \begin{bmatrix} M_{SML/S1_{x_1}} \\ M_{SML/S1_{y_1}} \\ M_{SML/S1_{z_1}} \end{bmatrix}, \tag{3.133}$$

$$\begin{bmatrix} W_{SML_x} \\ W_{SML_y} \\ W_{SML_z} \end{bmatrix} = T_{S1/SML} \begin{bmatrix} W_{SML_{x_{S1}}} \\ W_{SML_{y_{S1}}} \\ W_{SML_{z_{S1}}} \end{bmatrix}, \tag{3.134}$$

$$\begin{bmatrix} p_{E1_{x_1}} \\ p_{E1_{y_1}} \\ p_{E1_{z_1}} \end{bmatrix} = T_{SML/WK1} \begin{bmatrix} p_{E1_x} \\ p_{E1_y} \\ p_{E1_z} \end{bmatrix}, \tag{3.135}$$

$$\begin{bmatrix} v_{E1_{x_1}} \\ v_{E1_{y_1}} \\ v_{E1_{z_1}} \end{bmatrix} = T_{SML/WK1} \begin{bmatrix} v_{E1_x} \\ v_{E1_y} \\ v_{E1_z} \end{bmatrix}, \tag{3.136}$$

$$\begin{bmatrix} v_{SML_{x_{S1}}} \\ v_{SML_{y_{S1}}} \\ v_{SML_{z_{S1}}} \end{bmatrix} = T_{SML/S1} \begin{bmatrix} v_{SML_x} \\ v_{SML_y} \\ v_{SML_z} \end{bmatrix}, \tag{3.137}$$

$$\begin{bmatrix} a_{E1_{x_1}} \\ a_{E1_{y_1}} \\ a_{E1_{z_1}} \end{bmatrix} = T_{SML/WK1} \begin{bmatrix} a_{E1_x} \\ a_{E1_y} \\ a_{E1_z} \end{bmatrix}, \tag{3.138}$$

$$\begin{bmatrix} a_{SML_{x_{S1}}} \\ a_{SML_{y_{S1}}} \\ a_{SML_{z_{S1}}} \end{bmatrix} = T_{SML/S1} \begin{bmatrix} a_{SML_x} \\ a_{SML_y} \\ a_{SML_z} \end{bmatrix}. \tag{3.139}$$

Here, it should be noted that Equations (3.131), (3.133), (3.135), (3.136) and (3.138)

are valid only for the front left quarter of the vehicle. The vector transformations belonging to the other quarters can be obtained by changing the subscripts.

3.3.4.14. Inputs. According to the definition of q_1,

$$\delta_1 = q_1 \delta_S. \tag{3.140}$$

If the previous equations are scanned, it is seen that $\dot{\delta}_1$ and $\ddot{\delta}_1$ have to be found also. This is basically done by taking the derivative of Equation (3.140), and the results are as the following:

$$\dot{\delta}_1 = q_1 \dot{\delta}_S \tag{3.141}$$

$$\ddot{\delta}_1 = q_1 \ddot{\delta}_S \tag{3.142}$$

These three equations are valid only for the front left quarter of the vehicle. The equations belonging to the other quarters can be obtained by changing the subscripts.

By looking at Equations (3.140) - (3.142), it is concluded that δ_S, $\dot{\delta}_S$ and $\ddot{\delta}_S$ have to be obtained. This can be accomplished in two ways: Derivation of δ_S or integration of $\ddot{\delta}_S$. In simulations, it is good to avoid derivation. Therefore, integration of $\ddot{\delta}_S$ is preferred, meaning that δ_S and $\dot{\delta}_S$ are calculated using $\ddot{\delta}_S$. The construction of $\ddot{\delta}_S$ signal involves elementary calculus, so it is not explained here.

3.3.4.15. Outputs. $F_{W1/R_{z_1}}$, $F_{W2/R_{z_2}}$, $F_{W3/R_{z_3}}$, $F_{W4/R_{z_4}}$, $F_{SML/Ext_{x_{S1}}}$, $v_{SML_{x_{S1}}}$, $a_{SML_{y_{S1}}}$, δ_S, β, ϕ, θ, ψ and $\dot{\psi}$ are selected as the outputs. Except the side-slip angle, β, all of these variables can be directly taken out of the model. The side-slip angle is found as

$$\beta = \text{atan2}\left(v_{SML_{y_{S1}}}, v_{SML_{x_{S1}}}\right). \tag{3.143}$$

3.4. Modeling in Simulink

Since the simulation of the vehicle is about the case in which the vehicle moves, equations in Section 3.3.4 are used to prepare the model. The details about the equations are covered in Section 3.3.4, so they are not discussed again. Beyond equations, there are some facts which have to be considered while preparing the model. In this section, these facts are explained.

While preparing the model in Simulink, grouping the blocks makes it easy to handle the whole model. Of course, grouping is done according to the specifications of the equations. The primary groups are set according to the grouping done in Section 3.3.4. "Road - Wheels", "Suspensions", "External Force" and "Inputs" are some examples for the primary groups. Grouping in the secondary level is done according to the types of the equations. "Force Balance Equations", "Moment Balance Equations" and "Kinematic Relations" are some examples for the secondary groups.

According to Section 3.3.4.1, Magic Formula, which is the tyre model used, receives the vertical components of the forces on wheels as inputs. The horizontal components of the forces on wheels, on the other hand, are returned as outputs. This fact makes it necessary to make a distinction between the components of the forces on wheels. As the result, signals belonging to vertical and horizontal components flow in opposite directions in the model. This is a fact which has to be kept in mind while working with the model.

As a result of the nature of the relation between the road and the wheels, the vertical components of the forces on the wheels from the road can not be in the downward direction. Therefore, the nonlinear model is modified so that if one of the vertical components is downward, the simulation stops.

As stated before, the model involves nonlinearities which are due to the suspensions and the interaction between road and wheels. These nonlinearities are integrated into the model by means of lookup tables. Using lookup tables is the best choice be-

cause their negative effect on the performance of the model is small. The data for lookup tables are prepared before simulation. During simulation, lookup tables use the data to return results; and the results are used in other equations in the model.

Different maneuver types are included in the nonlinear model as input. They are namely “step”, “cornering”, “lane change”, “ramp”, “sine wave” and “custom” maneuvers.

4. SINGLE TRACK MODEL

The Single Track Model is a well-known approach in the vehicle dynamics literature. The simplicity of the model is a very important advantage. Due to its simplicity, the simulations run faster and it is very easy to diagnose for incidental mistakes. Despite the simplicity of the model, the obtained results do not differ from the results of a more complicated model too much. In these aspects, this approach is considered to be useful.

The definitions used in this section differ a bit, therefore they are explained in detail in the first part. In the second part, assumptions are discussed. Next, the equations of motion are presented. Finally, modeling in Simulink is discussed.

4.1. Definitions

It is very beneficial to make the definitions before starting to work with the Single Track Model. The definitions used in the Single Track Model are a little bit different, so all of them are explained in detail. To make it easier to understand, the definitions are discussed in the following order: Points, coordinate frames, masses, inertia components, lengths, velocities, accelerations, angles, angular velocities, forces and other constants.

Point O is a fixed point which is on the road surface. The center of gravity of the vehicle is represented with point G. Points F and R stand for the contact points of the front and rear wheels with the road, respectively. These points are seen in Figure 4.1 on page 56.

The $OXYZ$ coordinate frame is the fixed or reference coordinate frame. Its origin is at point O. The X and Y axes are on the road surface. The Z axis points the upward direction. The $Gxyz$ coordinate frame is attached to the vehicle and its origin is at point G. The x, y and z axes point the vehicle forward, left and upward directions, respectively. The $Fx_Fy_Fz_F$ coordinate frame is attached to the front wheel knuckle

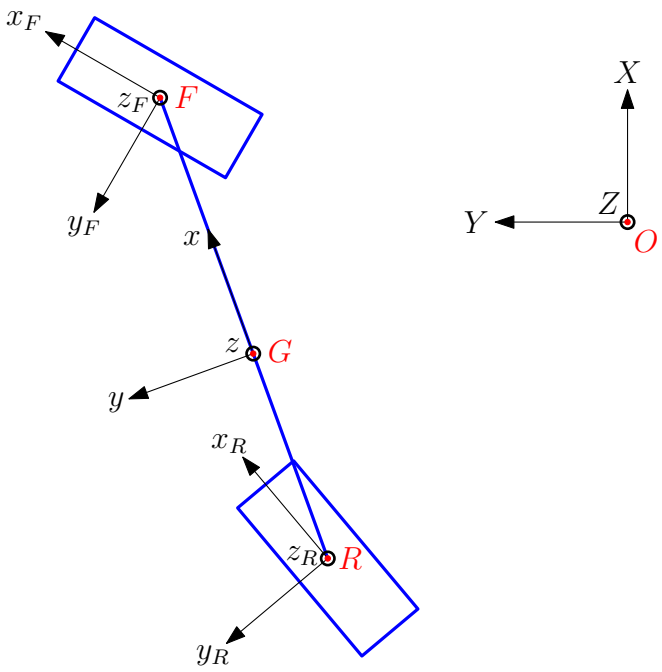

Figure 4.1. Representation of the points and the coordinate frames used in the Single Track Model

which means that it does not spin with the front wheel. Its origin is at point F. The x_F and y_F axes point the front wheel forward and left directions, respectively. The z_F axis points the vehicle upward direction. The $Rx_Ry_Rz_R$ coordinate frame is attached to the rear wheel knuckle which means that it does not spin with the rear wheel. Its origin is at point R. The x_R and y_R axes point the rear wheel forward and left directions, respectively. The z_R axis points the vehicle upward direction. These coordinate frames are seen in Figure 4.1.

m stands for the mass of the vehicle.

I_x, I_y, I_z, I_{xy}, I_{xz}, I_{yz} stand for the inertia components of the vehicle with respect to the $Gxyz$ coordinate frame. They are calculated according to Section A.4.1.1.

l_F stands for the length between the contact point of the front wheel with the road (point F) and the vehicle center of gravity (point G). l_R stands for the length between the contact point of the rear wheel with the road (point R) and the vehicle center of gravity (point G). They are seen in Figure 4.2 on page 57.

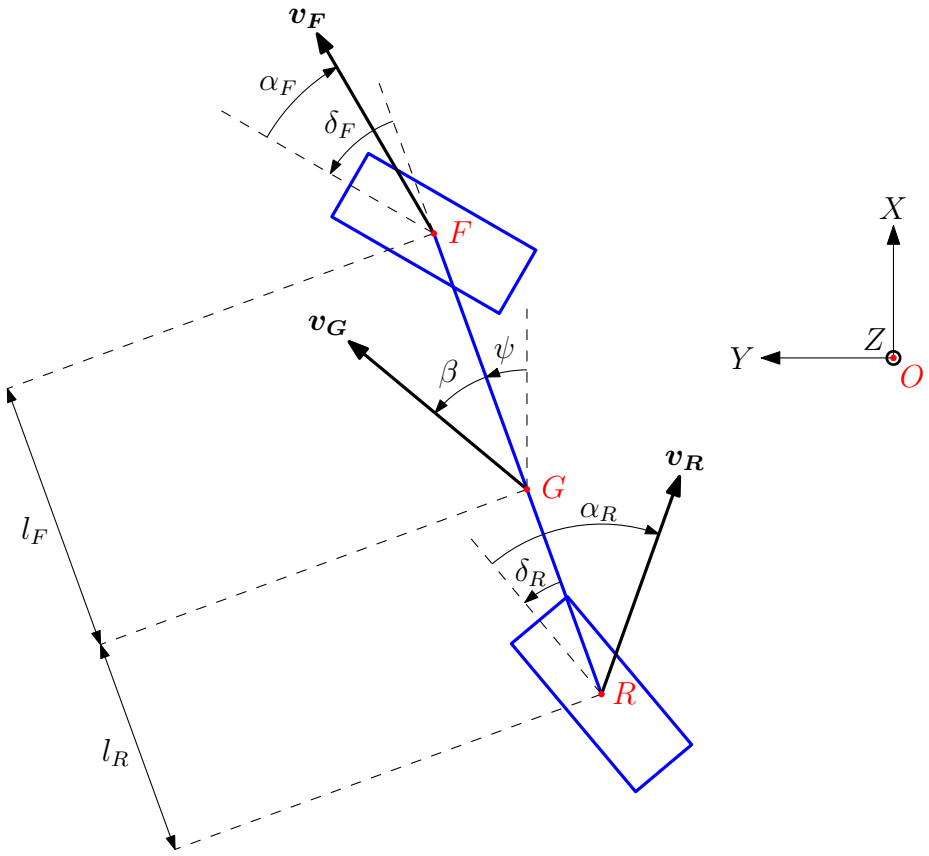

Figure 4.2. Representation of the lengths, velocities and angles used in the Single Track Model (Angles are shown in the positive direction.)

$\boldsymbol{v_G}$ stands for the velocity of the vehicle center of gravity (point G) with respect to the origin of the fixed coordinate frame (point O). $\boldsymbol{v_F}$ stands for the velocity of the contact point of the front wheel with the road (point F) with respect to the origin of the fixed coordinate frame (point O). $\boldsymbol{v_R}$ stands for the velocity of the contact point of the rear wheel with the road (point R) with respect to the origin of the fixed coordinate frame (point O). They are seen in Figure 4.2 on page 57.

$\boldsymbol{a_G}$ stands for the acceleration of the vehicle center of gravity (point G) with respect to the origin of the fixed coordinate frame (point O).

ψ stands for the yaw angle which is measured with respect to the X axis. A positive value means that the vehicle corners to the left whereas a negative value means that the vehicle corners to the right. δ_F stands for the front wheel steering angle which is measured with respect to the x axis. A positive value means that the wheel is turned to the left whereas a negative value means that the wheel is turned to the right. δ_R stands for the rear wheel steering angle which is measured with respect to the x axis. A positive value means that the wheel is turned to the left whereas a negative value means that the wheel is turned to the right. β stands for the side-slip angle which is measured with respect to the x axis. A positive value represents a counter-clockwise direction whereas a negative value represents a clockwise direction. α_F stands for the front wheel side-slip angle which is measured with respect to the x_F axis. A positive value represents a clockwise direction whereas a negative value represents a counter-clockwise direction. α_R stands for the rear wheel side-slip angle which is measured with respect to the x_R axis. A positive value represents a clockwise direction whereas a negative value represents a counter-clockwise direction. These angles are seen in Figure 4.2 on page 57. In addition, δ_S stands for the steering wheel angle. A positive value means that the vehicle corners to the left whereas a negative value means that the vehicle corners to the right.

$\boldsymbol{\omega}$ stands for the angular velocity of the vehicle with respect to the $OXYZ$ coordinate frame. According to the assumptions, the only component of the angular velocity of the vehicle is the yaw rate $\dot{\psi}$ which is shown in Figure 4.3 on page 59.

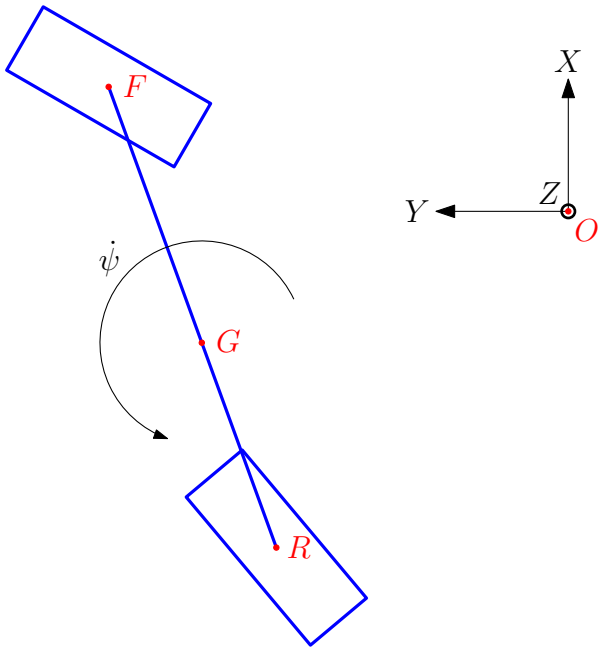

Figure 4.3. Top view of the Single Track Model while performing yaw

$\boldsymbol{F_F}$ and $\boldsymbol{F_R}$ stand for the forces on the front and rear wheels from the road, respectively. $\boldsymbol{W}$ represents the weight of the vehicle.

c_F and c_R stand for the linear tire stiffness parameters of the front and rear wheels, respectively. They are positive quantities. q_F and q_R stand for the front and rear steering coefficient, respectively. They are positive quantities.

4.2. Assumptions

Assumptions are treated in two parts: Starting assumptions and internal assumptions. It is very important to note that there is no functional difference between these two groups of assumptions. This classification is done only to emphasize that some assumptions are made when necessary (internal assumptions) while others are made before starting to work with the equations (starting assumptions).

4.2.1. Starting Assumptions

Assumption 4.1. The road is flat and even.

Assumption 4.2. Initially, the vehicle moves along the X axis in a straight and stable manner.

Assumption 4.3. There is no drag force applied on the vehicle. As a result of this assumption, wind effects are also neglected.

Assumption 4.4. No moments are applied on the wheels from the road.

Assumption 4.5. Vehicle center of gravity (point G) is on the road level.

Assumption 4.6. The vehicle does not perform roll and pitch.

Assumption 4.7. The inertia components I_{xz} and I_{yz} are equal to zero.

Assumption 4.8. The wheel longitudinal axis components of the forces, which are applied on the wheels from the road, are zero.

Assumption 4.9. The wheel lateral axis components of the forces, which are applied on the wheels from the road, are proportional to the wheel side-slip angles.

4.2.2. Internal Assumptions

Assumption 4.10. Side-slip angle is small.

Assumption 4.11. Front wheel side-slip angle is small.

Assumption 4.12. Rear wheel side-slip angle is small.

Assumption 4.13. Front wheel steering angle is small.

Assumption 4.14. Rear wheel steering angle is small.

Assumption 4.15. The vehicle longitudinal axis component of the velocity is constant.

Assumption 4.16. The vehicle does not perform bounce.

4.3. Equations of Motion

The derivation of the equations of motion of the Single Track Model is explained in detail in Section C. Therefore, details of the derivation are not discussed again in this section. The necessary equations are selected from Section C and included here.

The main subject of this study is the estimation of the side-slip angle β using the yaw rate $\dot{\psi}$. So, in the state-space description, the state variables are β and $\dot{\psi}$. In addition, the vehicle in concern is front steered. Equation (C.62) describes this case. Rewriting this equation yields

$$\dot{x} = \begin{bmatrix} -\frac{c_F+c_R}{mv_{G_x}} & \frac{c_R l_R - c_F l_F}{m{v_{G_x}}^2} - 1 \\ \frac{c_R l_R - c_F l_F}{I_z} & -\frac{c_R {l_R}^2 + c_F {l_F}^2}{I_z v_{G_x}} \end{bmatrix} x + \begin{bmatrix} \frac{c_F}{mv_{G_x}} \\ \frac{c_F l_F}{I_z} \end{bmatrix} u \tag{4.1}$$

where

$$x = \begin{bmatrix} \beta \\ \dot{\psi} \end{bmatrix} \tag{4.2}$$

and

$$u = \delta_F. \tag{4.3}$$

If the output is selected as the side-slip angle β, it is represented with the equation

$$y = \begin{bmatrix} 1 & 0 \end{bmatrix} x. \tag{4.4}$$

If it is selected as the yaw rate $\dot{\psi}$, it is represented with the equation

$$y = \begin{bmatrix} 0 & 1 \end{bmatrix} x. \tag{4.5}$$

4.4. Modeling in Simulink

To be able to obtain results, a Simulink model is created using the equations of motion of the Single Track Model. In addition to the equations of motion, some other facts have to be discussed to be able to create the model. In this section, these facts are explained.

Since the Simulink model involves integration blocks, the initial conditions of some of the variables have to be known. Assumption 4.2 is adequate to determine the initial conditions as the following:

$$\delta_S = 0 \tag{4.6}$$

$$\dot{\delta}_S = 0 \tag{4.7}$$

$$\ddot{\delta}_S = 0 \tag{4.8}$$

$$\beta = 0 \tag{4.9}$$

$$\psi = 0 \tag{4.10}$$

$$\dot{\psi} = 0 \tag{4.11}$$

In Section 4.3, the equations of motion for the front steered case are represented. However, the front and rear steered case is used in the Simulink model. This is done because the model is easily converted to the front steered case by setting the rear steering coefficient to zero.

To make the model more realistic, the input is introduced to the model in terms of the steering wheel angle. Because of that, the relation between the steering wheel angle and the wheel steering angles has to be defined. This is easily done as the following:

$$\delta_F = \delta_S q_F \tag{4.12}$$

$$\delta_R = \delta_S q_R \tag{4.13}$$

Also, different maneuver types are included in the model as input. They are namely “step”, “cornering”, “lane change”, “ramp”, “sine wave” and “custom” maneuvers.

5. PARAMETER VALUES OF THE NONLINEAR MODEL

In this section, parameter values of the vehicle, which is used with the nonlinear model, are set. Vehicle data are provided in terms of MSC Adams/Car data. Results of a simulation, which is done under certain conditions using MSC Adams/Car, are also provided. However, some of the parameter values have to be set again because the nonlinear model and MSC Adams/Car do not behave exactly same. Here, the aim is to make the simulation results as close as possible by changing some of the parameter values. Obviously, this involves a lot of trials.

First, conditions which are set while obtaining the provided simulation results have to be known. The only loads on the vehicle are the two front passengers and the fuel. By looking at the provided graphs, it is seen that the longitudinal velocity is 59.841 km/h when the maneuvering starts. This is seen in Figure 5.7 on page 68. By looking at this figure, it is also concluded that the longitudinal velocity is not kept constant. Therefore, the constants of the PI controller (C_I and C_P) are set to zero in the nonlinear model. The information about the steering is also important. The type of the steering input is step. Initially, the steering wheel angle is zero degrees. When the simulation time is two seconds, the steering wheel angle is changed to 45° in 0.2 s. This is also seen in Figure 5.1 on page 64.

Next, it is necessary to discuss which parameter values are changed to make the simulation results similar. Primary parameters such as masses, inertias, positions, suspension parameters and tyre parameters are not used in this work. The selected parameters are h_1, h_2, h_3, h_4, l, n_1, n_2, n_3 and n_4. The values of these parameters are changed and the simulation results are investigated.

Before making trials and trying to fit the results, the effects of parameter variations on the results have to be studied. If the effects are known, it becomes easier to select the parameter value to be changed; saving a lot of time. Here, each parameter value is changed and the changes in the simulation results are compared. The

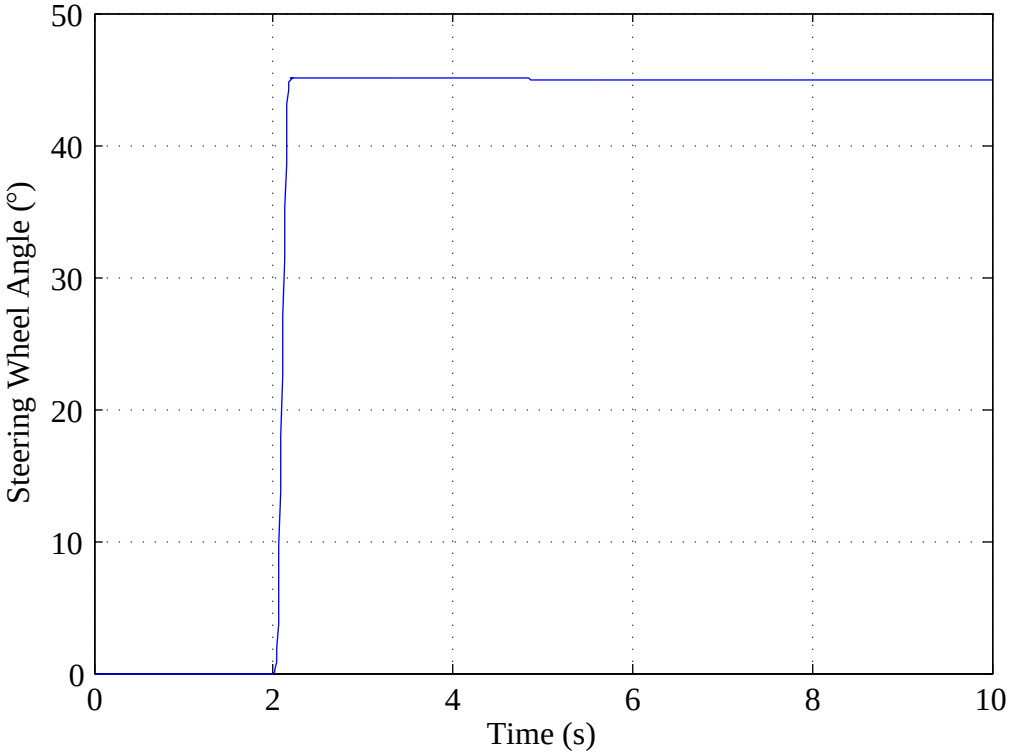

Figure 5.1. The steering wheel input

details are not explained because a lot of trials are done and representing them here is impossible. Among the selected parameters, l seems to be the most dominant one. The lateral acceleration, side-slip angle and yaw rate curves are mostly affected by the changes in l. When the vertical forces on wheels are considered, it is seen that changes in l, n_1, n_2, n_3 and n_4 affect the curves in the same amount. When the roll angle is considered, the domination of n_1, n_2, n_3 and n_4 is seen. It is seen that the roll angle curve is affected mostly by the variations in these parameters.

Analyzing the effects of parameter variations on the results makes it possible to define a method. First of all, the lateral acceleration, side-slip angle and yaw rate curves are fitted by varying l. After some trials, the value selected for l is 3000 mm. The results are seen in Figures 5.2, 5.3 and 5.4 on pages 65, 65 and 66, respectively.

Then, the roll angle curve is fitted by varying n_1, n_2, n_3 and n_4. This is seen in

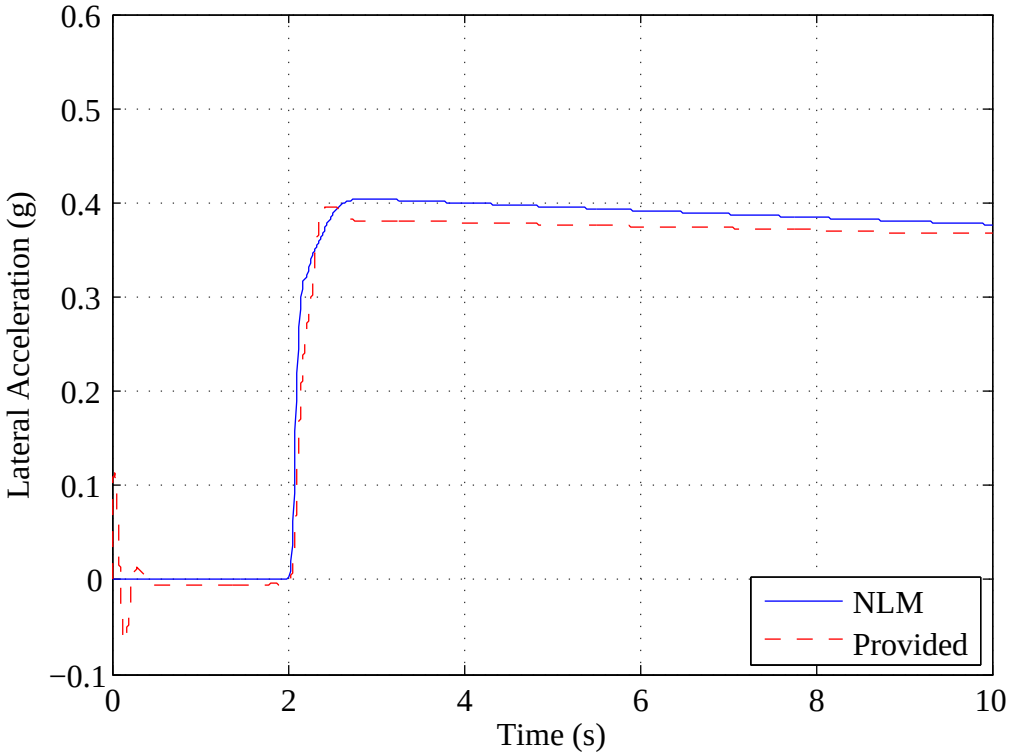

Figure 5.2. Lateral acceleration curves obtained from the nonlinear model and the provided results

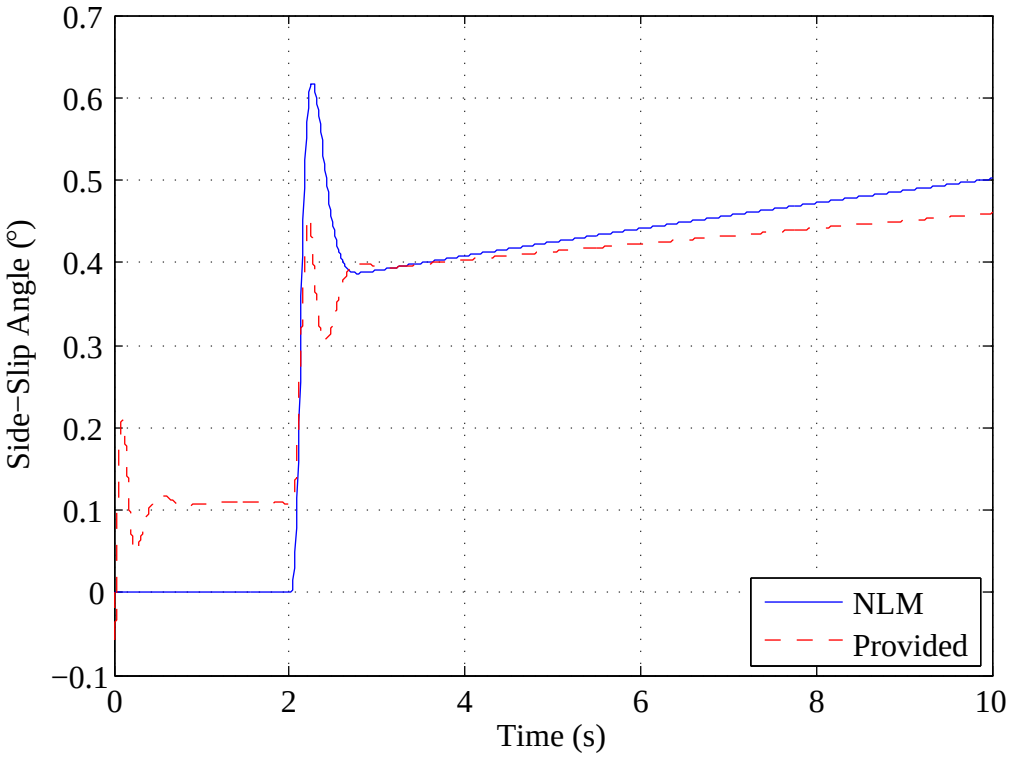

Figure 5.3. Side-slip angle curves obtained from the nonlinear model and the provided results

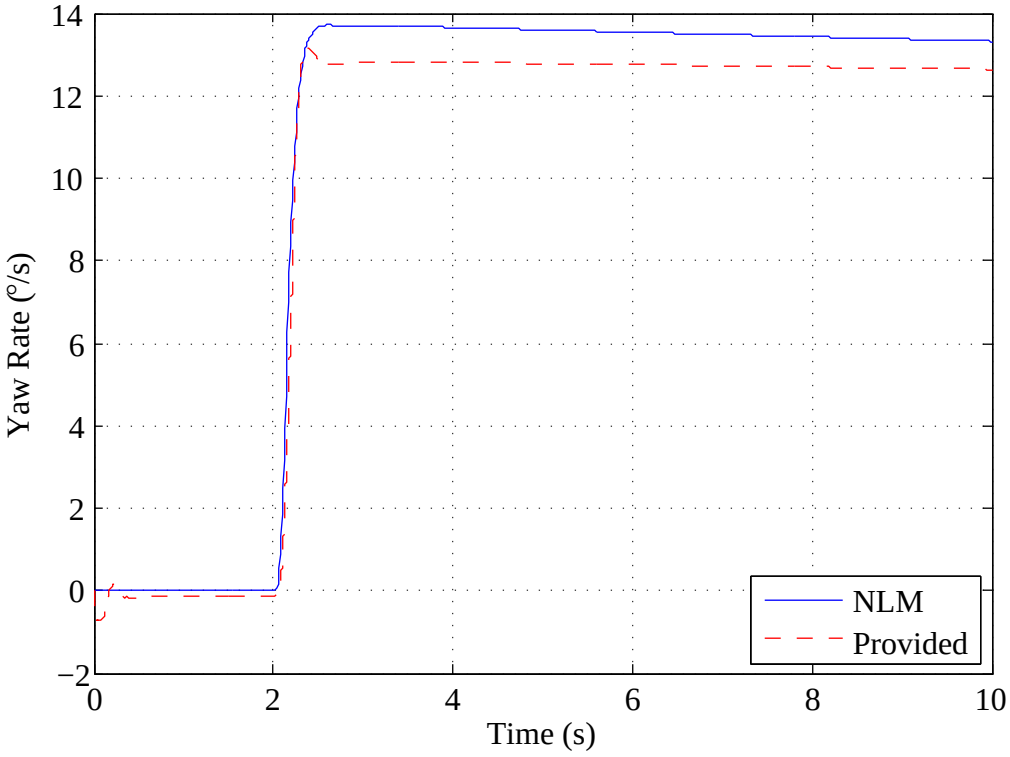

Figure 5.4. Yaw rate curves obtained from the nonlinear model and the provided results

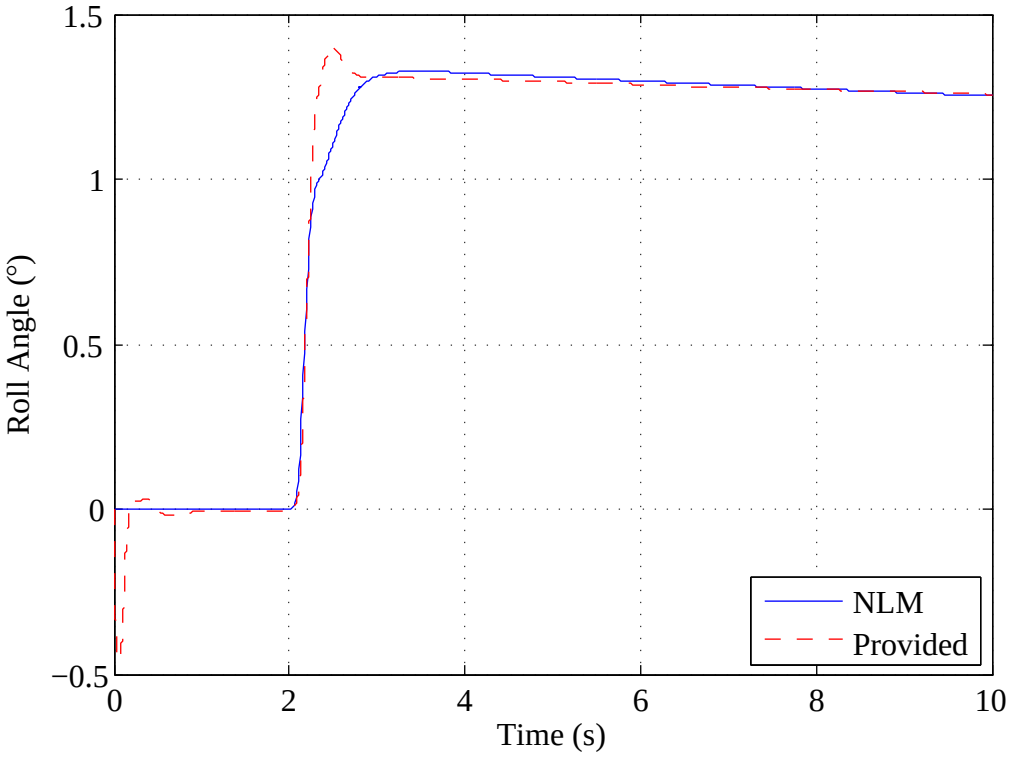

Figure 5.5. Roll angle curves obtained from the nonlinear model and the provided results

Figure 5.5 on page 66. The selected value for these parameters is -280 mm.

Finally, the minor changes are obtained by varying h_1, h_2, h_3 and h_4. The value of these parameters is 320 mm. The curves of vertical forces on wheels and longitudinal velocity are included too. They are seen in Figure 5.6 and in Figure 5.7 on page 68.

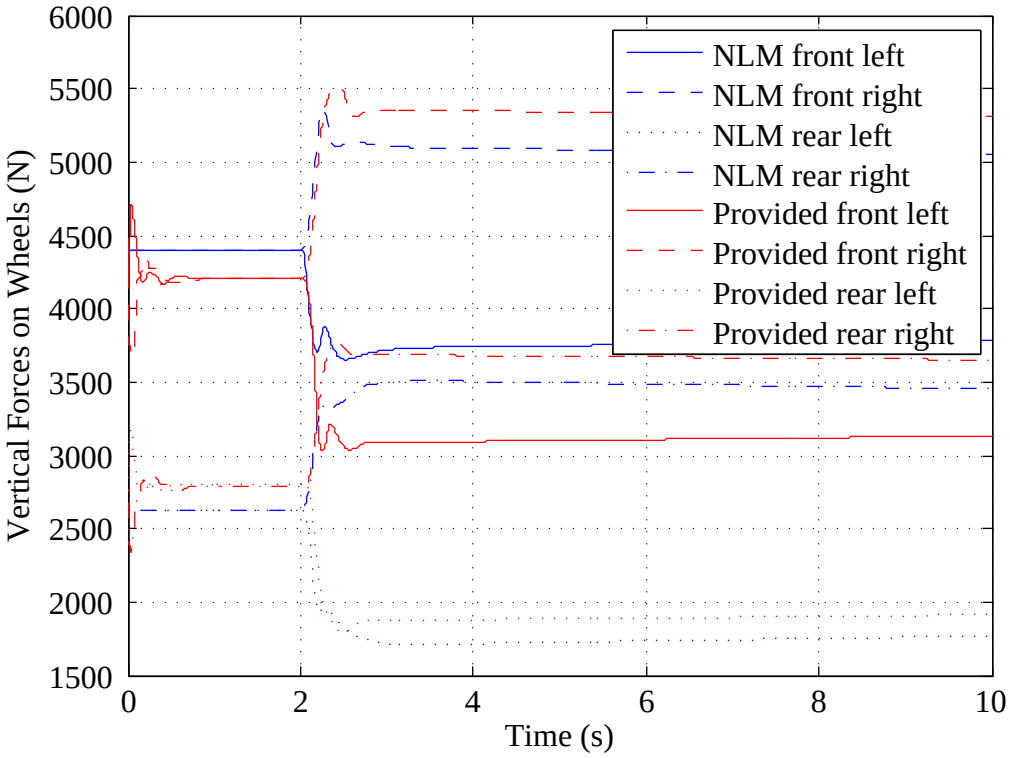

Figure 5.6. Curves of the vertical forces on wheels obtained from the nonlinear model and the provided results

Because of the structural differences between the nonlinear model and the MSC Adams/Car software, exact fit of the curves is not possible. However, the results are satisfactory. The shifts in the curves of the vertical forces are due to the difference in load distribution. The distribution of the load on the front and rear wheels is dependent on the parameters, especially l. Since the parameter values show differences, the shifts are expected. Both curves representing the side-slip angles do not reach steady-states until the simulations end. This is due to the decreasing longitudinal velocity of the vehicle.

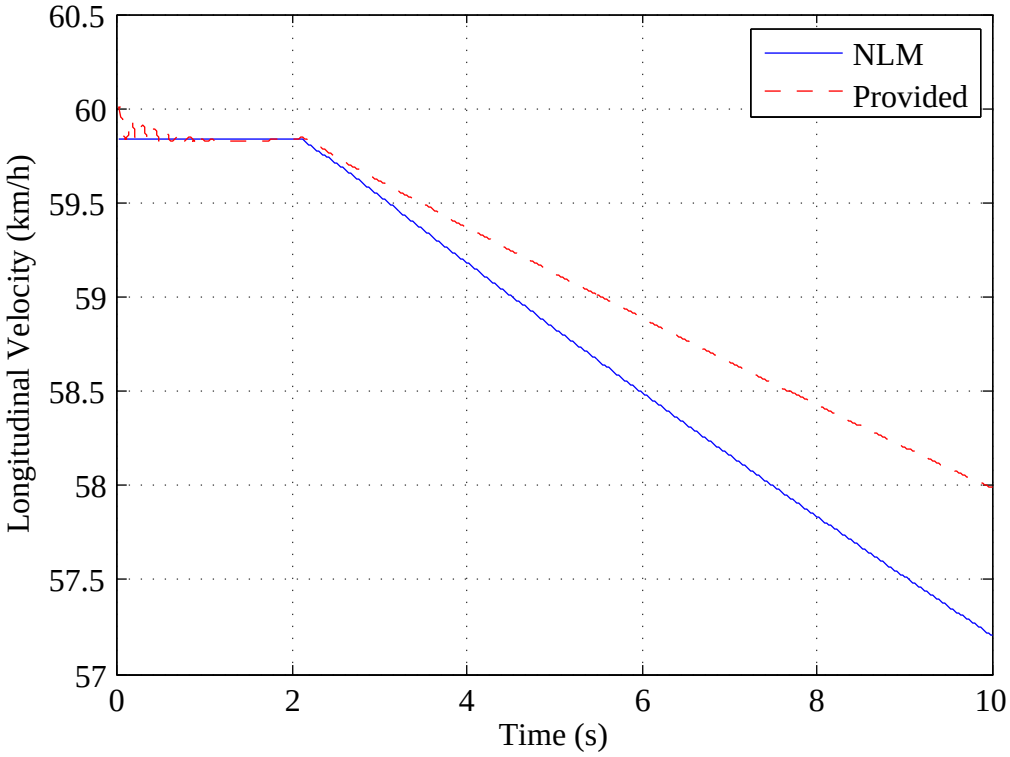

Figure 5.7. Longitudinal velocity curves obtained from the nonlinear model and the provided results

6. PARAMETER VALUES OF THE SINGLE TRACK MODEL

Previously, the parameter values of the vehicle, which is used with the nonlinear model, are set. In this section, a set of parameter values is found for the vehicle which is used with the Single Track Model. The parameter values have to be set so that the nonlinear model and the Single Track Model generate similar outputs for the same inputs. For this purpose, a constrained nonlinear optimization algorithm is used and the parameter values for the Single Track Model are obtained. Then, the responses of the two models are compared by means of bode plots. Finally, the models are fed with the same inputs and their outputs are compared.

In the Single Track Model, it is assumed that the vehicle longitudinal axis component of the velocity is constant. The behavior of the nonlinear model has to be similar. To provide this, the constants of the PI controller have to be set in the nonlinear model. After a number of trials, it is found that 300000 N/m and 13000 Ns/m are appropriate values for C_I and C_P, respectively. Also, the longitudinal velocity is set to 60 km/h in both of the models. It is also necessary to remind the loading condition of the vehicle which is used in the nonlinear model. The only loads on that vehicle are the two front passengers and the fuel. Since the Single Track Model is used in this section, the definitions made in Section 4 are also valid here.

The state-space description of the Single Track Model is as the following:

$$\dot{x} = Ax + Bu \tag{6.1}$$

$$y = Cx + Du \tag{6.2}$$

Here, it is beneficial to remind that

$$x = \begin{bmatrix} \beta \\ \dot{\psi} \end{bmatrix}, \tag{6.3}$$

$$u = \delta_F. \tag{6.4}$$

The side-slip angle β and the yaw rate $\dot{\psi}$ are outputs for both of the models. Therefore, the output is set as

$$y = \begin{bmatrix} \beta \\ \dot{\psi} \end{bmatrix} \tag{6.5}$$

by setting

$$C = \begin{bmatrix} 1 & 0 \\ 0 & 1 \end{bmatrix} \tag{6.6}$$

and

$$D = 0. \tag{6.7}$$

Before using the constrained nonlinear optimization algorithm, the nonlinear model has to be put in the state-space form. To do this, the "linmod" function of MATLAB is used. This function extracts continuous or discrete-time linear state-space model of a system around the operating point. The "linmod" function is executed using the nonlinear model and the matrices A, B, C and D are obtained for the nonlinear model. In addition, it is necessary to check the stability of the obtained state-space model. For this purpose, the eigenvalues of the matrix A are investigated. As the result, it is seen that all of the eigenvalues have negative real parts which means that the stability criterion is satisfied.

Now that both of the models are in the state-space form, it is possible to find the

parameter values of the vehicle which is used with the Single Track Model. The values of the parameters v_{G_x}, m, I_z, c_F, c_R, l_F and l_R have to be found in order to define the Single Track Model completely. The distance between points F and R is set to three m, that is

$$l_F + l_R = 3. \tag{6.8}$$

Also, it is assumed that

$$c_F = c_R. \tag{6.9}$$

For the constrained nonlinear optimization algorithm, the initial values of the remaining parameters have to be supplied. This is done by looking at the parameter values of the vehicle which is used with the nonlinear model. The initial values of the parameters are set as the following:

$$v_{G_x} = 16.6667 \tag{6.10}$$
$$m = 1432.6 \tag{6.11}$$
$$I_z = 2100 \tag{6.12}$$
$$c_F = 94000 \tag{6.13}$$
$$l_F = 1.0679 \tag{6.14}$$

The optimization returns the following values for these parameters:

$$v_{G_x} = 16.76 \tag{6.15}$$
$$m = 903.84 \tag{6.16}$$
$$I_z = 2103.08 \tag{6.17}$$
$$c_F = 94007.99 \tag{6.18}$$
$$l_F = 1.31 \tag{6.19}$$

Simply,

$$l_R = 1.69, \tag{6.20}$$

$$c_R = 94007.99. \tag{6.21}$$

It is also required to check the values of the eigenvalues of the matrix A to see if the system, which is found for the Single Track Model, is stable. All of the eigenvalues have negative real parts which means that the stability criterion is satisfied.

Looking at the bode plots of the obtained systems is useful because bode plots show how systems behave. Bode plots are generated for both of the models in a longitudinal velocity range from 10 km/h to 150 km/h with 10 km/h increments. However, all of the results are not shown here. In the figures, the first output is the side-slip angle β and the second output is the yaw rate $\dot{\psi}$. Figure 6.1 on page 73 shows the bode plots for a longitudinal velocity of 30 km/h. The systems show a little bit of difference in this figure, but this difference is acceptable. Figure 6.2 on page 74 shows the bode plots for a longitudinal velocity of 60 km/h. It is not surprising that the bode plots are very close to each other at 60 km/h. The nonlinear model is linearized at the longitudinal velocity of 60 km/h. Therefore, this condition gives the best result, as it is seen in the figure. Figure 6.3 on page 75 shows the bode plots for a longitudinal velocity of 90 km/h. Again, the bode plots are not coincident. As the longitudinal velocity increases starting from 60 km/h, it is expected that the bode plots separate from each other. Even if the bode plots are not coincident at different longitudinal velocities, it is seen that they are very close to each other at each case. This shows that the values of vehicle parameters used in the Single Track Model are selected correctly.

Also, the bode plots for the nonlinear model and the Single Track Model, which are obtained as the longitudinal velocity changes from 10 km/h to 150 km/h with 10 km/h increments, are included. Figure 6.4 on page 76 and Figure 6.5 on page 77 show these bode plots. By analyzing the similarity of these figures, it is concluded that the

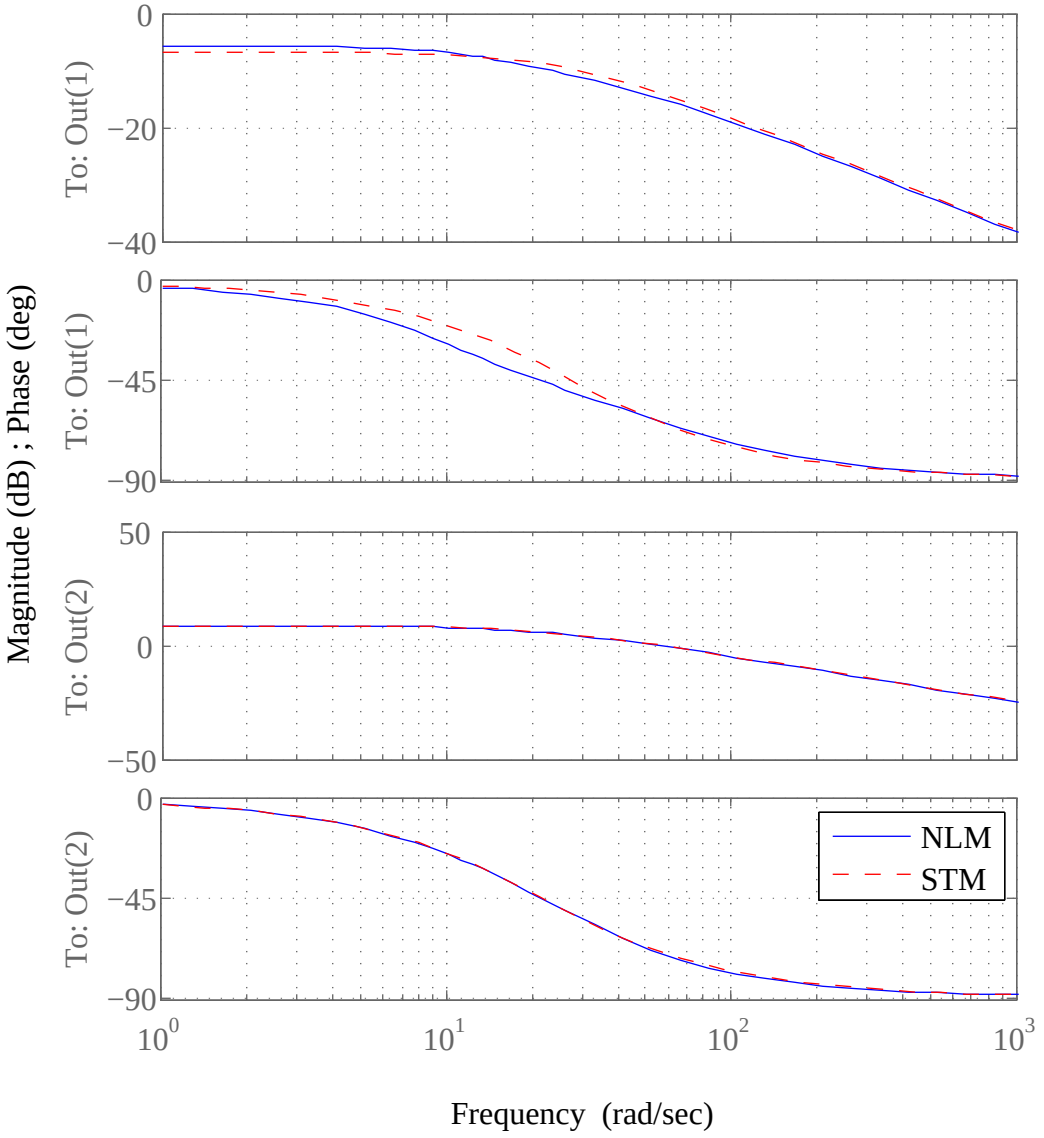

Figure 6.1. The bode plots of the nonlinear model and the Single Track Model at a longitudinal velocity of 30 km/h (The first output is the side-slip angle β and the second output is the yaw rate $\dot{\psi}$.)

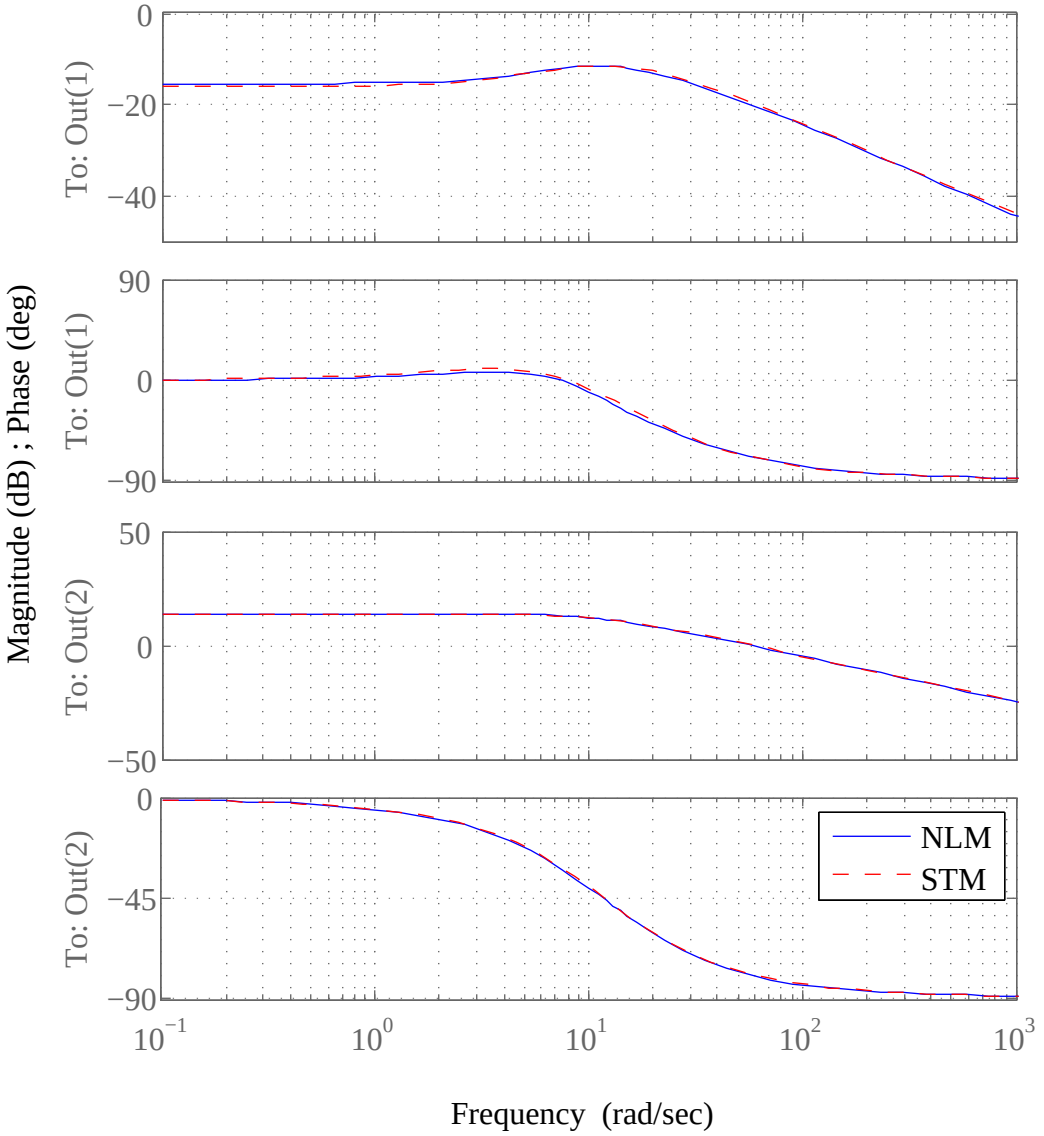

Figure 6.2. The bode plots of the nonlinear model and the Single Track Model at a longitudinal velocity of 60 km/h (The first output is the side-slip angle β and the second output is the yaw rate $\dot{\psi}$.)

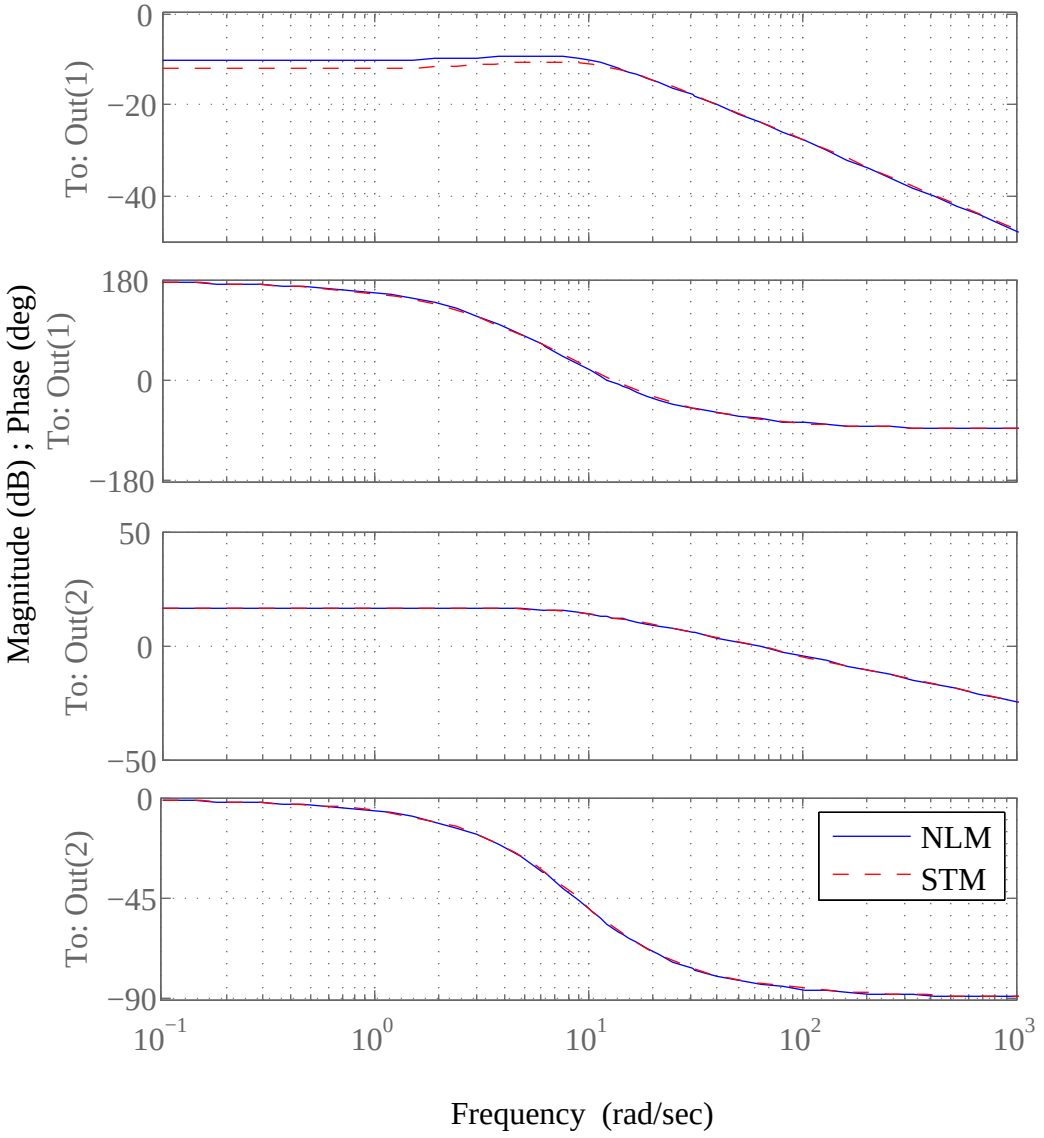

Figure 6.3. The bode plots of the nonlinear model and the Single Track Model at a longitudinal velocity of 90 km/h (The first output is the side-slip angle β and the second output is the yaw rate $\dot{\psi}$.)

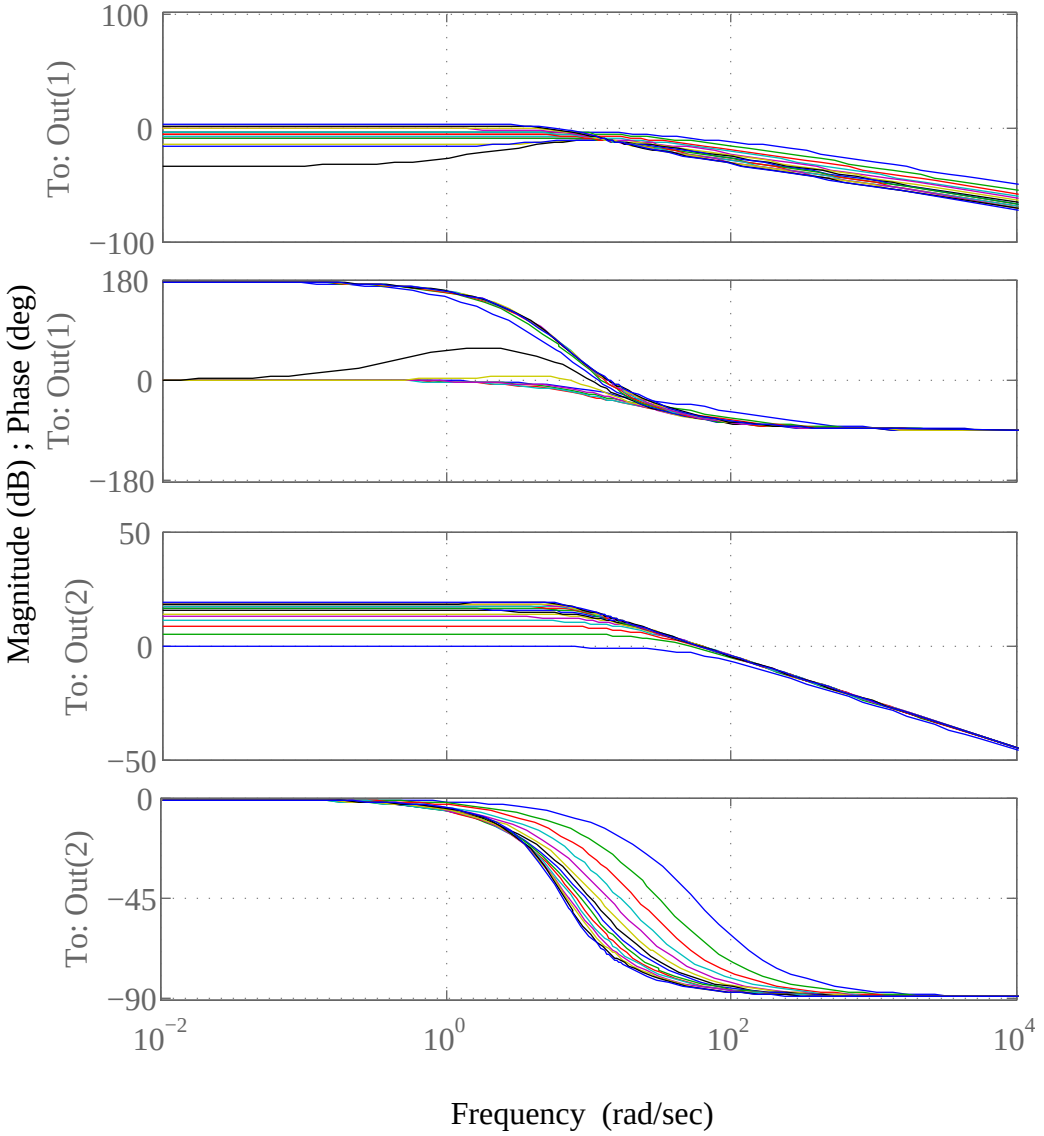

Figure 6.4. The bode plots of the nonlinear model for longitudinal velocities changing from 10 km/h to 150 km/h with 10 km/h increments (The first output is the side-slip angle β and the second output is the yaw rate $\dot{\psi}$.)

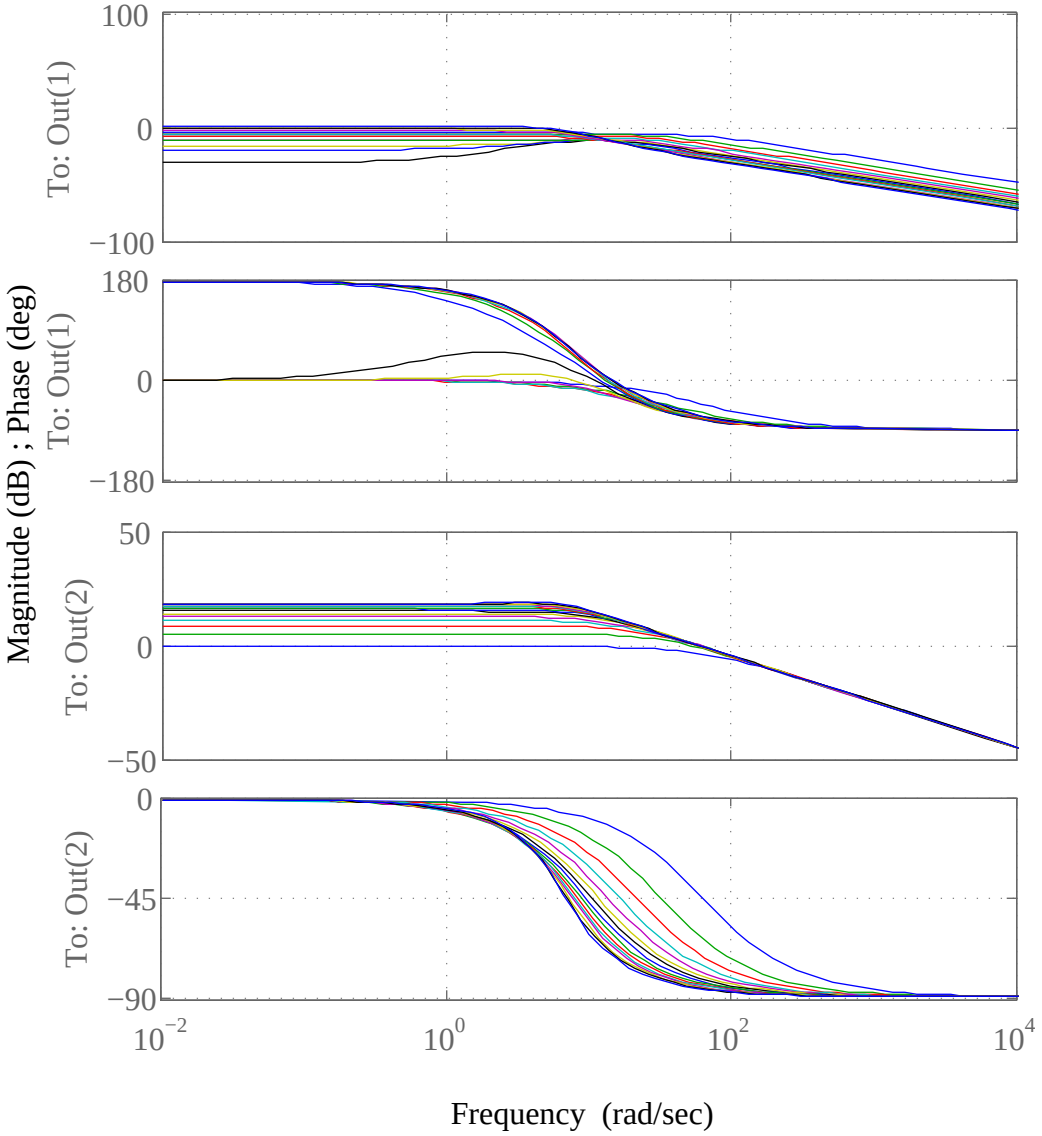

Figure 6.5. The bode plots of the Single Track Model for longitudinal velocities changing from 10 km/h to 150 km/h with 10 km/h increments (The first output is the side-slip angle β and the second output is the yaw rate $\dot{\psi}$.)

values of vehicle parameters used in the Single Track Model are selected correctly.

To further investigate the behaviors of the models, they are simulated with the same steering wheel inputs. The longitudinal velocity is 60 km/h in all of the simulations. In the first set of simulations, steering wheel input is a sine wave with an amplitude of 45° and a period of 2.2 s, which is also seen in Figure 6.6. The results of the simulations are seen in Figure 6.7 and 6.8 on page 79. As seen in these two figures, the side-slip angle and the yaw rate curves are very similar.

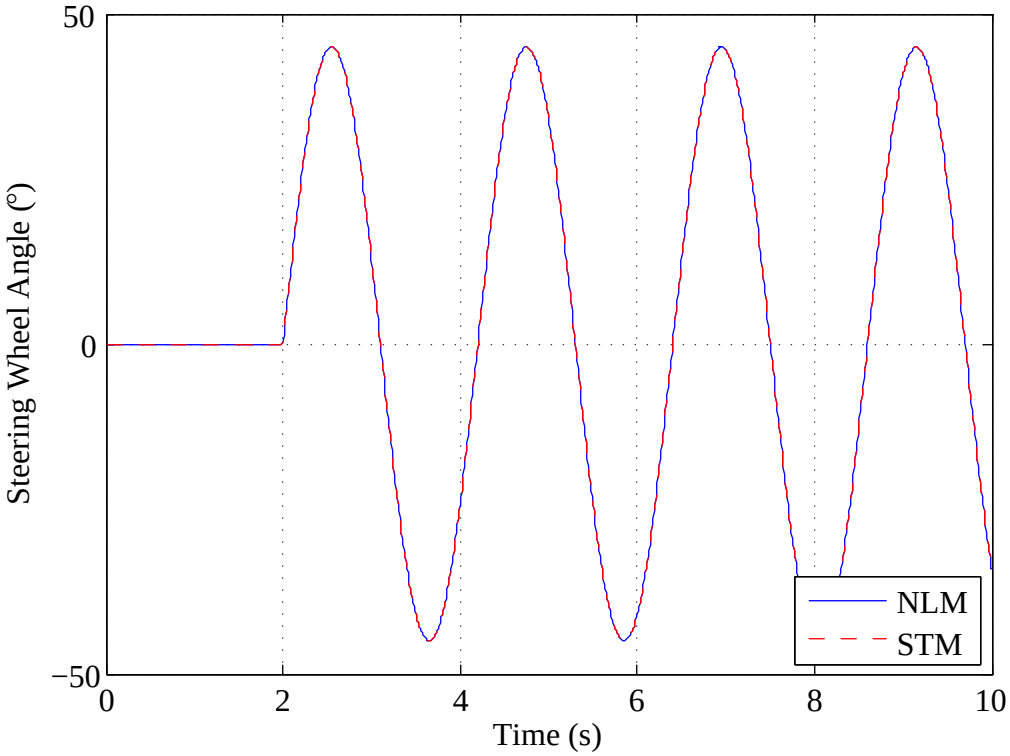

Figure 6.6. The sine wave steering wheel input for the nonlinear model and the Single Track Model

In the second set of simulations, steering wheel input is a step input. The steering wheel angle increases to 45° in 0.2 s, which is also seen in Figure 6.9 on page 80. The results of the simulations are seen in Figure 6.10 on page 80 and in Figure 6.11 on page 81. Side-slip angle curves show slight difference, but this difference is acceptable. On the other hand, the yaw rate curves are very close to each other.

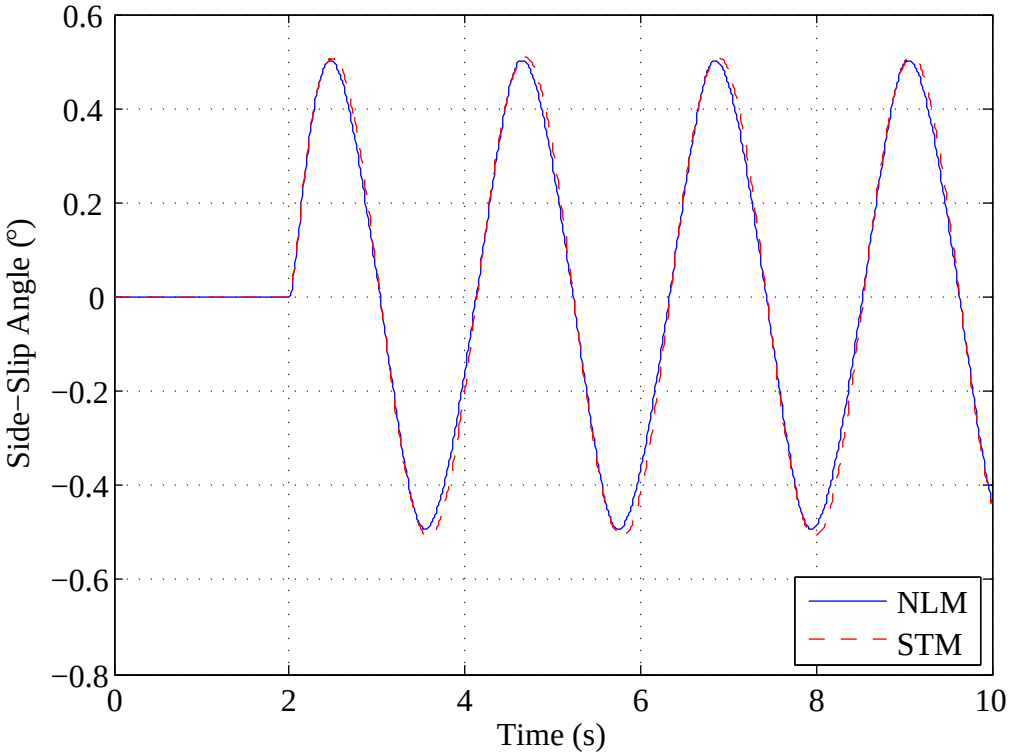

Figure 6.7. The side-slip angles of the nonlinear model and the Single Track Model with the sine wave steering wheel input

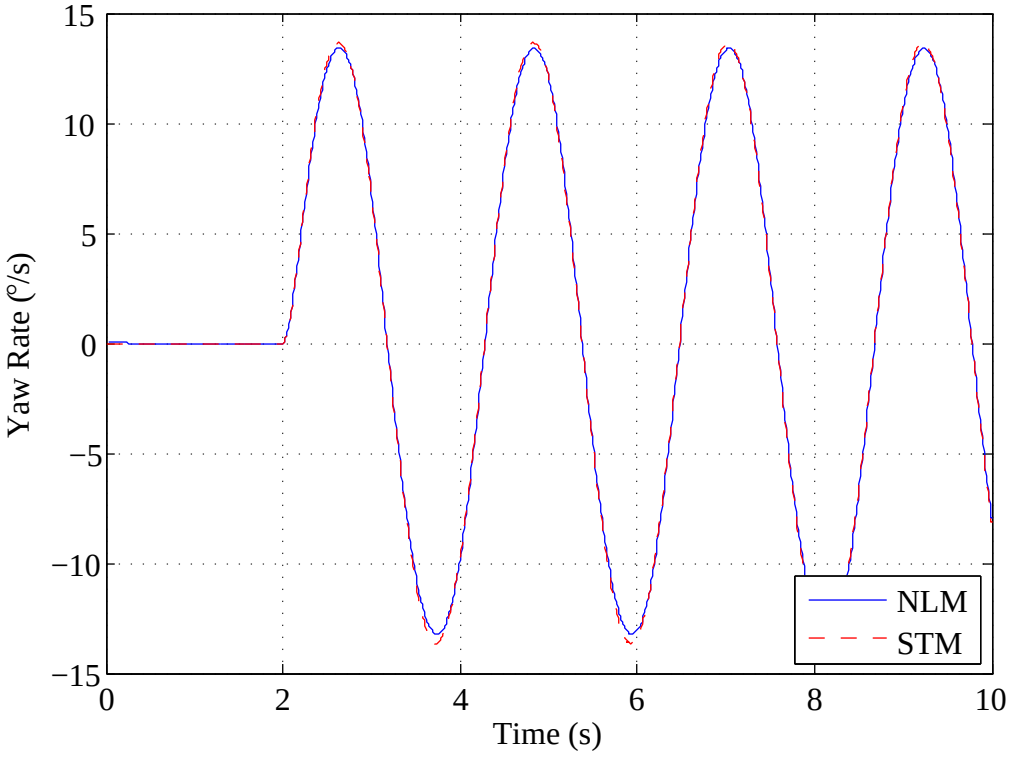

Figure 6.8. The yaw rates of the nonlinear model and the Single Track Model with the sine wave steering wheel input

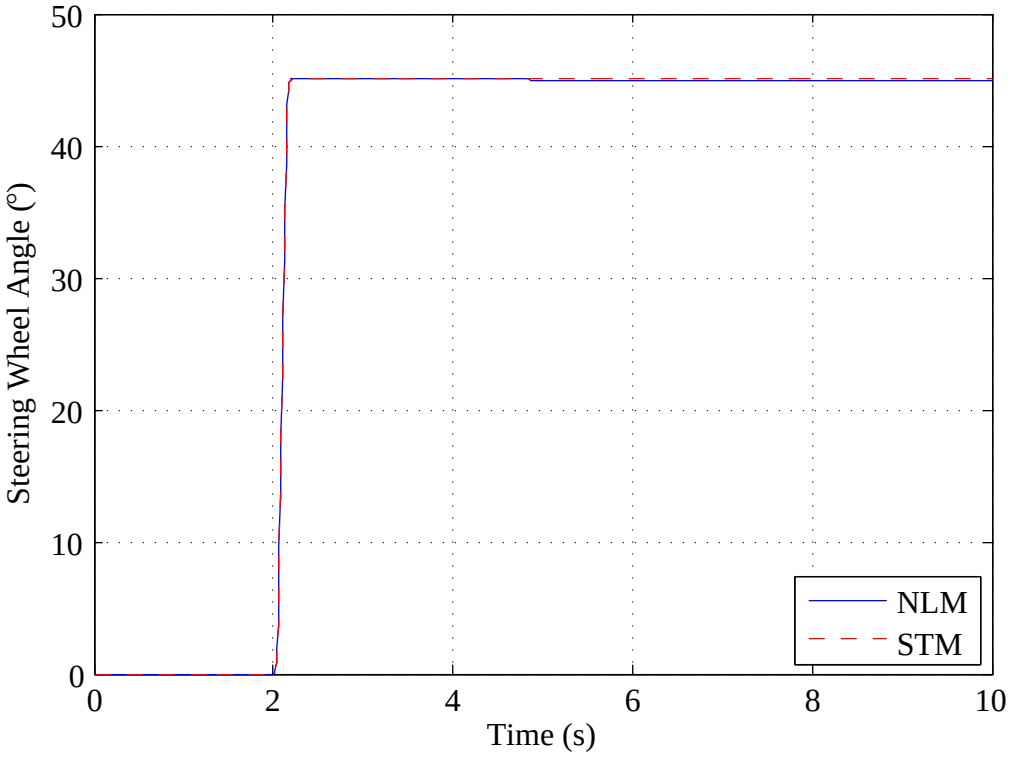

Figure 6.9. The step steering wheel input for the nonlinear model and the Single Track Model

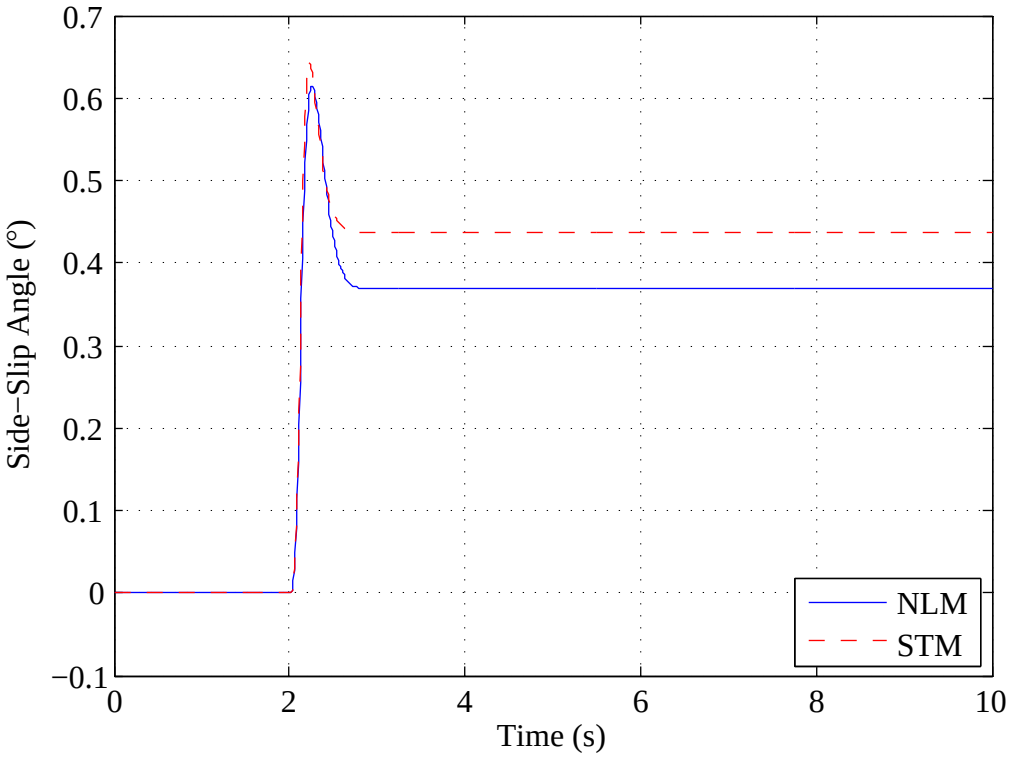

Figure 6.10. The side-slip angles of the nonlinear model and the Single Track Model with the step steering wheel input

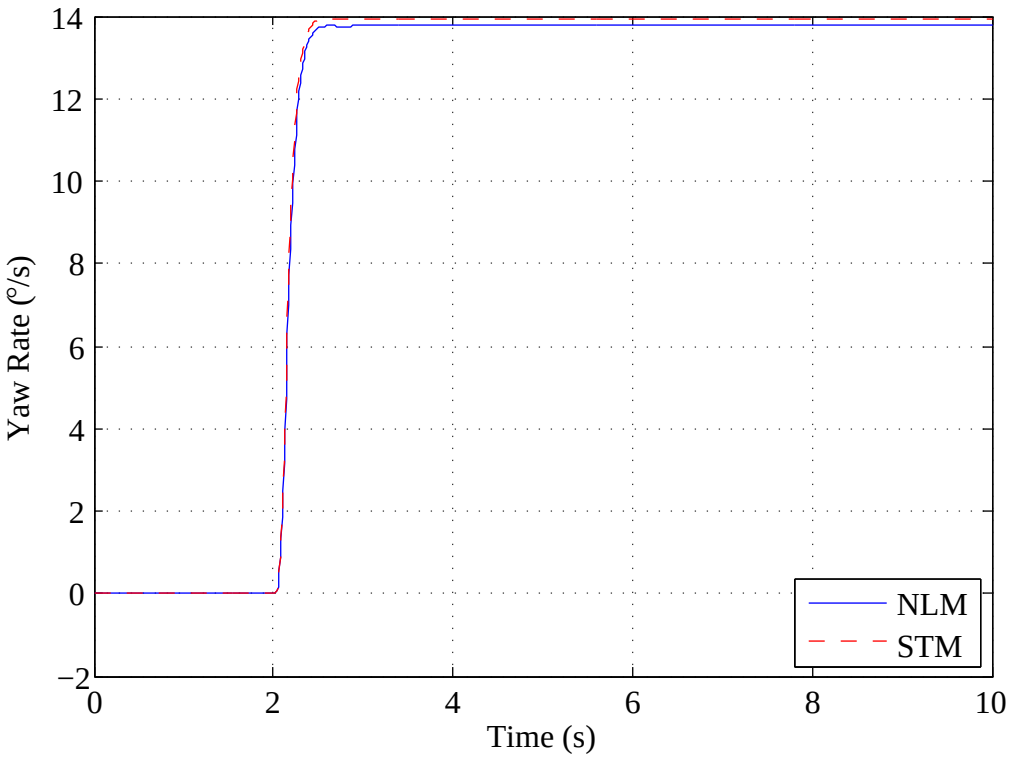

Figure 6.11. The yaw rates of the nonlinear model and the Single Track Model with the step steering wheel input

7. ESTIMATOR DESIGN BASED ON THE SINGLE TRACK MODEL

Estimation can be summarized as guessing a signal by using another measured signal. A basic estimation scheme is seen in Figure 7.1. In this figure, the dynamic system G is fed by the input w. z is the output to be estimated and y is the measured output. The estimator E outputs the estimated value z_{Est}. e stands for the error and it is the difference between the real and the estimated values; namely z and z_{Est}.

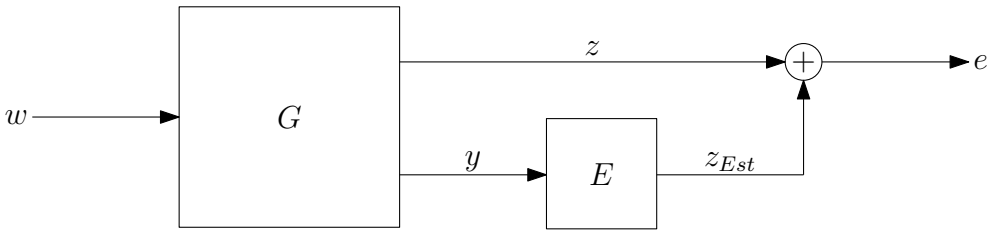

Figure 7.1. A basic estimation scheme

Here, it should be noted that the real output z does not exist in real-life applications because it can not be measured. As a result of that, e can not be calculated in real-life applications. At this point, a question may arise about the existence of these two signals in Figure 7.1. During the design stage, the internal dynamics of the system G is known; this information is necessary to be able to design the estimator. Therefore the two outputs of the system and thus the error can be obtained. However, in real-life applications, the internal dynamics of the system is not known. In this case, the only data is the measured output y. Using this measurement and the designed estimator E, the estimated output z_{Est} is found.

In the case of this study, the estimation of the side-slip angle β is done. It is considered that the yaw rate $\dot{\psi}$ is measured with a sensor. The estimation is done by using this measurement. As stated before, the longitudinal velocity of the vehicle is assumed to be constant. Therefore, the only remaining input to the system is the front wheel steering angle which is designated with δ_F. Figure 7.2 on page 83 is obtained by changing the notations in Figure 7.1.

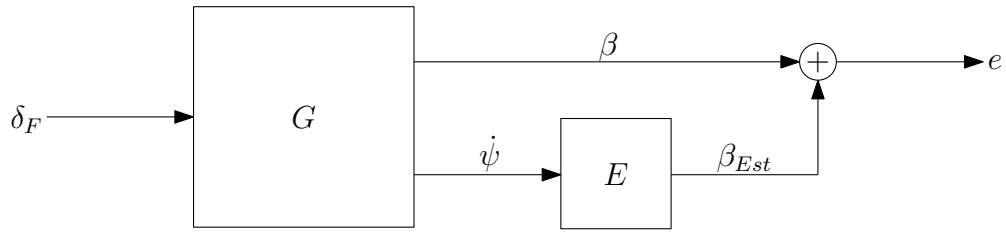

Figure 7.2. A basic estimation scheme with modified parameters

Here, of course, the right choice of the estimator E is very important. It has to perform as desired for the specified conditions. More specifically, the error e has to be less than the defined value. This is done by minimizing the effect of the input on the error, which is explained in detail later.

The parameters, which are involved in a system, play an important role in defining the system behavior for some given input. The estimator is designed according to a set of parameters, and it is expected to perform well when the values of some of these parameters change. The fact that some of the parameter values can change means that the system is "uncertain". If the system is uncertain, the uncertain terms has to be taken out and represented separately before starting to design the estimator. This process is called the "linear fractional transformation (LFT)".

The parameters, which are considered to be uncertain, have to be selected first. This is done by changing the parameter values in the same amounts and running tests. After that, the outputs are compared. If the system is more sensitive to a parameter, it is expected that the outputs change more when the value of that parameter is changed. Obviously, the system is more sensitive to the parameters which are considered to be uncertain. By looking at the sensitivity of the system, these parameters are selected. This has to be done before the uncertainty analysis, so the sensitivity analysis is done in the first part of this section.

After the sensitivity analysis, the uncertainty analysis takes place. The second part of this section is devoted to the uncertainty analysis.

Looking at Figure 7.2, one can easily observe that the only disturbance to the

system is the front wheel steering angle δ_F. Clearly, a variation in its value affects the whole system. This is why the estimator is designed considering the input, in this case the front wheel steering angle. The estimator is designed so that it performs well in any condition. If the conditions can be limited, it is clear that the estimator performs better. Limiting the input provides better functioning of the estimator. This is done by adding a "weighing function" so that the input is filtered. This process is the third part of this section.

The system is put into the LFT form and fine-tuned via a weighing function. In other words, the pre-work is done and the system is finally ready to be used in the estimator design. Therefore, the last part of this section is devoted to estimator design. The robust estimator design is done onto an uncertain plant using static multipliers.

7.1. Sensitivity Analysis

The first step of robust estimator design involves the analysis of model sensitivities to variations in parameter values. If the parameters, to which a system is most sensitive, are known, the uncertainties related to these parameters can be taken out of the equations of the system. In this section, the aim is to determine these parameters. To do this, the effects of the parameter value variations on the outputs have to be known. This analysis is done for both the nonlinear model and the Single Track Model using the methodology in [17]. The methodology is not discussed in detail, however it is summarized as the following: First, the model is simulated with the actual inputs and parameters while recording the output values at each time step. Then, one of the parameters is selected and its value is changed. The model is simulated again while recording the output values at each time step. Next, for each time step, the differences of the outputs are calculated. Then, the absolute values of the differences are found and summed up, returning the total absolute errors for each output. Total absolute errors show how sensitive the model is to the changes in the value of the selected parameter. The same process is applied for other parameters too. Here, it is necessary to remind that only one parameter value is changed at a time. Finally, the total absolute errors are compared and the parameters, to which the model is most sensitive, are

determined.

As stated before, the analysis is done for both of the models, namely the nonlinear model and the Single Track Model. Some of the facts are valid for both of the models and discussing these facts is necessary. The outputs, which are analyzed, are selected as the side-slip angle β and the yaw rate $\dot{\psi}$. Both of the models are simulated at longitudinal velocities of 20, 40, 60 and 80 km/h. Always a step steering wheel input is applied. The steering wheel angle increases to 45° in 0.2 s. All of the selected parameter values are changed from -25 per cent to 25 per cent with five per cent increments.

The selected parameters for the nonlinear model are p_{SMU/P_x}, m_{SMU}, I_{SMU_z} and v_{SMLi_X}. The longitudinal velocity has to be kept constant in simulations, so C_I and C_P are set to 300000 N/m and 13000 Ns/m, respectively. Vehicle parameter values are determined in Section 5 and these values are used in the simulations. Also, the loading condition of the vehicle has to be determined. The only loads on the vehicle are the two front passengers and the fuel. Here, it is not possible to represent all of the total absolute error graphs obtained for the nonlinear model. Therefore, only the results of the simulation with the longitudinal velocity of 60 km/h are included. These results are seen in Figures 7.3 and 7.4 on page 86.

The selected parameters for the Single Track Model are l_F, l_R, m, I_z, c_F, c_R and v_{G_x}. The definitions of these parameters can be found in Section 4. Vehicle parameter values are determined in Section 6 and these values are used in the simulations. Here, it is not possible to represent all of the total absolute error graphs obtained for the Single Track Model. Therefore, only the results of the simulation with the longitudinal velocity of 60 km/h are included. These results are seen in Figures 7.5 and 7.6 on page 87.

After studying the total absolute error graphs obtained for the nonlinear model and the Single Track Model, it is seen that both of the models are most sensitive to the changes in the values of longitudinal velocities. Accordingly, the longitudinal velocity is chosen as the uncertain parameter. To confirm this choice, bode plots of both of the

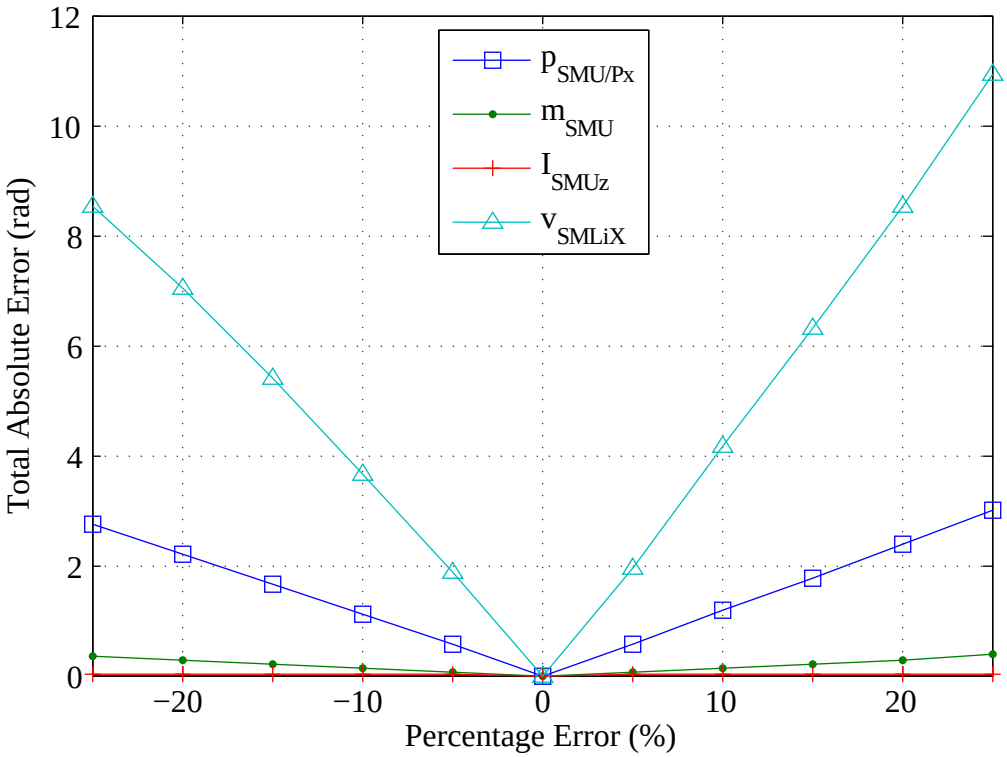

Figure 7.3. Side-slip angle total absolute error graph of the nonlinear model at a longitudinal velocity of 60 km/h

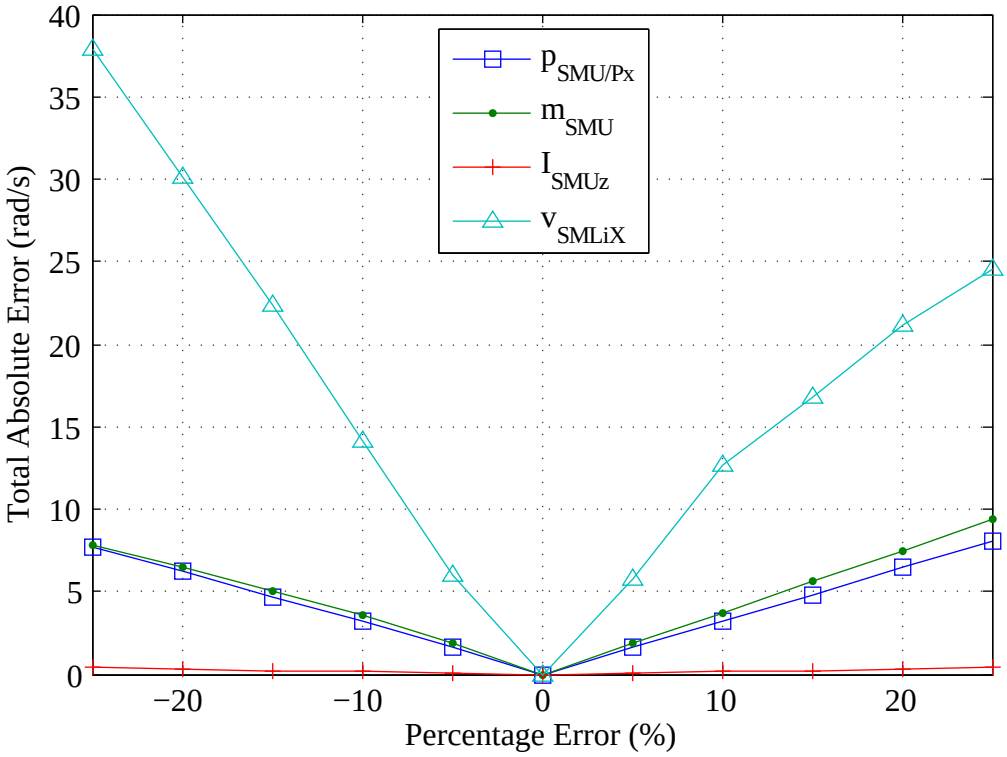

Figure 7.4. Yaw rate total absolute error graph of the nonlinear model at a longitudinal velocity of 60 km/h

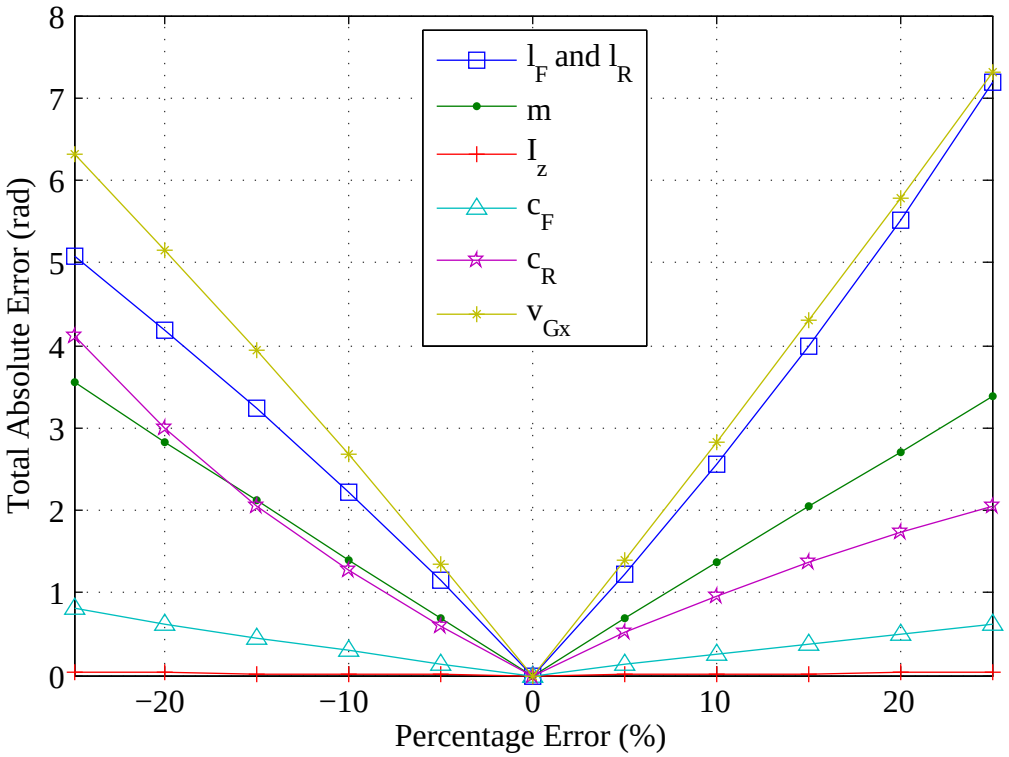

Figure 7.5. Side-slip angle total absolute error graph of the Single Track Model at a longitudinal velocity of 60 km/h

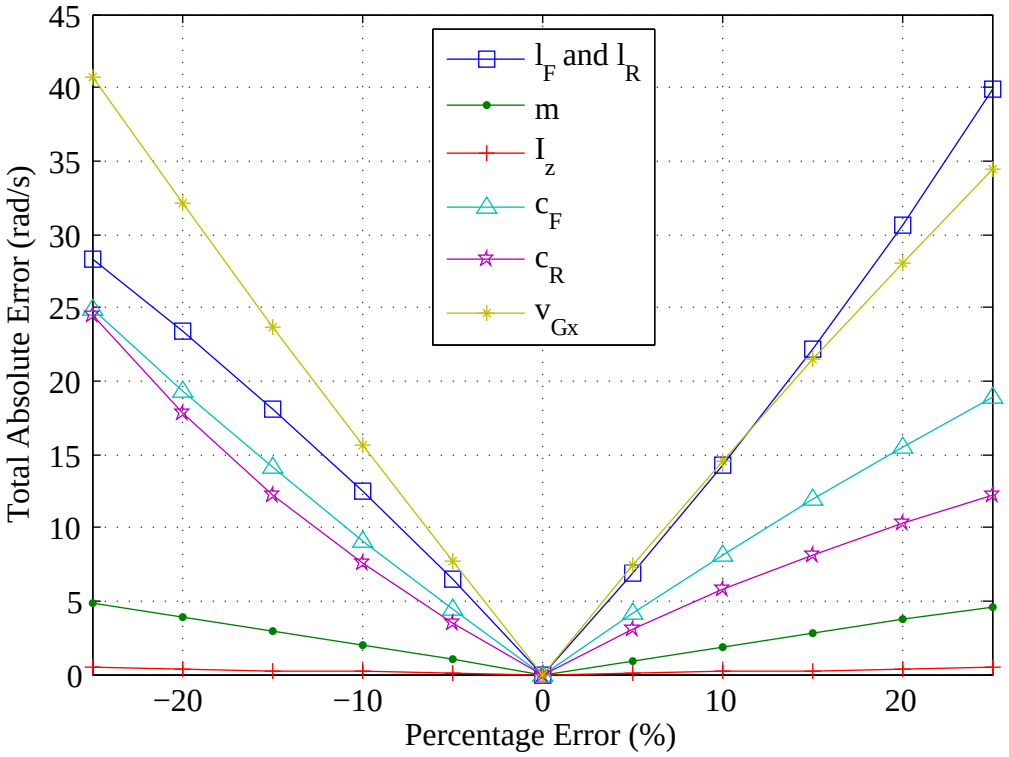

Figure 7.6. Yaw rate total absolute error graph of the Single Track Model at a longitudinal velocity of 60 km/h

models are also analyzed as an additional work. The bode plots are generated while the values of the selected parameters are changed. Here, only some of the bode plots are shown in Figures 7.7 - 7.14 on pages 89 - 96. Looking at these bode plots, it is concluded that the largest change is obtained when the longitudinal velocity is varied. Accordingly, the selection of the longitudinal velocity as the uncertain parameter is confirmed.

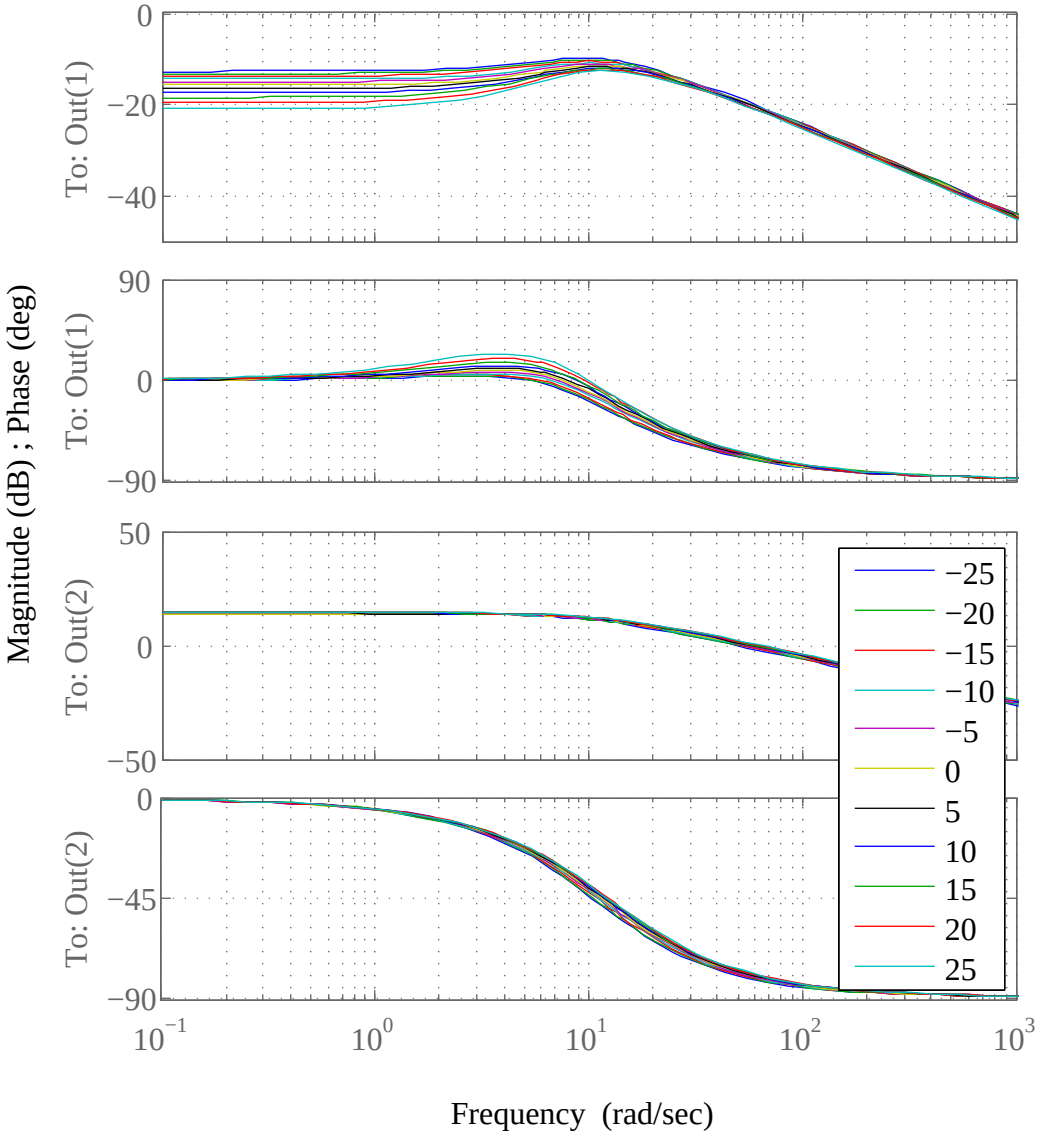

Figure 7.7. Bode plots of the nonlinear model as p_{SMU/P_x} is changed at a longitudinal velocity of 60 km/h (The first output is the side-slip angle β and the second output is the yaw rate $\dot{\psi}$.)

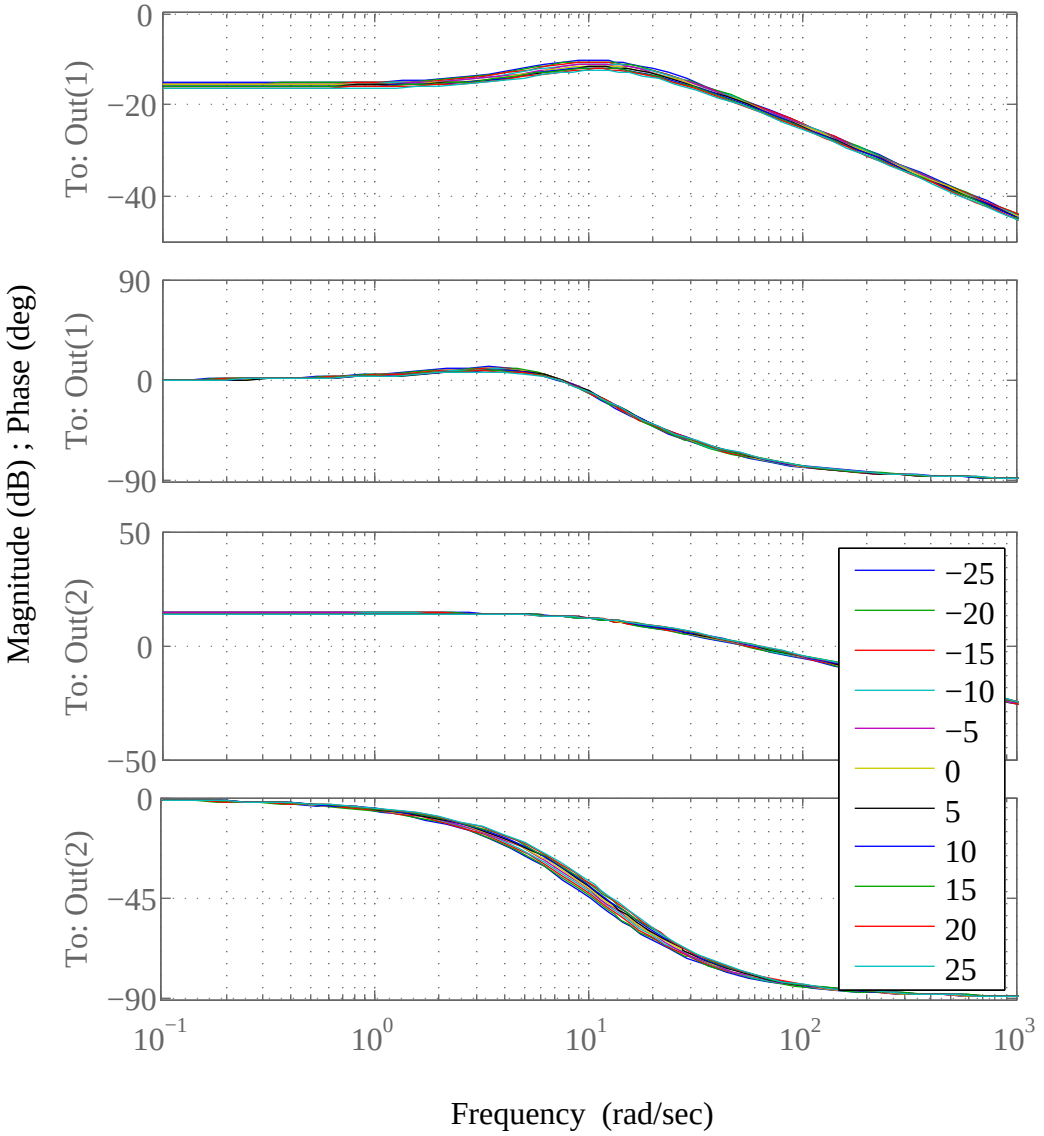

Figure 7.8. Bode plots of the nonlinear model as m_{SMU} is changed at a longitudinal velocity of 60 km/h (The first output is the side-slip angle β and the second output is the yaw rate $\dot{\psi}$.)

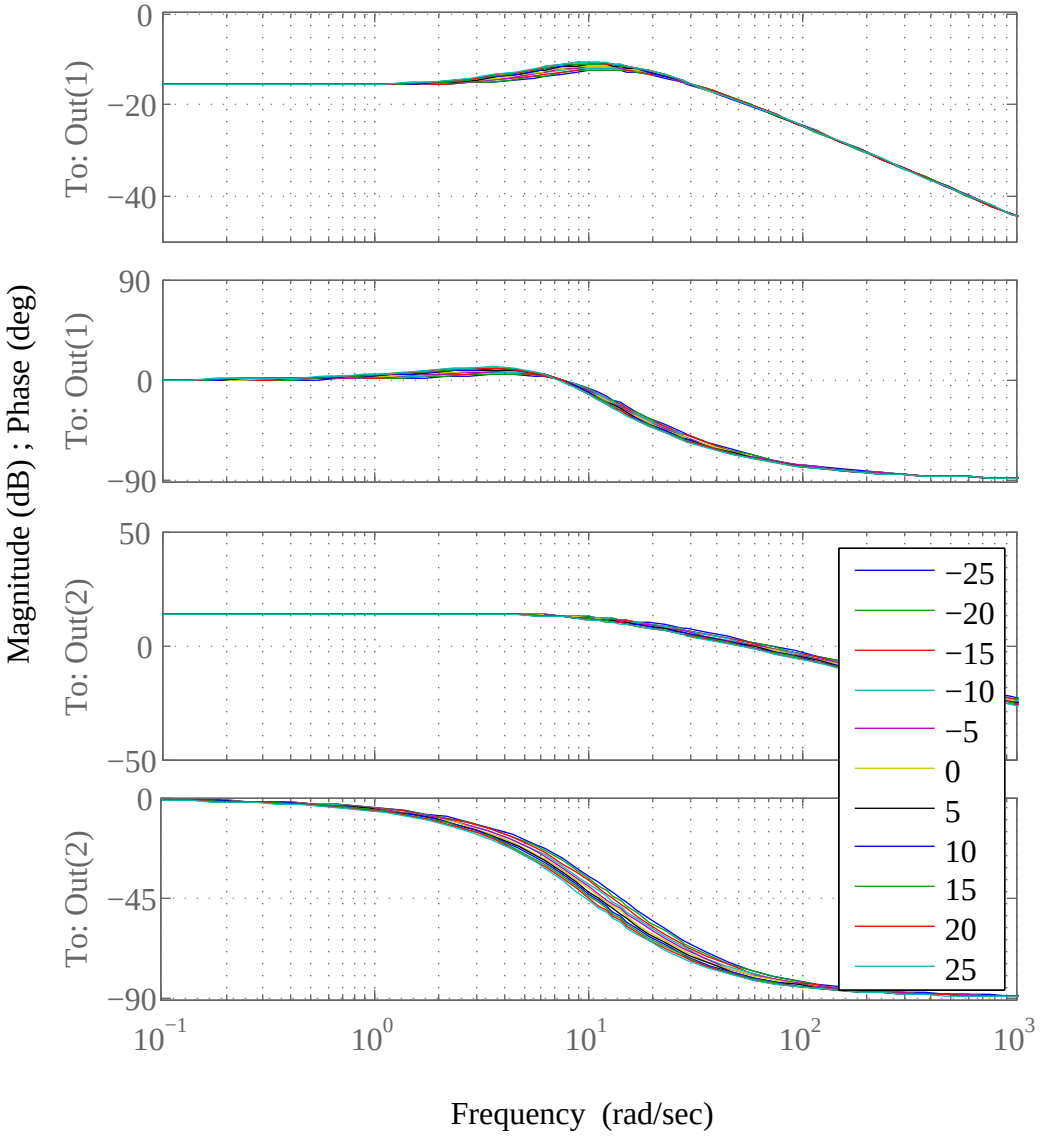

Figure 7.9. Bode plots of the nonlinear model as I_{SMU_z} is changed at a longitudinal velocity of 60 km/h (The first output is the side-slip angle β and the second output is the yaw rate $\dot{\psi}$.)

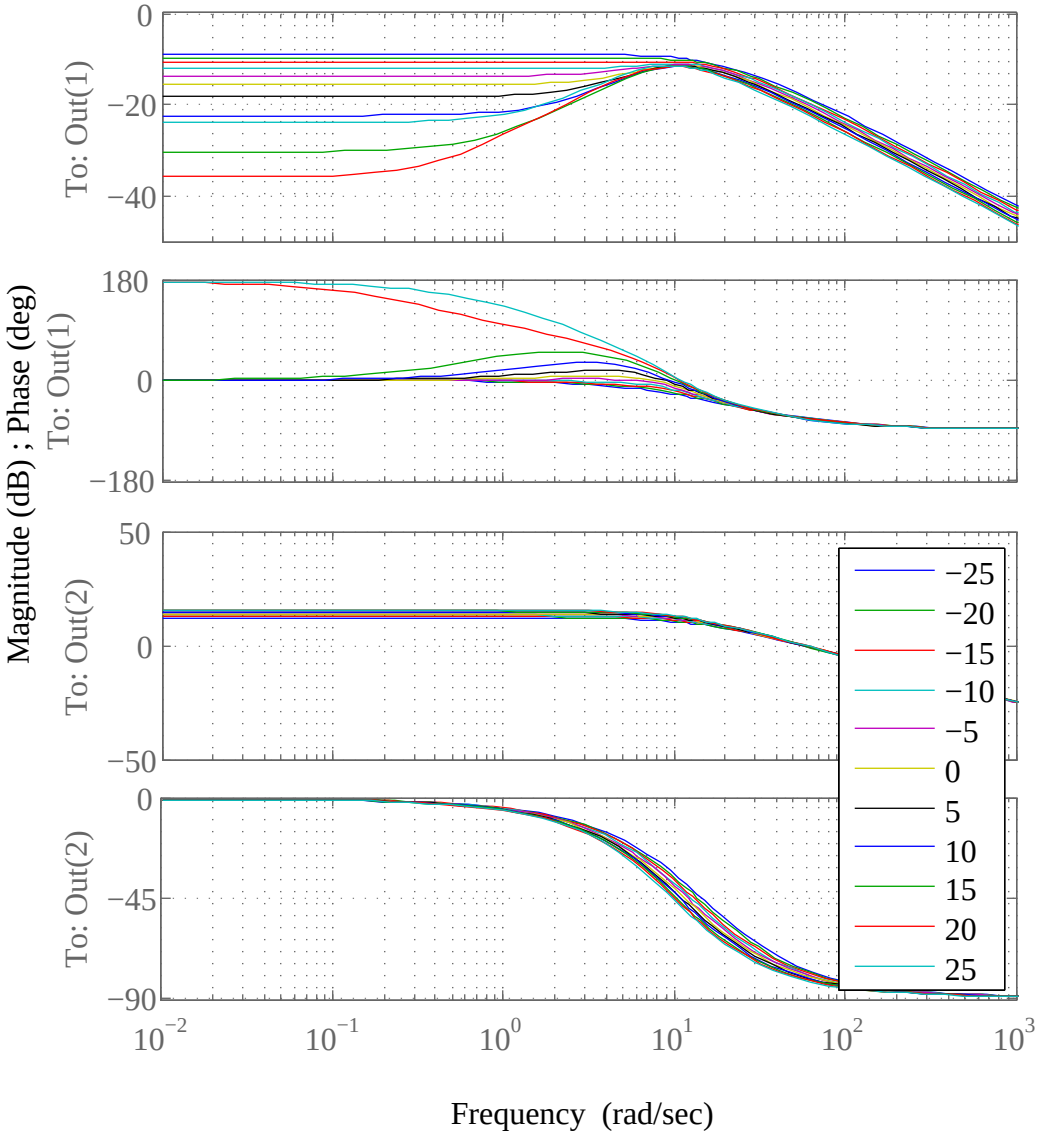

Figure 7.10. Bode plots of the nonlinear model as v_{SMLi_X} is changed at a longitudinal velocity of 60 km/h (The first output is the side-slip angle β and the second output is the yaw rate $\dot{\psi}$.)

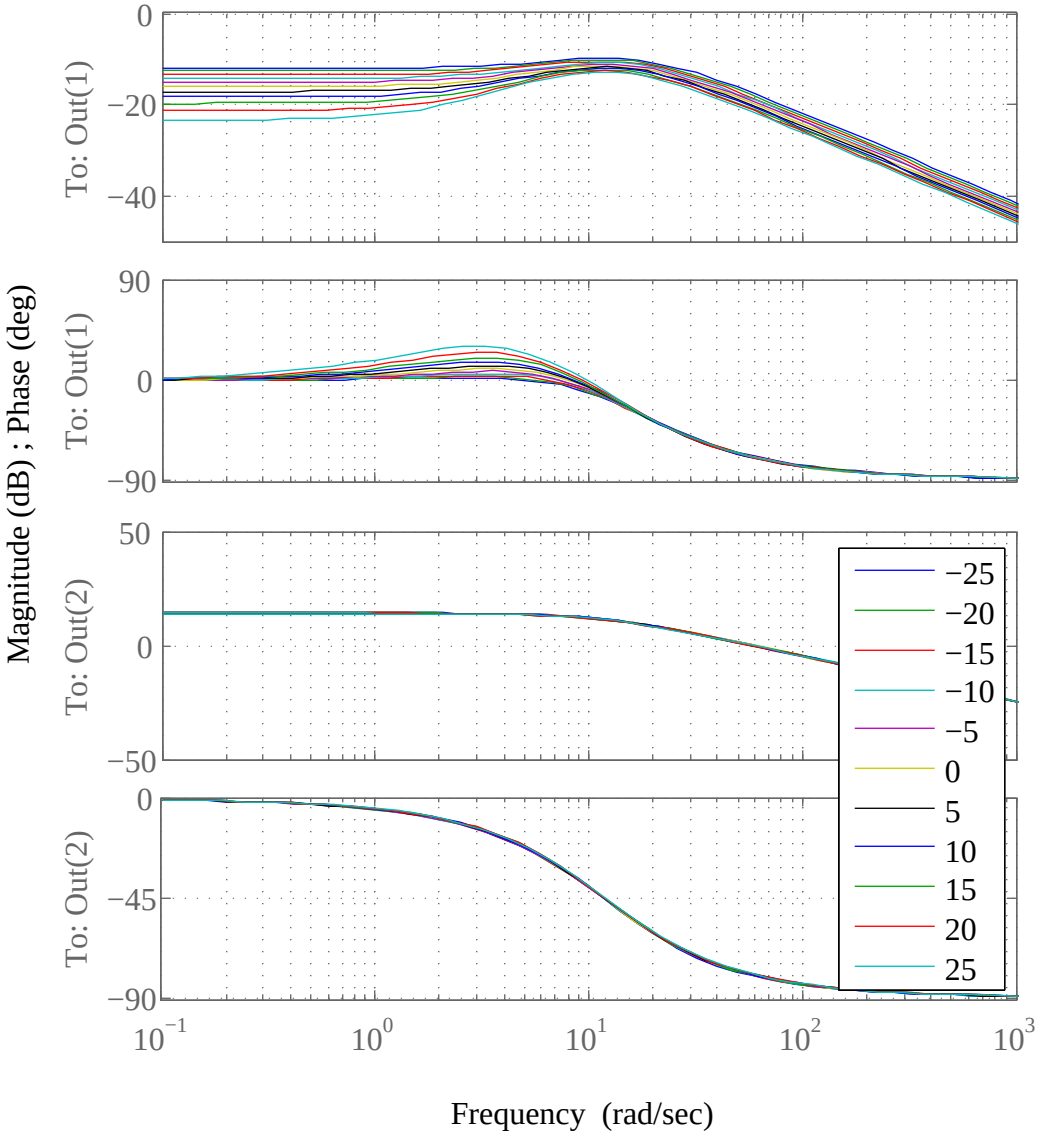

Figure 7.11. Bode plots of the Single Track Model as m is changed at a longitudinal velocity of 60 km/h (The first output is the side-slip angle β and the second output is the yaw rate $\dot{\psi}$.)

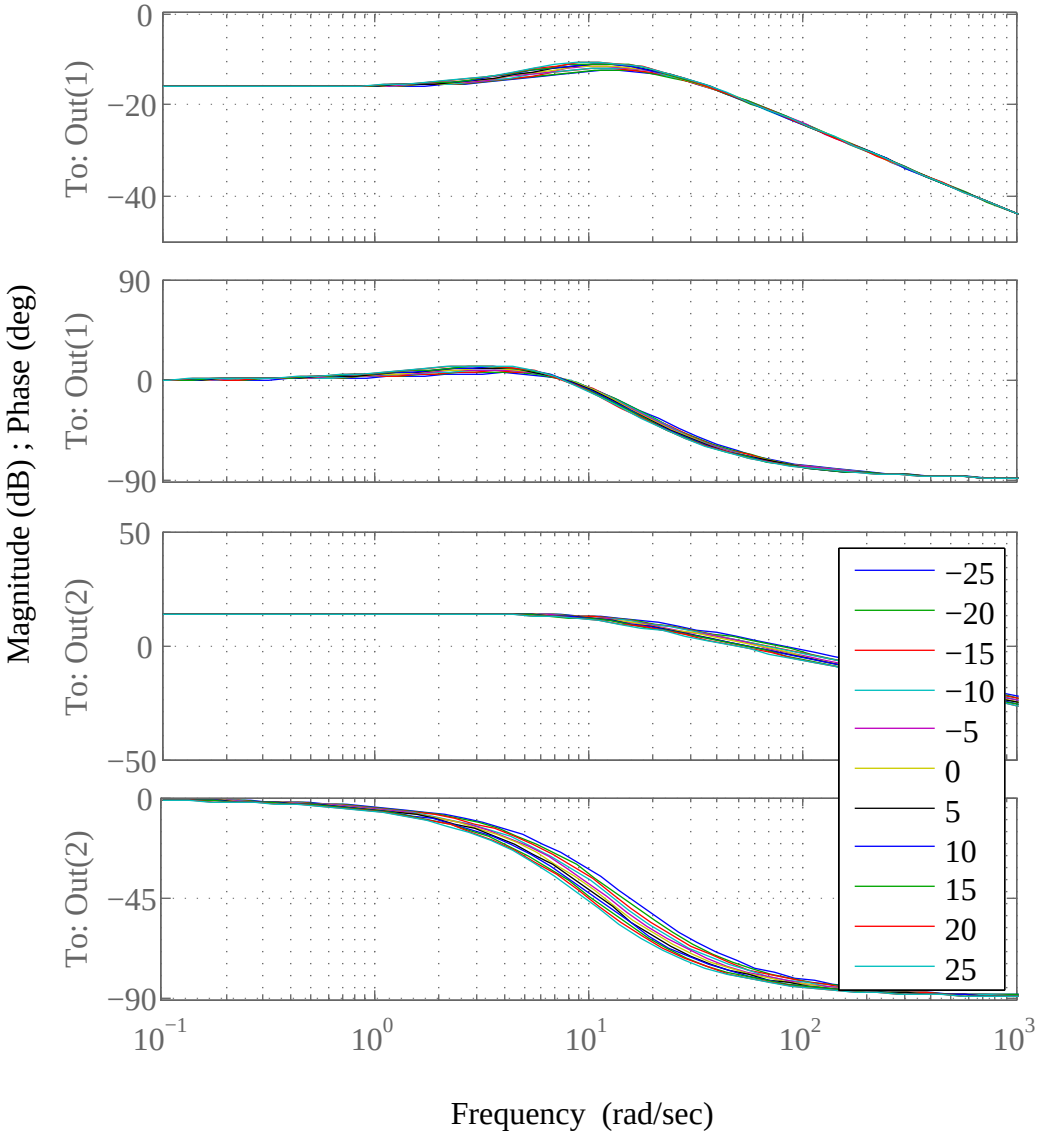

Figure 7.12. Bode plots of the Single Track Model as I_z is changed at a longitudinal velocity of 60 km/h (The first output is the side-slip angle β and the second output is the yaw rate $\dot{\psi}$.)

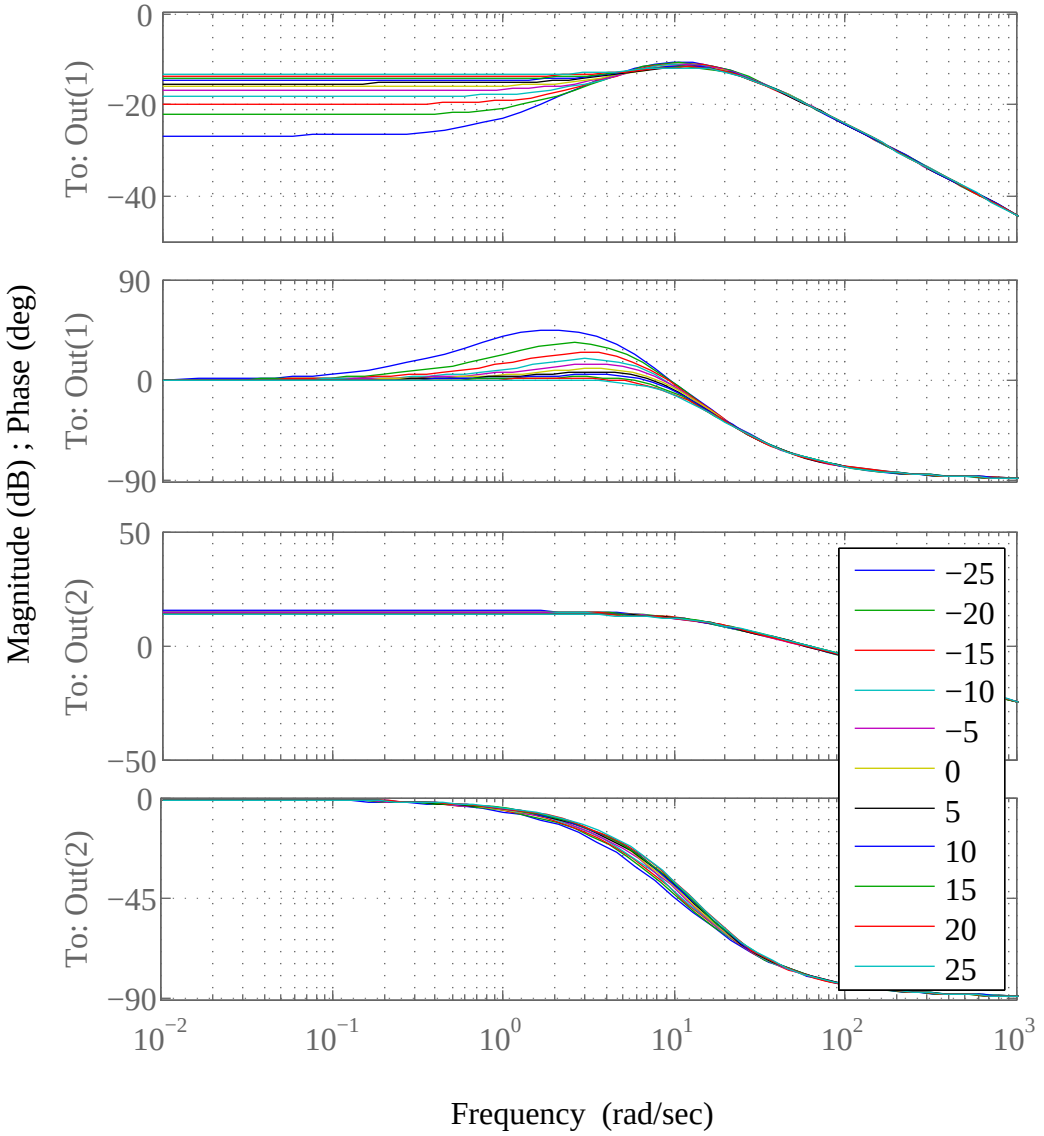

Figure 7.13. Bode plots of the Single Track Model as c_R is changed at a longitudinal velocity of 60 km/h (The first output is the side-slip angle β and the second output is the yaw rate $\dot{\psi}$.)

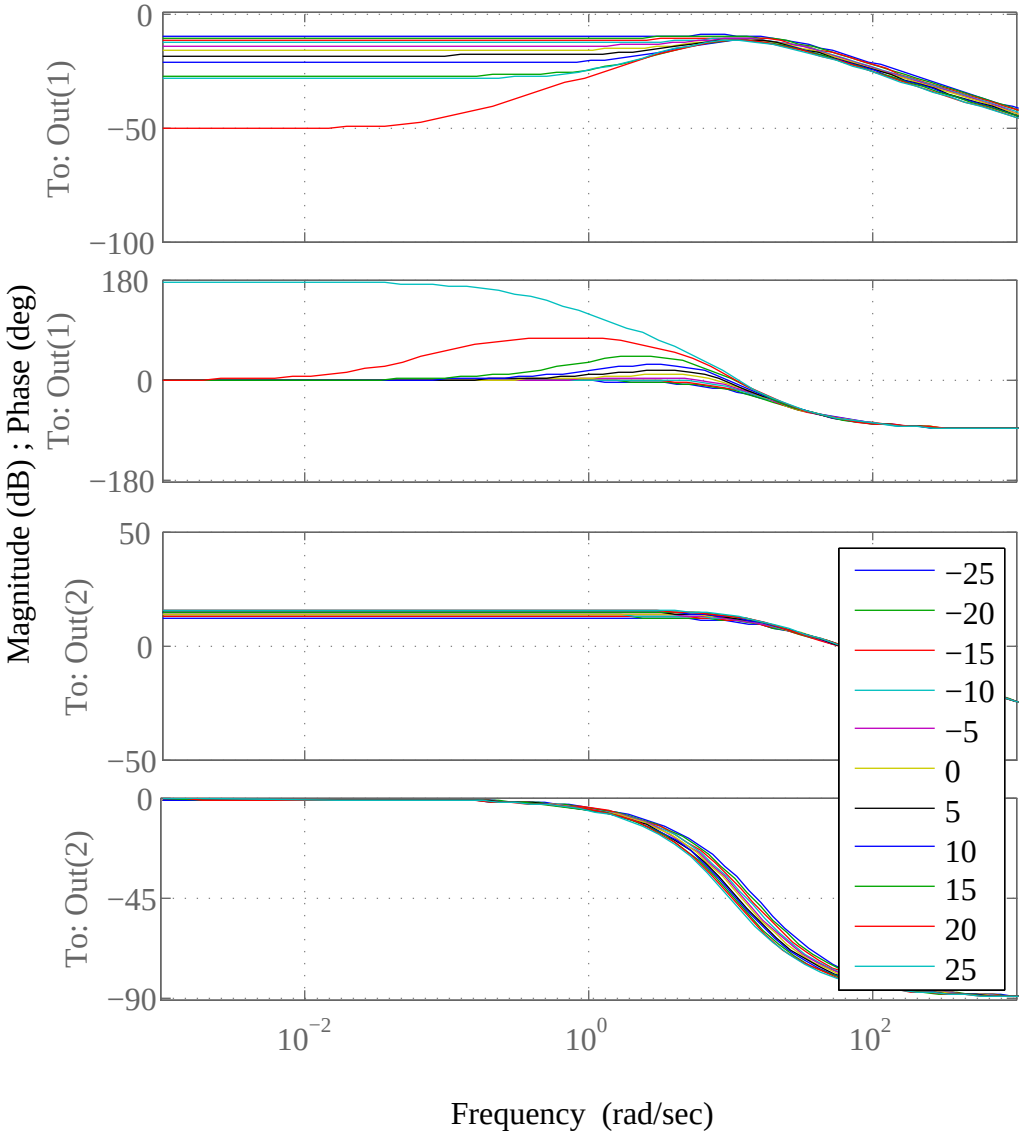

Figure 7.14. Bode plots of the Single Track Model as v_{G_x} is changed at a longitudinal velocity of 60 km/h (The first output is the side-slip angle β and the second output is the yaw rate $\dot{\psi}$.)

7.2. Uncertainty Analysis

From now on, the Single Track Model is used to design the estimator. As stated before, the estimator is designed based on the Single Track Model, and then it is used with the nonlinear model to analyze its performance. After the sensitivity analysis, the next step is the uncertainty analysis which is done in this section. At the end of this section, the uncertain parameters are represented separately which makes it easier to deal with them in the following steps.

This section is divided into three parts. The first part deals with the initial system where the system is explained in detail. In the second part, the uncertainty due to the longitudinal component of the velocity is taken out. Finally in the third part, the obtained plant is normalized.

7.2.1. The Initial System

Any system can be represented in the state-space form as

$$\dot{x} = Ax + Bw, \tag{7.1}$$

$$y = Cx + Dw. \tag{7.2}$$

where w, x and y stand for the input, state and output vectors of the system. The sizes of these vectors are dependent on the system itself. In the case of this study, estimation of a parameter is done by using another parameter. This clearly explains why there have to be two outputs of the system. This means that vector y is made up of two scalars. The state-space representation of the system is then rewritten as

$$\dot{x} = Ax + Bw, \tag{7.3}$$

$$y_1 = C_1x + D_1w, \tag{7.4}$$

$$y_2 = C_2x + D_2w. \tag{7.5}$$

For the sake of simplicity, the above equation set is written as the following:

$$\dot{x} = Ax + Bw \tag{7.6}$$

$$y = C_y x + D_y w \tag{7.7}$$

$$z = C_z x + D_z w \tag{7.8}$$

Finally, the system is represented as the following:

$$\dot{x} = Ax + Bw \tag{7.9}$$

$$\begin{bmatrix} y \\ z \end{bmatrix} = \begin{bmatrix} C_y \\ C_z \end{bmatrix} x + \begin{bmatrix} D_y \\ D_z \end{bmatrix} w \tag{7.10}$$

The block representation of the initial system is seen in Figure 7.15 where

$$G(s) = \begin{bmatrix} C_y \\ C_z \end{bmatrix} (sI - A)^{-1} B + \begin{bmatrix} D_y \\ D_z \end{bmatrix} := \left[\begin{array}{c|c} A & B \\ \hline C_y & D_y \\ C_z & D_z \end{array}\right]. \tag{7.11}$$

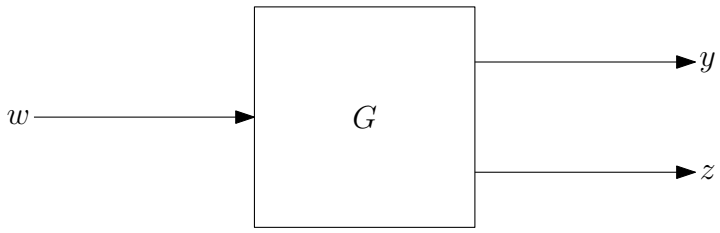

Figure 7.15. The block representation of the initial system

It is necessary to define the inputs, states and outputs of the system. As stated before, the Single Track Model with only front steering is used in this study. Therefore, the only input to the system is the front wheel steering angle. Accordingly,

$$w = \delta_F. \tag{7.12}$$

The state vector is defined as

$$x = \begin{bmatrix} \beta \\ \dot{\psi} \end{bmatrix}. \tag{7.13}$$

The outputs of the system are the side-slip angle and the yaw rate; which means that

$$y = \dot{\psi}, \tag{7.14}$$

$$z = \beta. \tag{7.15}$$

Using these definitions, the system reduces to

$$\dot{x} = Ax + Bw, \tag{7.16}$$

$$y = C_y x, \tag{7.17}$$

$$z = C_z x \tag{7.18}$$

where

$$C_y = \begin{bmatrix} 0 & 1 \end{bmatrix}, \tag{7.19}$$

$$C_z = \begin{bmatrix} 1 & 0 \end{bmatrix}. \tag{7.20}$$

It is stated that the Single Track Model with only front steering is used in this study. Considering this fact, the system is written as

$$\dot{x} = \begin{bmatrix} -\frac{c_F + c_R}{m v_{G_x}} & \frac{c_R l_R - c_F l_F}{m {v_{G_x}}^2} - 1 \\ \frac{c_R l_R - c_F l_F}{I_z} & -\frac{c_R {l_R}^2 + c_F {l_F}^2}{I_z v_{G_x}} \end{bmatrix} x + \begin{bmatrix} \frac{c_F}{m v_{G_x}} \\ \frac{c_F l_F}{I_z} \end{bmatrix} w, \tag{7.21}$$

$$y = \begin{bmatrix} 0 & 1 \end{bmatrix} x, \tag{7.22}$$

$$z = \begin{bmatrix} 1 & 0 \end{bmatrix} x. \tag{7.23}$$

7.2.2. Pulling Out the Uncertainty

When a system is considered, representing the uncertainties separately is beneficial during the estimator construction stage. As stated before, the uncertainty due to the longitudinal component of the velocity is taken out of the system.

The starting equation is

$$\dot{x} = Ax + Bw. \tag{7.24}$$

The term v_{G_x} is considered to be uncertain. Therefore, it is thought to change around a value v_0, which can also be written as

$$v_{G_x} = v_0 + \delta. \tag{7.25}$$

After the necessary calculations, the following set of equations is found:

$$\dot{x} = A'x + B_p p + B_w w \tag{7.26}$$

$$q = C_q x + D_{qp} p + D_{qw} w \tag{7.27}$$

$$p = \Delta q \tag{7.28}$$

$$\Delta = \delta I \tag{7.29}$$

Including the outputs,

$$\dot{x} = A'x + B_p p + B_w w, \tag{7.30}$$

$$q = C_q x + D_{qp} p + D_{qw} w, \tag{7.31}$$

$$y = C_y x, \tag{7.32}$$

$$z = C_z x, \tag{7.33}$$

$$p = \Delta q, \tag{7.34}$$

$$\Delta = \delta I. \tag{7.35}$$

The above equation set is put into the common form as

$$\dot{x} = A'x + B_p p + B_w w, \tag{7.36}$$

$$q = C_q x + D_{qp} p + D_{qw} w, \tag{7.37}$$

$$y = C_y x + D_{yp} p + D_{yw} w, \tag{7.38}$$

$$z = C_z x + D_{zp} p + D_{zw} w, \tag{7.39}$$

$$p = \Delta q, \tag{7.40}$$

$$\Delta = \delta I \tag{7.41}$$

where

$$D_{yp} = 0, \tag{7.42}$$

$$D_{yw} = 0, \tag{7.43}$$

$$D_{zp} = 0, \tag{7.44}$$

$$D_{zw} = 0. \tag{7.45}$$

These equations can be put into a more compact form as

$$\dot{x} = A'x + \begin{bmatrix} B_p & B_w \end{bmatrix} \begin{bmatrix} p \\ w \end{bmatrix}, \tag{7.46}$$

$$\begin{bmatrix} q \\ y \\ z \end{bmatrix} = \begin{bmatrix} C_q \\ C_y \\ C_z \end{bmatrix} x + \begin{bmatrix} D_{qp} & D_{qw} \\ D_{yp} & D_{yw} \\ D_{zp} & D_{zw} \end{bmatrix} \begin{bmatrix} p \\ w \end{bmatrix}, \tag{7.47}$$

$$p = \Delta q, \tag{7.48}$$

$$\Delta = \delta I \tag{7.49}$$

or, equivalently,

$$\begin{bmatrix} q \\ y \\ z \end{bmatrix} = \left[\begin{array}{c|cc} A' & B_p & B_w \\ \hline C_q & D_{qp} & D_{qw} \\ C_y & D_{yp} & D_{yw} \\ C_z & D_{zp} & D_{zw} \end{array}\right] \begin{bmatrix} p \\ w \end{bmatrix}, \tag{7.50}$$

$$p = \Delta q, \tag{7.51}$$

$$\Delta = \delta I. \tag{7.52}$$

The block representation of the system is seen in Figure 7.16 where

$$G_u(s) = \begin{bmatrix} C_q \\ C_y \\ C_z \end{bmatrix} (sI - A')^{-1} \begin{bmatrix} B_p & B_w \end{bmatrix} + \begin{bmatrix} D_{qp} & D_{qw} \\ D_{yp} & D_{yw} \\ D_{zp} & D_{zw} \end{bmatrix} \tag{7.53}$$

and

$$\Delta = \delta I. \tag{7.54}$$

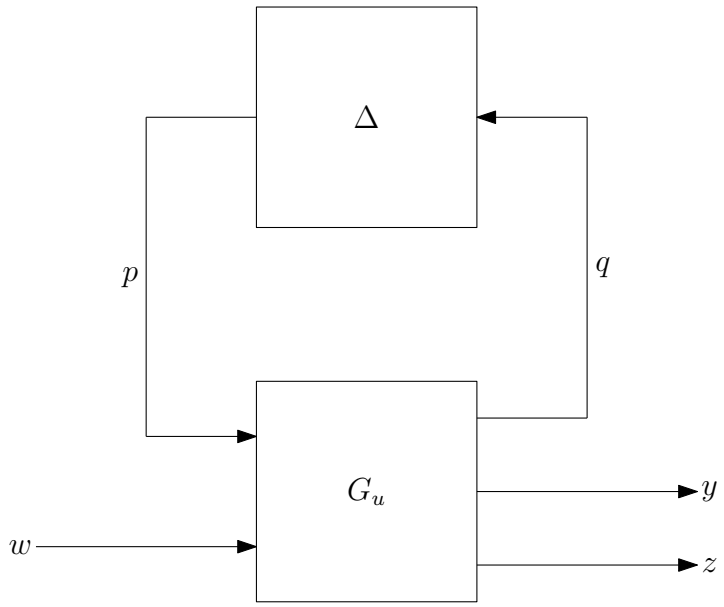

Figure 7.16. The block representation of the system with the uncertainty taken out

7.2.3. Normalization

It is better to change the value of δ between zero and one during the uncertainty analysis. Therefore, normalization should be done.

Firstly, δ is written as

$$\delta = v^* \delta^*. \tag{7.55}$$

Using Equations (7.25), (7.29) and (7.55),

$$v_{G_x} = v_0 + v^* \delta^*, \tag{7.56}$$

$$\Delta = v^* \delta^* I. \tag{7.57}$$

The relation between p and q is rewritten as

$$p = \Delta q \tag{7.58a}$$

$$= v^* \delta^* I q \tag{7.58b}$$

$$= \underbrace{\delta^* I}_{\Delta_n} \underbrace{v^* q}_{q_n} \tag{7.58c}$$

$$= \Delta_n q_n. \tag{7.58d}$$

The application of these equations to the plant results in

$$\dot{x} = A' x + B_p p + B_w w, \tag{7.59}$$

$$q_n = v^* C_q x + v^* D_{qp} p + v^* D_{qw} w, \tag{7.60}$$

$$y = C_y x + D_{yp} p + D_{yw} w, \tag{7.61}$$

$$z = C_z x + D_{zp} p + D_{zw} w, \tag{7.62}$$

$$p = \Delta_n q_n, \tag{7.63}$$

$$\Delta_n = \delta^* I. \tag{7.64}$$

This equation set is written in a more compact form as

$$\dot{x} = A'x + \begin{bmatrix} B_p & B_w \end{bmatrix} \begin{bmatrix} p \\ w \end{bmatrix}, \tag{7.65}$$

$$\begin{bmatrix} q_n \\ y \\ z \end{bmatrix} = \begin{bmatrix} v^*C_q \\ C_y \\ C_z \end{bmatrix} x + \begin{bmatrix} v^*D_{qp} & v^*D_{qw} \\ D_{yp} & D_{yw} \\ D_{zp} & D_{zw} \end{bmatrix} \begin{bmatrix} p \\ w \end{bmatrix}, \tag{7.66}$$

$$p = \Delta_n q_n, \tag{7.67}$$

$$\Delta_n = \delta^* I \tag{7.68}$$

or, equivalently,

$$\begin{bmatrix} q_n \\ y \\ z \end{bmatrix} = \left[\begin{array}{c|cc} A' & B_p & B_w \\ \hline v^*C_q & v^*D_{qp} & v^*D_{qw} \\ C_y & D_{yp} & D_{yw} \\ C_z & D_{zp} & D_{zw} \end{array}\right] \begin{bmatrix} p \\ w \end{bmatrix}, \tag{7.69}$$

$$p = \Delta_n q_n, \tag{7.70}$$

$$\Delta_n = \delta^* I. \tag{7.71}$$

The block representation of the system is seen in Figure 7.17 on page 105 where

$$G_n(s) = \begin{bmatrix} v^*C_q \\ C_y \\ C_z \end{bmatrix} (sI - A')^{-1} \begin{bmatrix} B_p & B_w \end{bmatrix} + \begin{bmatrix} v^*D_{qp} & v^*D_{qw} \\ D_{yp} & D_{yw} \\ D_{zp} & D_{zw} \end{bmatrix} \tag{7.72}$$

and

$$\Delta_n = \delta^* I. \tag{7.73}$$

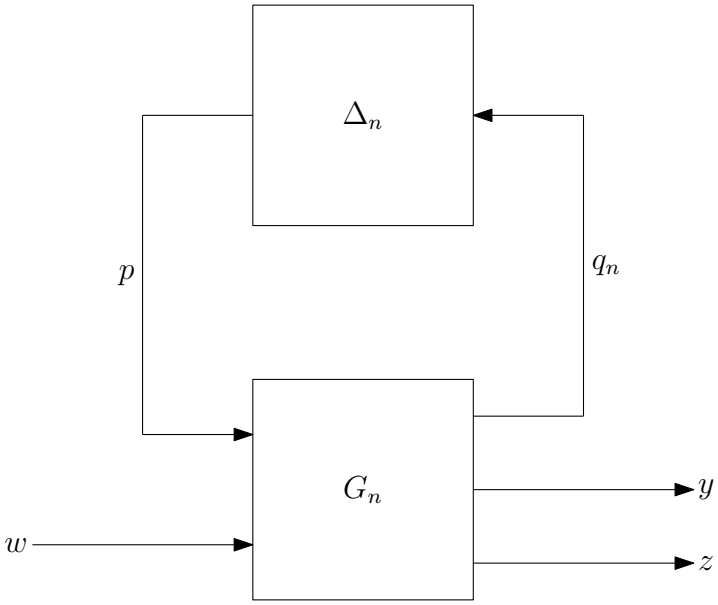

Figure 7.17. The block representation of the normalized system with the uncertainty taken out

As the final representation of the system is obtained, it is appropriate to write the matrices explicitly. The matrices involved are as the following:

$$A' = \begin{bmatrix} -\frac{1}{v_0}\frac{c_F+c_R}{m} & \frac{1}{{v_0}^2}\frac{c_R l_R - c_F l_F}{m} - 1 \\ \frac{c_R l_R - c_F l_F}{I_z} & -\frac{1}{v_0}\frac{c_F {l_F}^2 + c_R {l_R}^2}{I_z} \end{bmatrix} \tag{7.74}$$

$$B_p = \begin{bmatrix} 1 & 0 & \frac{1}{v_0}\frac{c_R l_R - c_F l_F}{m} \\ 0 & 1 & 0 \end{bmatrix} \tag{7.75}$$

$$B_w = \begin{bmatrix} \frac{1}{v_0}\frac{c_F}{m} \\ \frac{c_F l_F}{I_z} \end{bmatrix} \tag{7.76}$$

$$C_q = \begin{bmatrix} \frac{1}{{v_0}^2}\frac{c_F+c_R}{m} & \frac{1}{{v_0}^3}\frac{c_F l_F - c_R l_R}{m} \\ 0 & \frac{1}{{v_0}^2}\frac{c_F {l_F}^2 + c_R {l_R}^2}{I_z} \\ 0 & -\frac{1}{{v_0}^2} \end{bmatrix} \tag{7.77}$$

$$C_y = \begin{bmatrix} 0 & 1 \end{bmatrix} \tag{7.78}$$

$$C_z = \begin{bmatrix} 1 & 0 \end{bmatrix} \tag{7.79}$$

$$D_{qp} = \begin{bmatrix} -\frac{1}{v_0} & 0 & \frac{1}{{v_0}^2}\frac{c_F l_F - c_R l_R}{m} \\ 0 & -\frac{1}{v_0} & 0 \\ 0 & 0 & -\frac{1}{v_0} \end{bmatrix} \tag{7.80}$$

$$D_{yp} = \begin{bmatrix} 0 & 0 & 0 \end{bmatrix} \tag{7.81}$$

$$D_{zp} = \begin{bmatrix} 0 & 0 & 0 \end{bmatrix} \tag{7.82}$$

$$D_{qw} = \begin{bmatrix} -\frac{1}{{v_0}^2}\frac{c_F}{m} \\ 0 \\ 0 \end{bmatrix} \tag{7.83}$$

$$D_{yw} = 0 \tag{7.84}$$

$$D_{zw} = 0 \tag{7.85}$$

$$\Delta_n = \begin{bmatrix} \delta^* & 0 & 0 \\ 0 & \delta^* & 0 \\ 0 & 0 & \delta^* \end{bmatrix} \tag{7.86}$$

7.3. Frequency Weighing

The system shown in Figure 7.17 on page 105 is actually ready for estimator construction. However, another additional step is essential to improve the performance of the estimator. This step is the addition of a weighing function.

A weighing function basically modifies the input, commonly by means of filters. This provides the elimination of the undesired signals. Frequency weighing is the elimination of signals according to their frequencies. The well-known analog filters, which are used in frequency weighing, are the low-pass, band-pass and high-pass filters. A low-pass filter eliminates the signals which have higher frequencies than the specified value. A band-pass filter offers passage to the signals which have frequencies between two specified values. Finally, a high-pass filter eliminates the signals which have lower frequencies than the specified value. Figure 7.18 illustrates the responses of a low-pass, band-pass and high-pass filter, respectively.

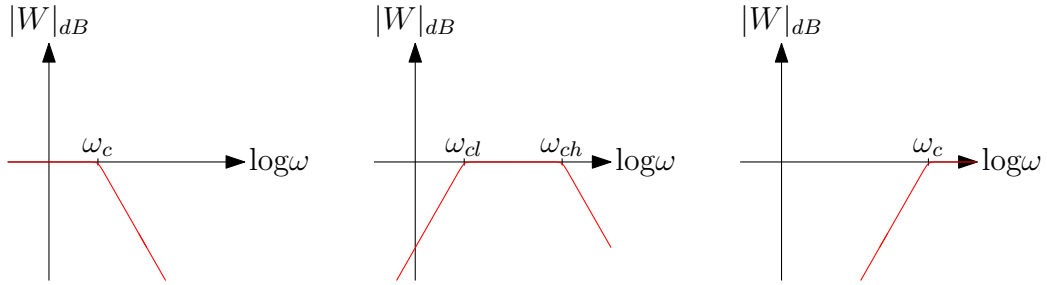

Figure 7.18. The responses of a low-pass, band-pass and high-pass filter, respectively

In the case of Figure 7.17 on page 105, the only input to the system is the front wheel steering angle which is designated with w. This means that the system response is totally dependent on the value of the front wheel steering angle. Therefore, limiting the input in the frequency aspect constraints the system. Accordingly, the estimator is constructed using a constrained system. As the result, the estimator performs better, which turns out to be an important fact.

As stated before, the aim is to filter the input signal. There are two reasons for doing that. The first reason is eliminating the unwanted noise, if there is any. The second reason is eliminating the frequencies which are impossible to be achieved in real

life. In both cases, the higher frequencies are undesired, so a low-pass filter is used. To limit the input, the weighing function has to be placed just after the input signal. Figure 7.19 shows the system after the weighing function W is added.

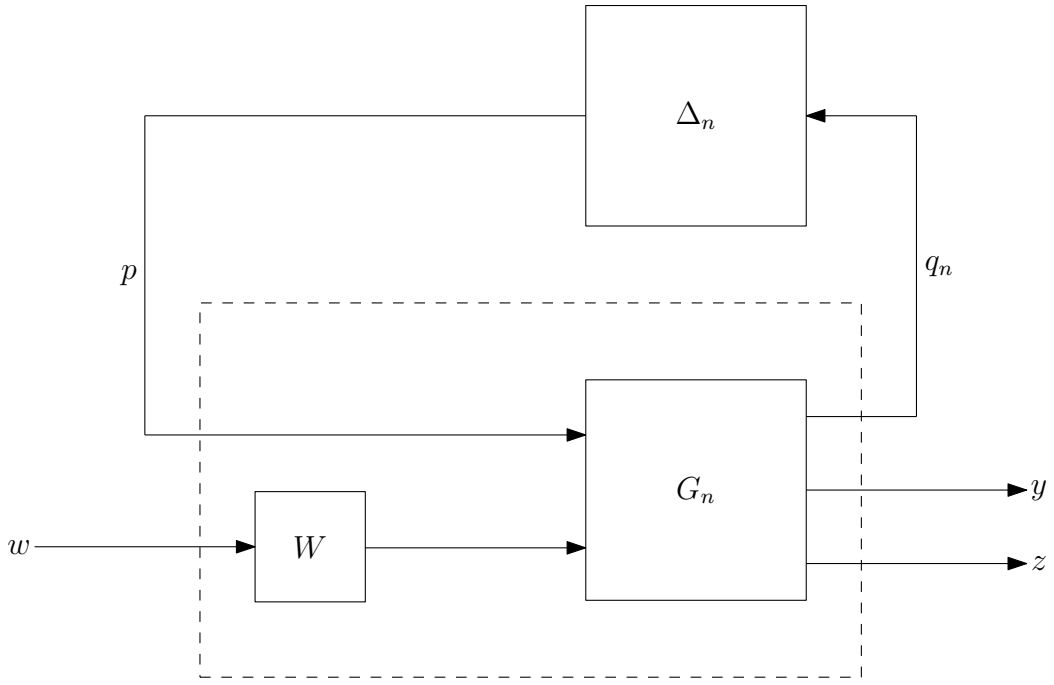

Figure 7.19. The block representation of the normalized system with the uncertainty taken out and the weighing function added

It is easily seen that the dashed block represents a system with the same inputs and outputs as G_n. If the state-space description for the dashed block is determined, the estimator can be constructed. However, the dashed block includes the weighing function which shows nonlinear characteristics. Accordingly, the state-space description for the dashed block can be found using a computational tool. The "linmod" function of MATLAB is used for this purpose.

The "linmod" function returns the state-space matrices of the system. Figure 7.20 on page 109 shows the system after the use of the "linmod" function where

$$G_w(s) = \begin{bmatrix} C_{wq} \\ C_{wy} \\ C_{wz} \end{bmatrix} (sI - A_w)^{-1} \begin{bmatrix} B_{wp} & B_{ww} \end{bmatrix} + \begin{bmatrix} D_{wqp} & D_{wqw} \\ D_{wyp} & D_{wyw} \\ D_{wzp} & D_{wzw} \end{bmatrix} \tag{7.87}$$

and

$$\Delta_n = \delta^* I. \tag{7.88}$$

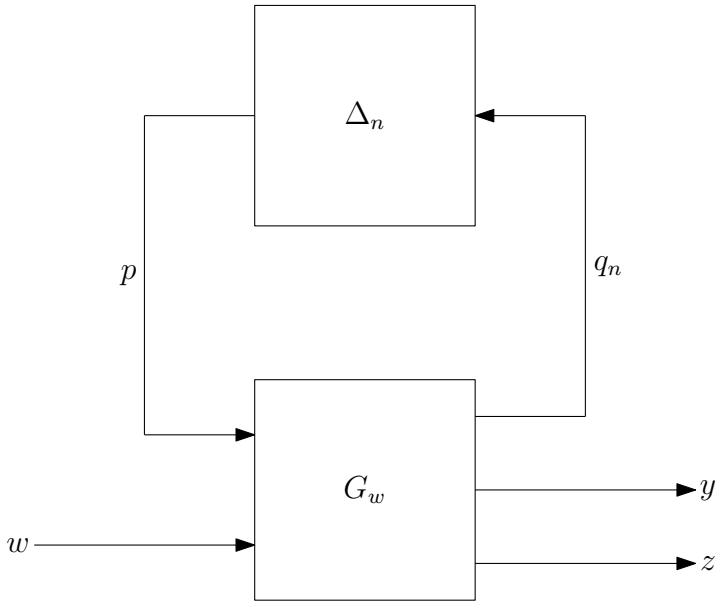

Figure 7.20. The block representation of the system after the use of the "linmod" function

During estimator construction, this system is often used. Therefore, the following changes in the names of the parameters and variables are done for the sake of simplicity. The parameters and variables of the newly obtained system are not to be confused with the previous ones, even if they are the same. Figure 7.21 on page 110 shows the final representation of the system where

$$G(s) = \begin{bmatrix} C_q \\ C_y \\ C_z \end{bmatrix} (sI - A)^{-1} \begin{bmatrix} B_p & B_w \end{bmatrix} + \begin{bmatrix} D_{qp} & D_{qw} \\ D_{yp} & D_{yw} \\ D_{zp} & D_{zw} \end{bmatrix} \tag{7.89}$$

and

$$\Delta = \delta I. \tag{7.90}$$

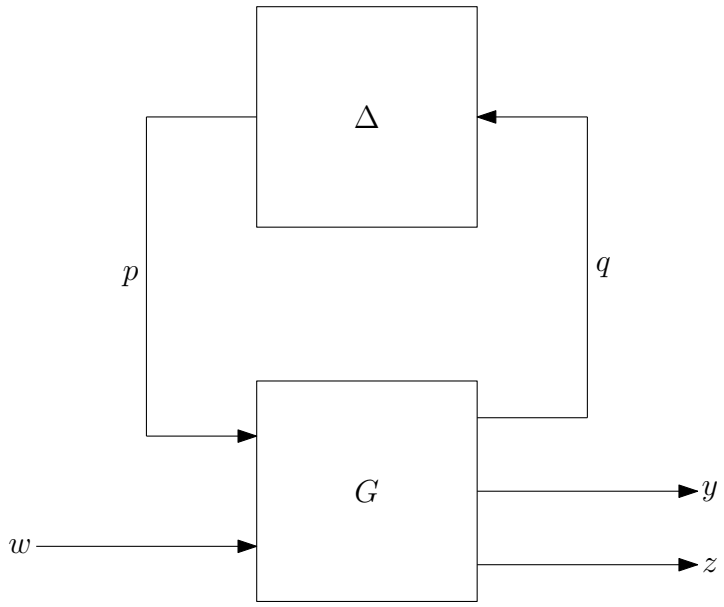

Figure 7.21. The block representation of the final system

This system can also be represented as

$$\begin{bmatrix} q \\ y \\ z \end{bmatrix} = \left[\begin{array}{c|cc} A & B_p & B_w \\ \hline C_q & D_{qp} & D_{qw} \\ C_y & D_{yp} & D_{yw} \\ C_z & D_{zp} & D_{zw} \end{array}\right] \begin{bmatrix} p \\ w \end{bmatrix}, \tag{7.91}$$

$$p = \Delta q, \tag{7.92}$$

$$\Delta = \delta I \tag{7.93}$$

or, equivalently,

$$\dot{x} = Ax + \begin{bmatrix} B_p & B_w \end{bmatrix} \begin{bmatrix} p \\ w \end{bmatrix}, \tag{7.94}$$

$$\begin{bmatrix} q \\ y \\ z \end{bmatrix} = \begin{bmatrix} C_q \\ C_y \\ C_z \end{bmatrix} x + \begin{bmatrix} D_{qp} & D_{qw} \\ D_{yp} & D_{yw} \\ D_{zp} & D_{zw} \end{bmatrix} \begin{bmatrix} p \\ w \end{bmatrix}, \tag{7.95}$$

$$p = \Delta q, \tag{7.96}$$

$$\Delta = \delta I. \tag{7.97}$$

Finally, the expanded form is as the following:

$$\dot{x} = Ax + B_p p + B_w w \tag{7.98}$$

$$q = C_q x + D_{qp} p + D_{qw} w \tag{7.99}$$

$$y = C_y x + D_{yp} p + D_{yw} w \tag{7.100}$$

$$z = C_z x + D_{zp} p + D_{zw} w \tag{7.101}$$

$$p = \Delta q \tag{7.102}$$

$$\Delta = \delta I \tag{7.103}$$

As stated before, the analog frequency filter has to be selected with care in order to design an estimator which has good performance. In this study, the input signal, which is the front wheel steering angle, is filtered. Therefore, driver behavior has to be investigated because it is the only fact which affects the front wheel steering angle. First, it is obvious that driver is not able to steer in the high frequency range, hence a low-pass filter is used. Next, the cutoff frequency has to be determined. Its value is selected as 4π rad/s because it is almost impossible to steer with an angular frequency higher than this value.

7.4. Estimator Design

An introduction to estimation is given at the beginning of Section 7. Here, however, a more detailed explanation is done. Figure 7.1 is redrawn with the addition of a dashed block as in Figure 7.22 on page 112. The dashed block T_{we} represents the transfer function from w to e. Looking at this figure, it is easy to observe that the error e is affected only by the input w via the transfer function T_{we}. If the plant is written as

$$G = \begin{bmatrix} G_1 \\ G_2 \end{bmatrix}, \tag{7.104}$$

it is easily found that

$$z = G_1 w, \tag{7.105}$$

$$y = G_2 w. \tag{7.106}$$

Looking at the figure,

$$z_{Est} = Ey, \tag{7.107}$$

$$e = z + z_{Est}. \tag{7.108}$$

Putting these four equations together, the error is found to be

$$e = (G_1 + EG_2)\, w \tag{7.109}$$

which can also be written as

$$e = T_{we} w. \tag{7.110}$$

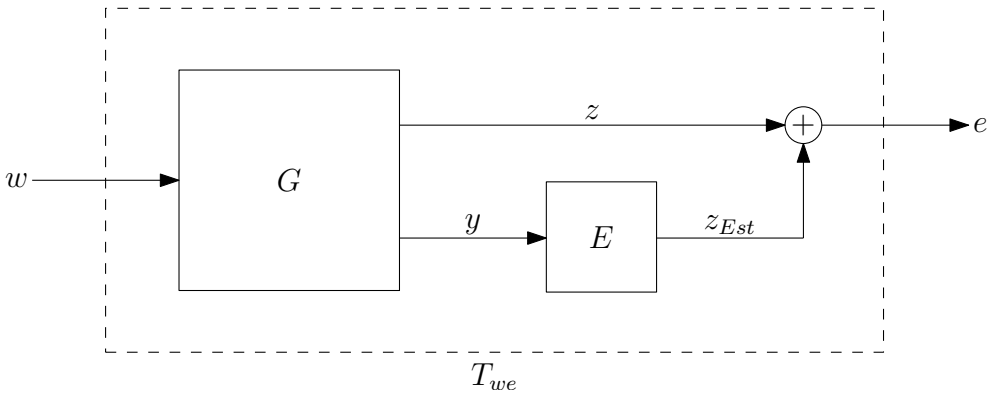

Figure 7.22. A basic estimation scheme

The performance of the estimator is measured according to the error. For acceptable performance, the error has to be less than a specified value. Hence, the error has to be minimized somehow. Since the only variable affecting the error is the input, it is concluded that the effect of the input on the error has to be minimized. This is done by minimizing the H_∞ or the H_2-norm of the transfer function T_{we}. The definitions of

them are given as

$$\left\|T_{we}\right\|_{\infty} := \sup_{\omega \in \Re} \bar{\sigma}\left(T_{we}\left(j\omega\right)\right) \tag{7.111}$$

and

$$\left\|T_{we}\right\|_{2}^{2} := \frac{1}{2\pi} \int_{-\infty}^{\infty} \text{Trace}\left(T_{we}(j\omega)^{*} T_{we}\left(j\omega\right)\right) d\omega. \tag{7.112}$$

For single-input single-output systems, the H_{∞}-norm is the peak of the corresponding Bode plot. It is also useful to discuss the signal-based interpretation of the H_{∞}-norm. The energy-to-energy interpretation of the H_{∞}-norm is written as

$$\left\|T_{we}\right\|_{\infty} = \sup_{w \neq 0} \frac{\left\|e\right\|_{2}}{\left\|w\right\|_{2}} \tag{7.113}$$

where $\left\|e\right\|_{2}$ and $\left\|w\right\|_{2}$ stand for the energy-norms of the error and input, respectively. They are defined as

$$\left\|e\right\|_{2}^{2} := \int_{0}^{\infty} e\left(t\right)^{T} e\left(t\right) dt \tag{7.114}$$

and

$$\left\|w\right\|_{2}^{2} := \int_{0}^{\infty} w\left(t\right)^{T} w\left(t\right) dt. \tag{7.115}$$

For single-input single-output systems, the H_{2}-norm is the area under the Bode plot. It is also useful to discuss the signal-based interpretations of the H_{2}-norm. The impulse-to-energy interpretation of the H_{2}-norm is written as

$$\left\|T_{we}\right\|_{2} = \sum_{i=1}^{m} \left\|e_{i}\right\|_{2}^{2}. \tag{7.116}$$

The energy-to-peak interpretation of the H_2-norm is only applicable to single-input single-output systems. It is written as

$$\left\|T_{we}\right\|_2 = \sup_{w\neq 0} \frac{\|e\|_\infty}{\|w\|_2}. \tag{7.117}$$

Finally, the white noise-to-variance interpretation of the H_2-norm is written as

$$\left\|T_{we}\right\|_2 = \lim_{t\to\infty} E\left(e\left(t\right)^T e\left(t\right)\right). \tag{7.118}$$

If G is an LTI transfer function, H_∞ and H_2 estimations can be denoted with LMIs. Convex optimization problems can be created using LMIs. Briefly, convex optimization is trying to minimize the output of a function such that the input of the function is always in a defined set. More specifically, $f\left(x\right)$ is to be minimized such that $x\in S$ where f is a convex function and S is a convex set. In a convex function, local minima is equal to the global minima. This means that if a minimum value is achieved in an interval, it is the minimum value for all of the outputs of the function. In a convex set, every point on a line, which joins any two points in the set, has to be an element of the set.

Until here, the uncertainty within the system are ignored. However, they exist in real-life applications. An estimator, which is designed ignoring the uncertainties, performs well in the lack of any uncertainty. But when the uncertainties take place, the error does not diminish. That means that the system is not robust. The aim is to design an estimator so that the error is kept in an acceptable interval when the uncertainties take place. As the result, it is beneficial to consider the uncertainties within the plant. This is referred to as "robust estimation".

The details of separating the troublesome terms are explained in Section 7.2.2. Figure 7.21 on page 110 shows a system with the uncertainties collected in Δ. Also, Figure 7.23 on page 115 shows the estimation problem when the uncertainties are taken out. Here, the characterization of Δ has to be done in terms of IQCs. This is done by

means of suitable multipliers which are considered in two groups: Static and dynamic multipliers. Static multipliers do not reflect the dynamics of a system, whereas dynamic multipliers do. In this study, static multipliers are used.

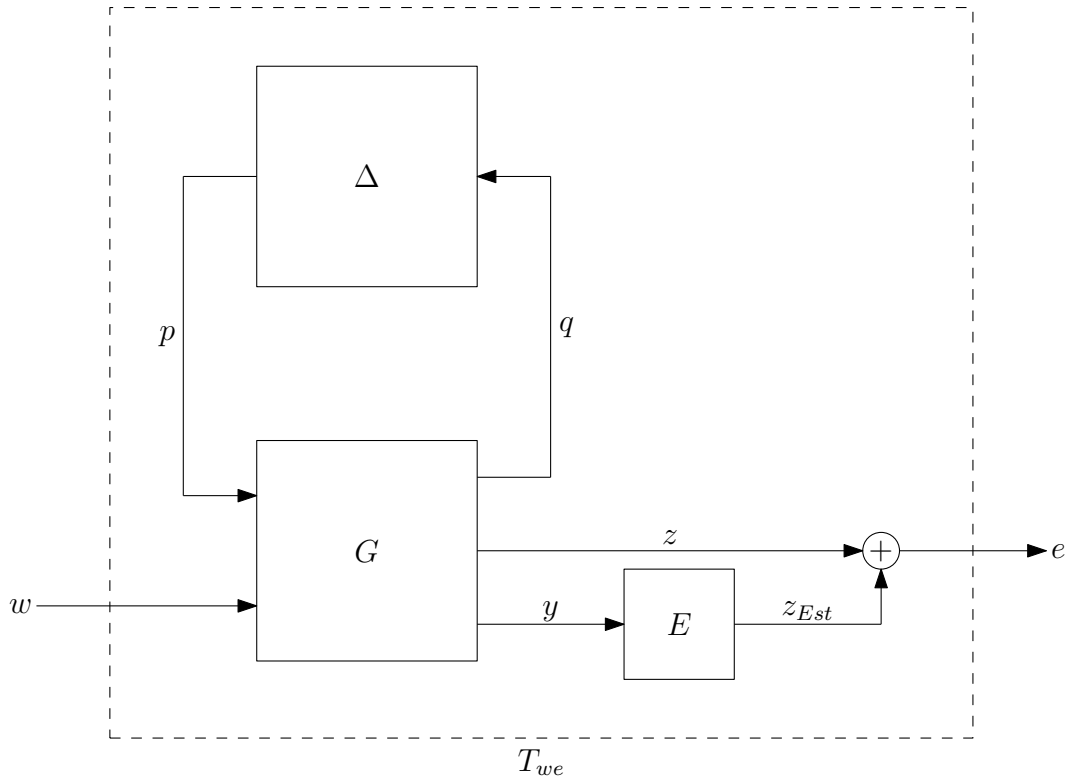

Figure 7.23. A basic estimation scheme with the uncertainties taken out

As stated before, all of the predictable uncertainties are collected in Δ. The aim is to find an estimator such that the H_∞ or the H_2-norm is minimized for all possible variations of Δ.

According to [16], the robust H_2 and H_∞-estimation problems where Δ is characterized by dynamic IQCs admit LMI solutions. As stated before, LMIs are convex optimization problems. Therefore, LMIs can be solved using techniques involved in convex optimization.

By trying to minimize the $\mathcal{L}_2$-gain of the system, an estimator can be found. Here, it is important to emphasize that this estimator is not the only estimator that can be found. It is an estimator found using the methodology in [16].

Theorem 7.1 ([16])**.** *There exists an estimator such that A and A_E are stable if the*

LMIs

$$\star^{*}\begin{bmatrix} 0 & 0 & I & 0 & 0 & 0 & 0 & 0 \\ 0 & 0 & 0 & I & 0 & 0 & 0 & 0 \\ I & 0 & 0 & 0 & 0 & 0 & 0 & 0 \\ 0 & I & 0 & 0 & 0 & 0 & 0 & 0 \\ 0 & 0 & 0 & 0 & P & Q & 0 & 0 \\ 0 & 0 & 0 & 0 & Q^T & R & 0 & 0 \\ 0 & 0 & 0 & 0 & 0 & 0 & \gamma^{-1}I & 0 \\ 0 & 0 & 0 & 0 & 0 & 0 & 0 & -\gamma I \end{bmatrix}$$

$$\begin{bmatrix} I & 0 & 0 & 0 \\ 0 & I & 0 & 0 \\ ZA & ZA & ZB_p & ZB_w \\ K & XA+LC_y & XB_p+LD_{yp} & XB_w+LD_{yw} \\ C_q & C_q & D_{qp} & D_{qw} \\ 0 & 0 & I & 0 \\ C_z+M & C_z+NC_y & D_{zp}+ND_{yp} & D_{zw}+ND_{yw} \\ 0 & 0 & 0 & I \end{bmatrix} \prec 0 \tag{7.119}$$

and

$$X - Z \succ 0 \tag{7.120}$$

are satisfied. This estimator is then written as

$$E(s) = C_E (sI - A_E)^{-1} B_E + D_E \tag{7.121}$$

where

$$A_E = (XA + LC_y - K)(X - Z)^{-1}, \tag{7.122}$$

$$B_E = L, \tag{7.123}$$

$$C_E = M(X - Z)^{-1}, \tag{7.124}$$

$$D_E = -N. \tag{7.125}$$

It should also be noted that Q is a skew-symmetric matrix and

$$R = -P. \tag{7.126}$$

As stated before, the two LMIs in the theorem lead to a convex optimization problem in matrix variables K, L, M, N, P, Q, R, X, Z and γ. In the solution, it is important to try to keep γ as minimum as possible.

The solution thereafter requires computational tools. YALMIP [21] and SeDuMi [22], which are toolboxes designed for use with MATLAB, are used in the solution of the convex optimization problem. YALMIP is a parser which can operate in conjunction with SeDuMi. Its command line interface makes using SeDuMi easier. SeDuMi is the solver. It is used to solve the convex optimization problem.

Two estimators are designed using the theory above. The first one is the "nominal" estimator, which means that uncertainties within the system are neglected. This estimator is designed using the previously determined parameter values for the Single Track Model and a longitudinal velocity of 60 km/h. As it is stated before, it is important to keep γ as minimum as possible. The solution of the convex optimization problem for the nominal estimator returns a value of $3.18 \cdot 10^{-6}$ for γ. The matrices,

which make up the estimator, are found as the following:

$$A_E = \begin{bmatrix} -2.84{\cdot}10^{2} & 1.35{\cdot}10 & 4.08 & 3.96{\cdot}10^{-1} & 2.48{\cdot}10^{-2} & 4.61{\cdot}10^{-4} & 4.38{\cdot}10^{-3} \\ 2.90{\cdot}10^{3} & -7.61{\cdot}10^{2} & -1.28{\cdot}10^{2} & -1.10{\cdot}10 & -6.73{\cdot}10^{-1} & -1.25{\cdot}10^{-2} & -1.19{\cdot}10^{-1} \\ -1.27{\cdot}10^{4} & 9.92{\cdot}10^{3} & 1.50{\cdot}10^{3} & 1.32{\cdot}10^{2} & 8.89 & 1.69{\cdot}10^{-1} & 1.60 \\ -1.07{\cdot}10^{5} & -9.40{\cdot}10^{4} & -1.43{\cdot}10^{4} & -1.35{\cdot}10^{3} & -9.42{\cdot}10 & -1.52 & -1.42{\cdot}10 \\ -5.77{\cdot}10^{5} & -4.46{\cdot}10^{4} & -8.14{\cdot}10^{3} & -6.77{\cdot}10^{2} & -5.61{\cdot}10 & -6.54 & -6.31{\cdot}10 \\ -1.34{\cdot}10^{6} & -2.84{\cdot}10^{5} & -4.54{\cdot}10^{4} & -4.26{\cdot}10^{3} & -2.60{\cdot}10^{2} & -2.12{\cdot}10 & -6.81{\cdot}10 \\ 1.39{\cdot}10^{7} & 2.97{\cdot}10^{6} & 4.60{\cdot}10^{5} & 4.28{\cdot}10^{4} & 2.84{\cdot}10^{3} & 4.94{\cdot}10 & 4.35{\cdot}10^{2} \end{bmatrix} \tag{7.127}$$

$$B_E = \begin{bmatrix} 6.21 \\ -1.71{\cdot}10^{2} \\ 1.62{\cdot}10^{3} \\ 4.93{\cdot}10^{2} \\ -1.98{\cdot}10^{5} \\ -7.57{\cdot}10^{4} \\ 2.42{\cdot}10^{4} \end{bmatrix} \tag{7.128}$$

$$C_E = \begin{bmatrix} -4.16 & -8.79{\cdot}10^{-1} & -1.41{\cdot}10^{-1} & -1.32{\cdot}10^{-2} & -8.06{\cdot}10^{-4} & -9.80{\cdot}10^{-5} & -1.58{\cdot}10^{-4} \end{bmatrix} \tag{7.129}$$

$$D_E = 9.31{\cdot}10^{-5} \tag{7.130}$$

The second estimator is the "robust" estimator, which means that uncertainties within the system are taken into account. As the result of the sensitivity analysis, the longitudinal velocity is the most sensitive parameter. This is why the uncertainties related with the longitudinal velocity are taken out in Section 7.2.2. This estimator is designed using the previously determined parameter values for the Single Track Model and a longitudinal velocity of 60 km/h. The uncertainty of the longitudinal velocity is set as 20 km/h. As it is stated before, it is important to keep γ as minimum as possible. The solution of the convex optimization problem for the robust estimator returns a value of $2.75 \cdot 10^{-1}$ for γ. The matrices, which make up the estimator, are

found as the following:

$$A_E = \begin{bmatrix} -3.33 \cdot 10 & -9.92 \cdot 10 \\ -1.24 \cdot 10 & -1.33 \cdot 10^2 \end{bmatrix} \tag{7.131}$$

$$B_E = \begin{bmatrix} -8.87 \cdot 10^{-2} \\ -5.41 \cdot 10^{-1} \end{bmatrix} \tag{7.132}$$

$$C_E = \begin{bmatrix} -9.26 & -2.81 \cdot 10 \end{bmatrix} \tag{7.133}$$

$$D_E = 2.90 \cdot 10^{-3} \tag{7.134}$$

8. TESTS WITH THE NONLINEAR MODEL

Here, the previously obtained nominal and robust estimators are connected to the nonlinear model. The tests are conducted with two kinds of steering wheel inputs. The first one is a sine wave steering wheel input with an amplitude of 45° and a period of 2.2 s. The second one is a step steering wheel input where the steering wheel angle increases to 45° in 0.2 s. The tests are conducted with the longitudinal velocities of 60 and 80 km/h. The obtained side-slip angle curves are represented in Figures 8.1 - 8.6 on pages 120 - 123.

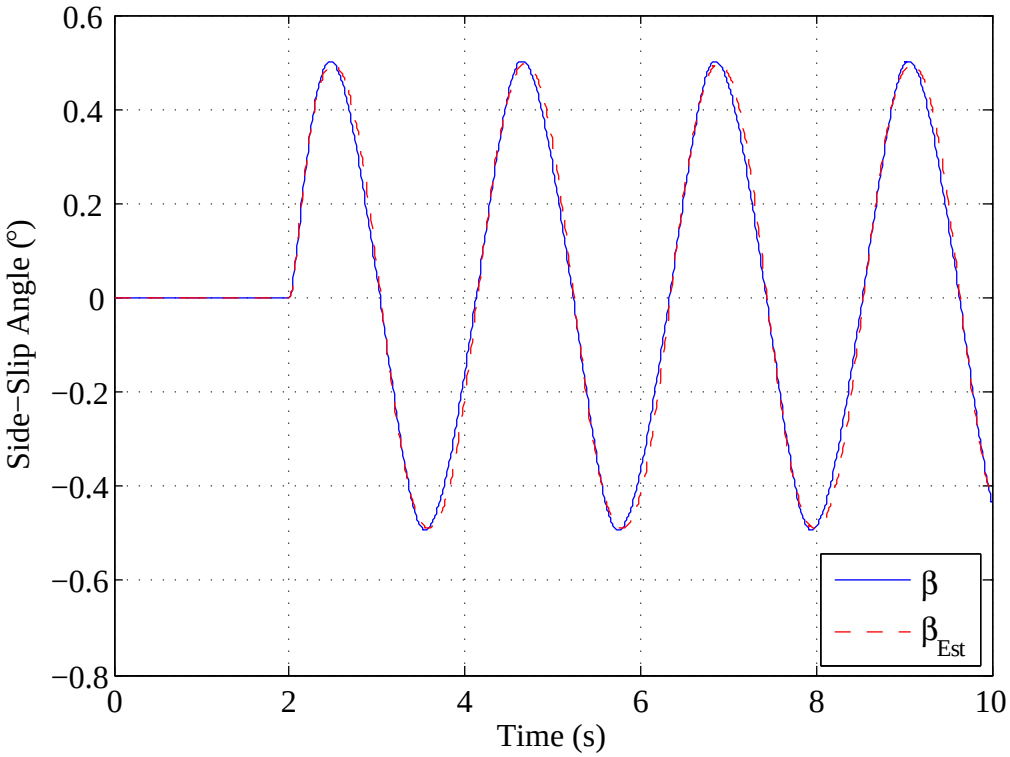

Figure 8.1. Nonlinear model with the sine wave steering wheel input at a longitudinal velocity of 60 km/h using the nominal estimator

For the sine wave steering wheel input case, the results show that the estimators perform better when the longitudinal velocity is 60 km/h. This is predictable because the nominal value of the longitudinal velocity is chosen as 60 km/h during the estimator design. As the longitudinal velocity is varied from 60 km/h, the difference between the estimated and real side-slip angle values increases. This is observed when the

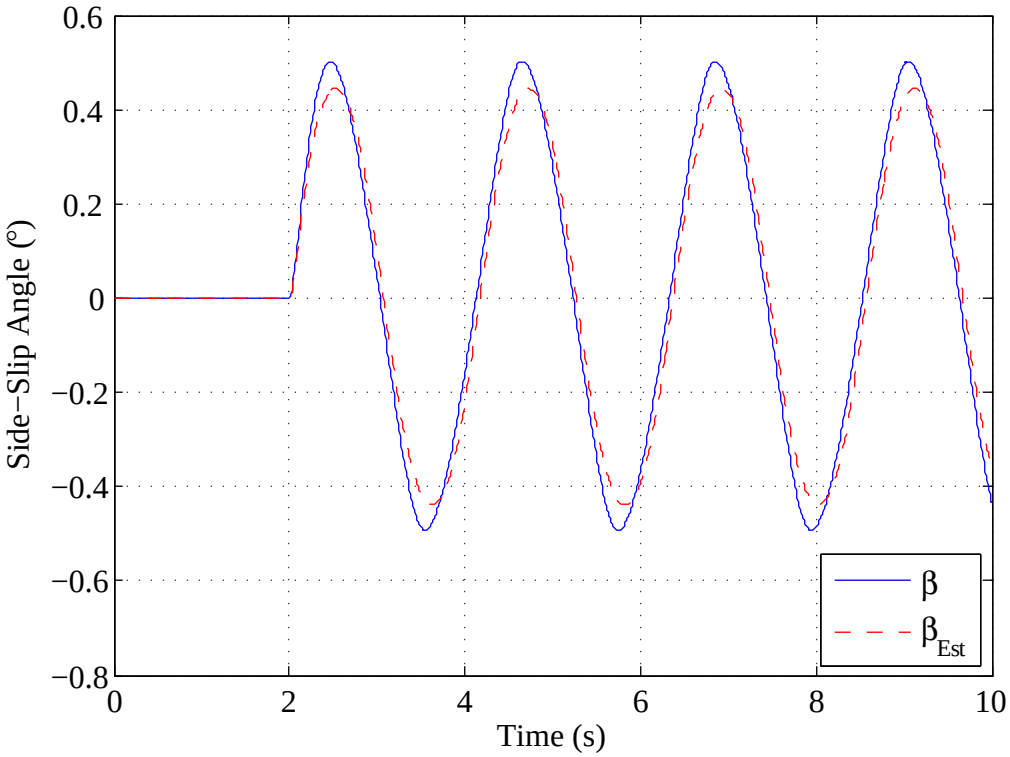

Figure 8.2. Nonlinear model with the sine wave steering wheel input at a longitudinal velocity of 60 km/h using the robust estimator

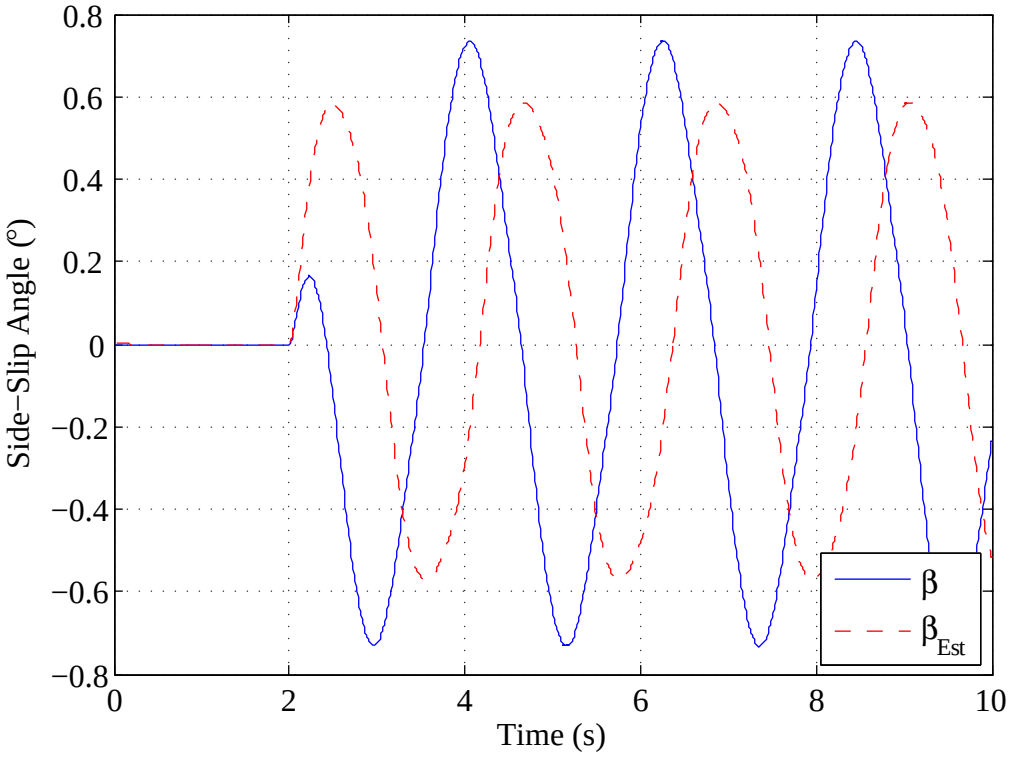

Figure 8.3. Nonlinear model with the sine wave steering wheel input at a longitudinal velocity of 80 km/h using the nominal estimator

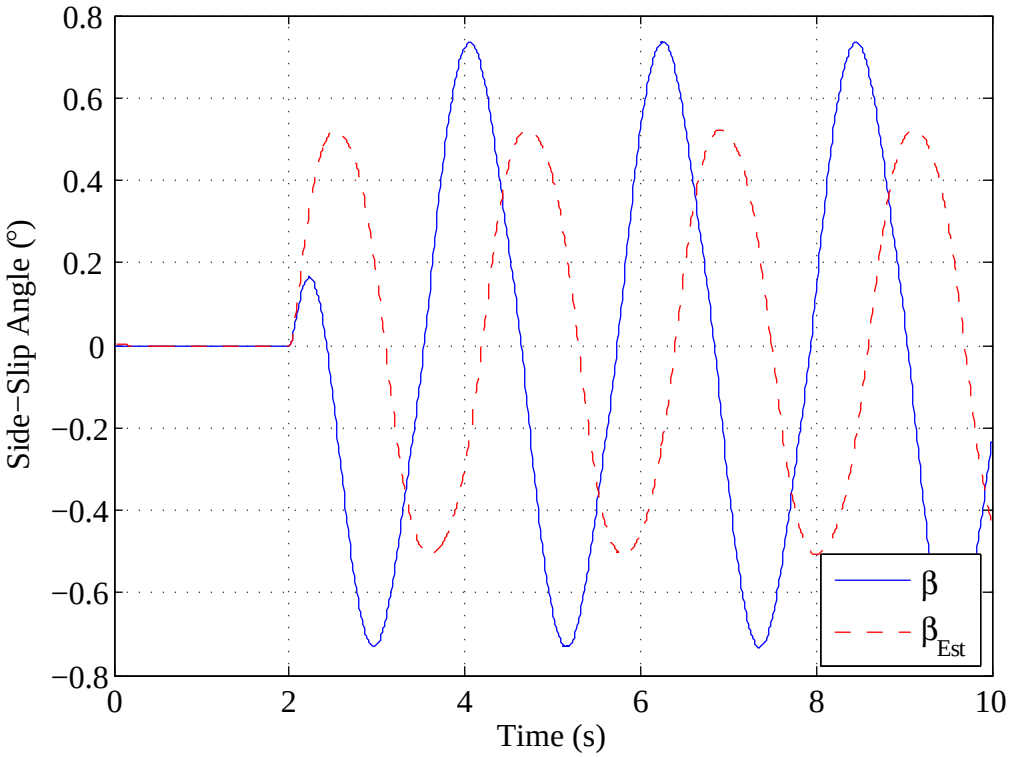

Figure 8.4. Nonlinear model with the sine wave steering wheel input at a longitudinal velocity of 80 km/h using the robust estimator

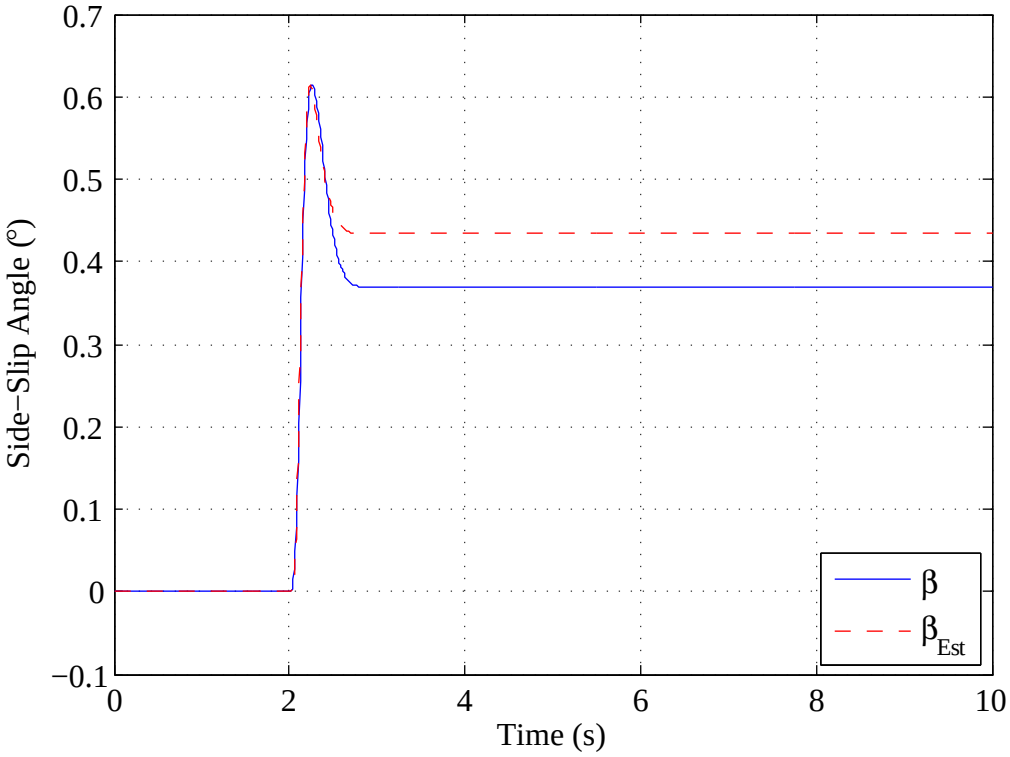

Figure 8.5. Nonlinear model with the step steering wheel input at a longitudinal velocity of 60 km/h using the nominal estimator

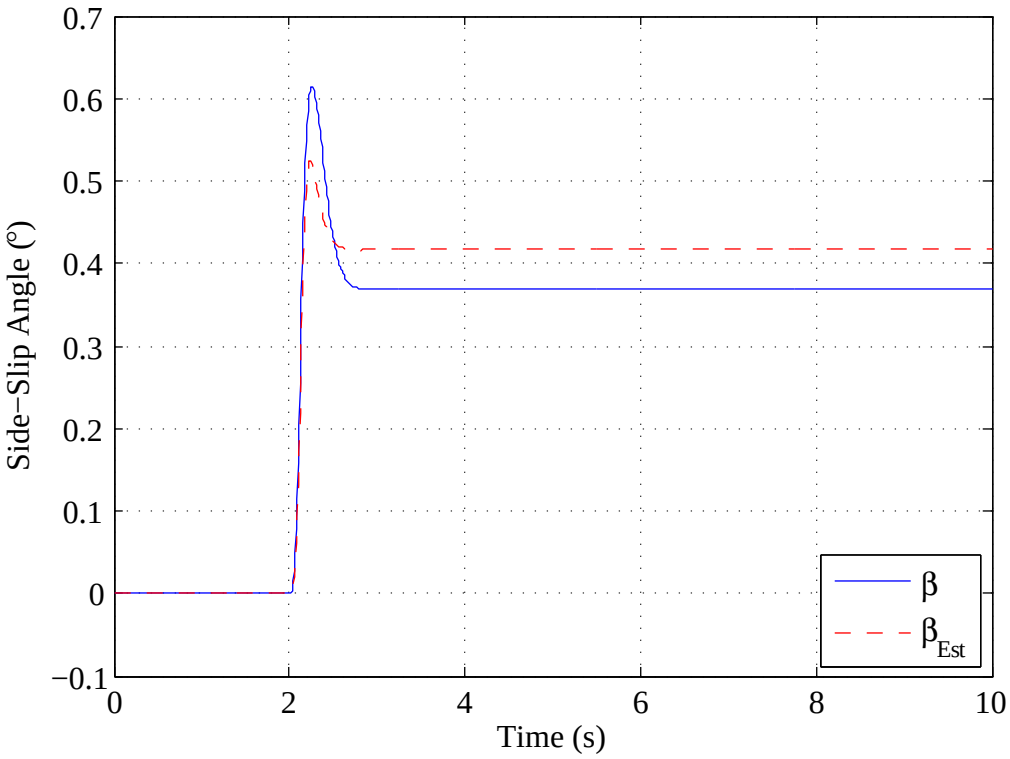

Figure 8.6. Nonlinear model with the step steering wheel input at a longitudinal velocity of 60 km/h using the robust estimator

longitudinal velocity is increased to 80 km/h.

Here, it is also necessary to compare the performances of the estimators. When the longitudinal velocity is 60 km/h, it is expected that the nominal estimator performs better because it is previously designed by using the nominal value of 60 km/h. Looking at the figures, it is concluded that the nominal estimator performs better when the longitudinal velocity is 60 km/h. Since the nominal estimator is designed without considering any uncertainty within the system, it is expected to perform worse than the robust estimator when the longitudinal velocity differs from the nominal value. This explains why the robust estimator performs better than the nominal estimator when the longitudinal velocity is 80 km/h.

The nonlinear model responds slightly worse when the steering wheel input is step. This is due to the rapid change of the steering wheel angle in the case of step steering wheel input.

9. TESTS WITH THE SINGLE TRACK MODEL

In this section, the previously obtained nominal and robust estimators are connected to the Single Track Model. The tests are conducted with two kinds of steering wheel inputs. The first one is a sine wave steering wheel input with an amplitude of 45° and a period of 2.2 s. The second one is a step steering wheel input where the steering wheel angle increases to 45° in 0.2 s. The tests are conducted with the longitudinal velocities of 60 and 80 km/h. The obtained side-slip angle curves are represented in Figures 9.1 - 9.6 on pages 124 - 127.

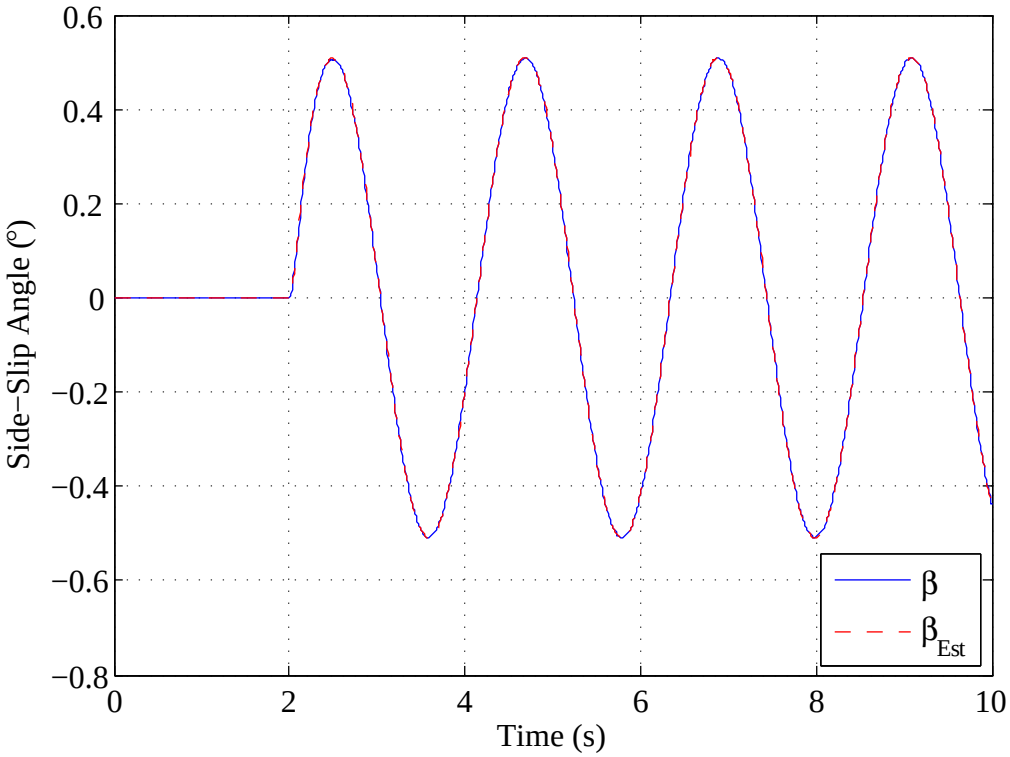

Figure 9.1. Single Track Model with the sine wave steering wheel input at a longitudinal velocity of 60 km/h using the nominal estimator

For the sine wave steering wheel input case, the results show that the estimators perform better when the longitudinal velocity is 60 km/h. This is predictable because the nominal value of the longitudinal velocity is chosen as 60 km/h during the estimator design. As the longitudinal velocity is varied from 60 km/h, the difference between the estimated and real side-slip angle values increases. This is observed when the

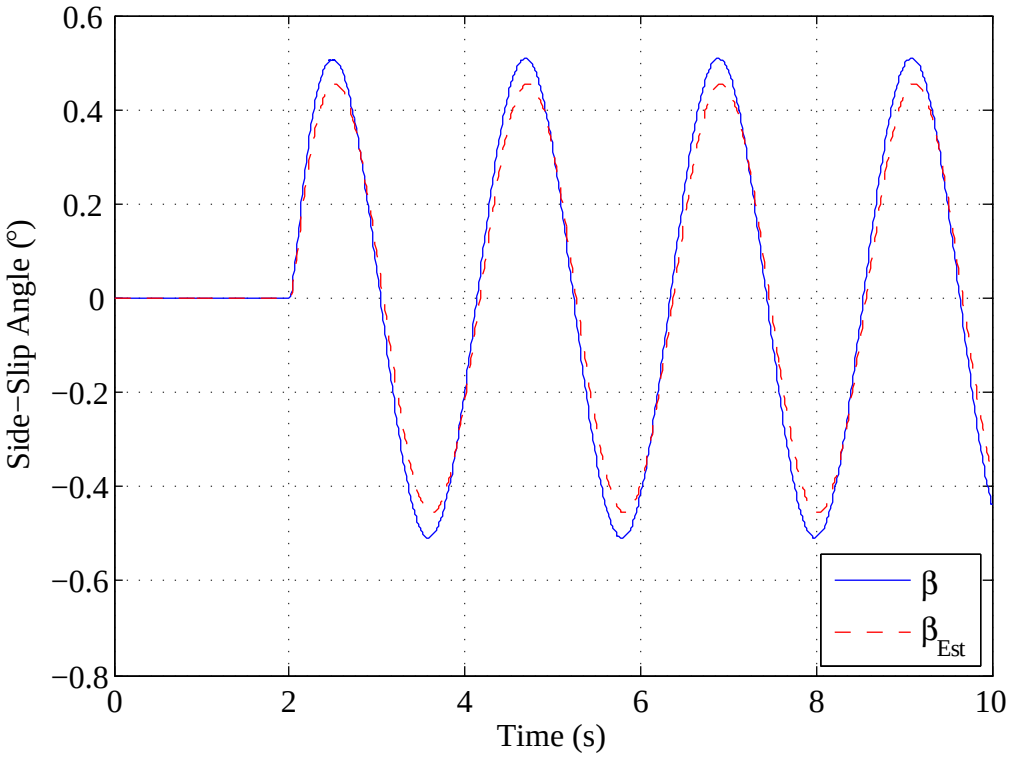

Figure 9.2. Single Track Model with the sine wave steering wheel input at a longitudinal velocity of 60 km/h using the robust estimator

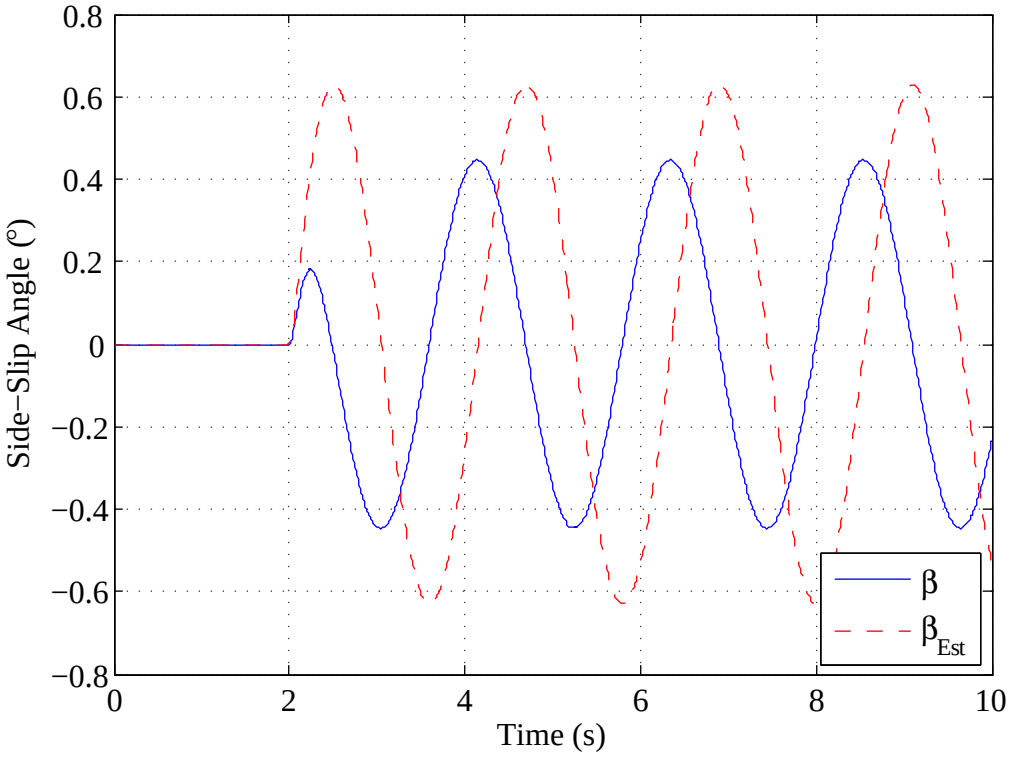

Figure 9.3. Single Track Model with the sine wave steering wheel input at a longitudinal velocity of 80 km/h using the nominal estimator

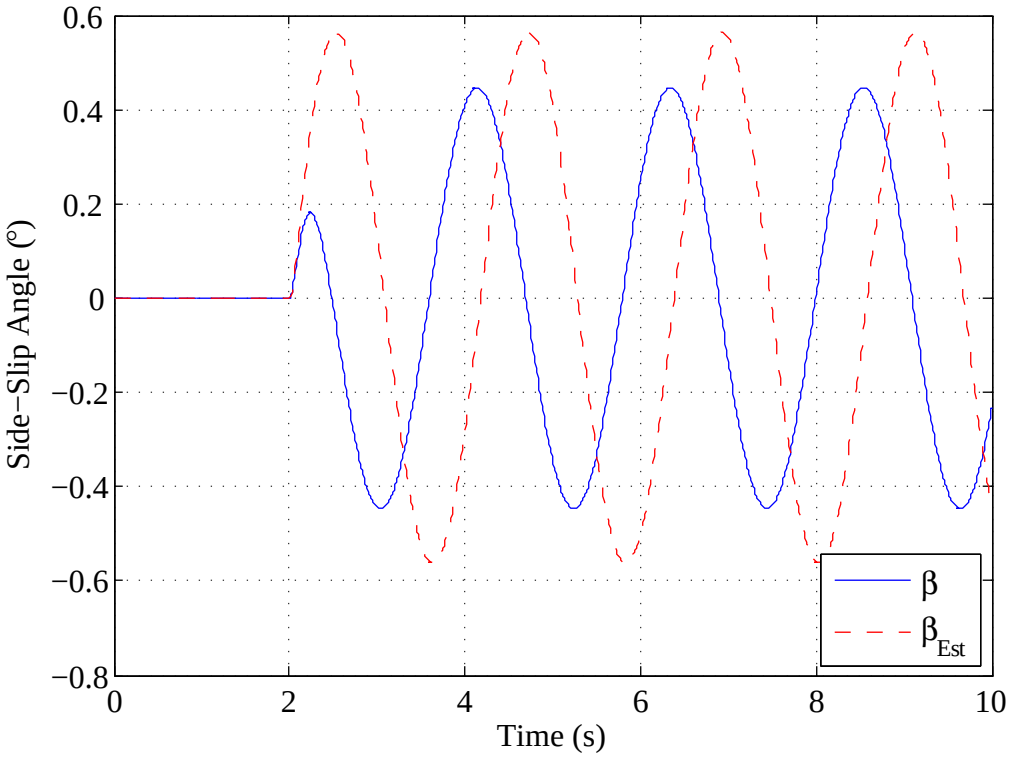

Figure 9.4. Single Track Model with the sine wave steering wheel input at a longitudinal velocity of 80 km/h using the robust estimator

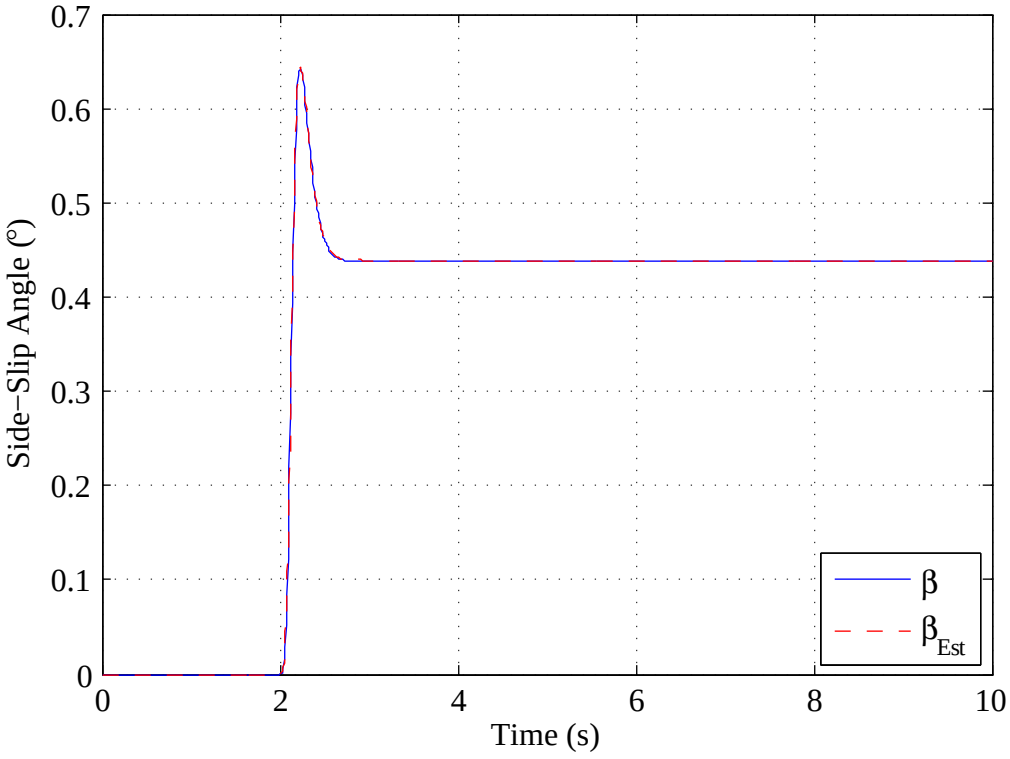

Figure 9.5. Single Track Model with the step steering wheel input at a longitudinal velocity of 60 km/h using the nominal estimator

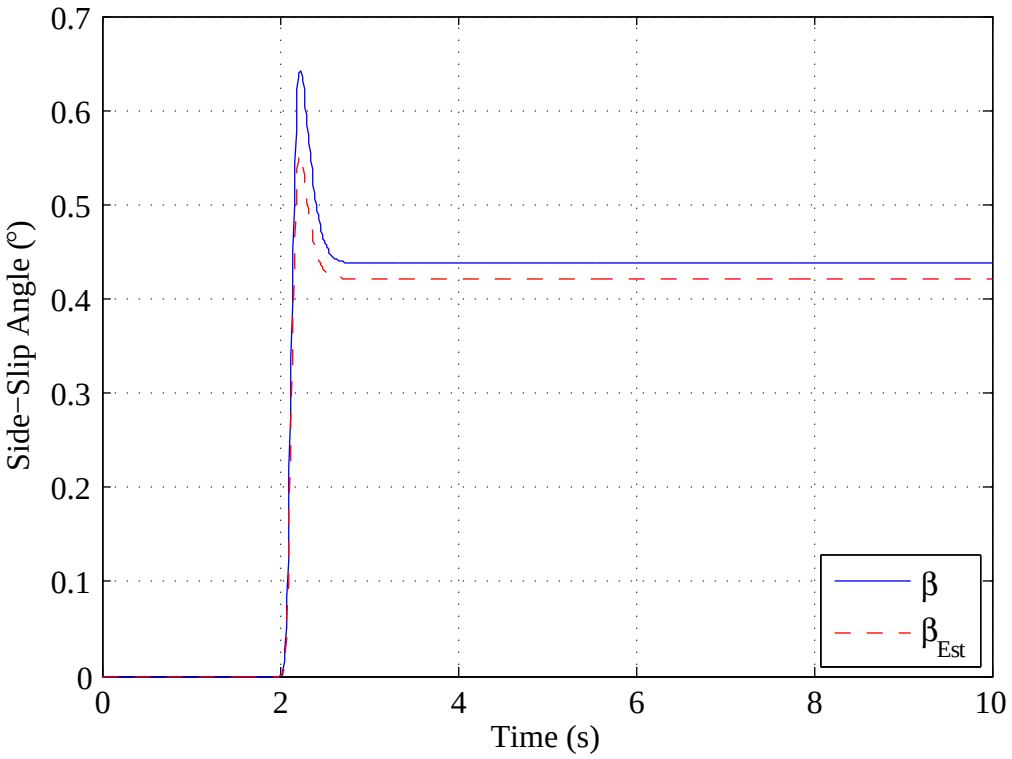

Figure 9.6. Single Track Model with the step steering wheel input at a longitudinal velocity of 60 km/h using the robust estimator

longitudinal velocity is increased to 80 km/h.

Here, it is also necessary to compare the performances of the estimators. When the longitudinal velocity is 60 km/h, it is expected that the nominal estimator performs better because it is previously designed by using the nominal value of 60 km/h. Looking at the figures, it is concluded that the nominal estimator performs better when the longitudinal velocity is 60 km/h. Since the nominal estimator is designed without considering any uncertainty within the system, it is expected to perform worse than the robust estimator when the longitudinal velocity differs from the nominal value. This explains why the robust estimator performs better than the nominal estimator when the longitudinal velocity is 80 km/h.

10. CONCLUSIONS

In this text, the behaviors and performances of two side-slip estimators (namely the "nominal" and the "robust" estimator) are studied. The estimator design is based on the well-known Single Track Model. The parameter values of the Single Track Model are determined according to a more complex nonlinear model so that the two models behave similarly. After the construction of the estimators, these two models are simulated using the estimators. The curves of both the real and estimated side-slip angles, which are obtained for different cases, are placed on the same graphs to be able to compare the difference between the real and estimated values of the side-slip angle.

The performances of the side-slip estimators are dependent on the model used. The estimators are designed considering the Single Track Model, so it is expected that the simulations with the Single Track Model return better results than the ones with the nonlinear model. When the results are compared, it is seen that this prediction is correct. For the same conditions and inputs, the difference between the real and estimated values of the side-slip angle (namely the "error") is smaller for the Single Track Model. Because of the nonlinearity of the nonlinear model, the estimator performance is lower. The nonlinear model includes many parts when compared with the Single Track Model. Also, all of the rotations (roll, pitch and yaw) are performed in the nonlinear model whereas only yaw is performed in the Single Track Model. In addition, the tyres and suspensions show nonlinear characteristics in the nonlinear model. Because of these facts, the performances of the estimators are lower when they are used with the nonlinear model.

It is observed that the performances of the side-slip estimators are also related with the type of the input. Therefore, it should be noted that the constructed estimator has to be tested with possible different inputs to see if the estimator is capable to work with all of the inputs which are given to the plant.

The side-slip estimators are designed using the nominal value of 60 km/h for the

longitudinal velocity. For both the Single Track Model and the nonlinear model, the estimation error increases as the longitudinal velocity varies. Therefore, it is concluded that the nominal values of the selected uncertain parameters have to be set carefully during estimator design using static multipliers. Also, the operating range has to be defined correctly for each parameter. After designing, the estimator has to be tested to see if it works well in the selected range for each uncertain parameter.

The simulations are done using different models (the Single Track Model and the nonlinear model) with varying inputs (steering wheel angle) and conditions (longitudinal velocity). By looking at the results, it is seen that some error exists in every simulation. Here, however, it is very important to note that error does not increase in any simulation as the simulation runs. This fact shows that the error is controlled and kept in a margin, even if the margin is different for each simulation.

As it is stated before, the designed side-slip estimators are fed by the yaw rate data. In other words, the estimator obtains the side-slip angle by processing the yaw rate data. The yaw rate data are obtained via the yaw rate sensors. It is possible to improve estimator performance by designing it so that lateral acceleration or lateral velocity data are input. But when this is done, a lateral acceleration sensor is required of course.

Another factor, which affects estimator performance, may be the selection of the uncertain parameters. As stated before, longitudinal velocity is the parameter to which the models are most sensitive. Therefore, it is selected as the uncertain parameter. However, side-slip estimator performance can be improved by including some other parameters as uncertain parameters. This increases estimator robustness. As estimator robustness increases, the side-slip estimation error is expected to decrease.

The whole estimator design is done using static multipliers during the characterization of the uncertainties in terms of IQCs. Using dynamic multipliers instead, may increase estimator performance because dynamic multipliers also account for the dynamics of the system. This makes the estimator operate better in different condi-

tions. In this case, the estimation error is expected to be less as a result of increased estimator performance.

APPENDIX A: PRELIMINARIES

In order to make the whole text easier to understand, the preliminaries are included. However, only the information, which is required and used, appear here. Therefore, this discussion is brief because the main purpose is to help the reader. A literature search has to be conducted for detailed information about the topics.

A.1. Vector Transformations in Two Dimensions

Studying vector transformations in two dimensions makes it easier to analyze more complex motions. Here, two coordinate frames are considered and the representations of a vector in these coordinate frames are studied. Then, the transformation matrices are found.

The first coordinate frame is made up of x, y and z axes. The x and y axes lie on the plane of interest. On the other hand, the z axis is normal to that plane.

The second coordinate frame is made up of x', y' and z' axes. The x' and y' axes lie on the plane of interest just like the x and y axes. The z' axis is normal to the plane.

To make it easier, it is assumed that the z and z' axes coincide. In this case, the origins of the coordinate frames must also coincide because the x, y, x' and y' axes must lie on the same plane. The $x'y'z'$ coordinate frame is rotated about the z' axis in the positive sense with respect to the xyz coordinate frame. This is seen in Figure A.1 on page 132 with the addition of an arbitrarily chosen vector $\boldsymbol{A}$ which also lies on the plane of interest.

A vector can be written in the component form according to any coordinate frame. Vector $\boldsymbol{A}$ is written in the component form according to the xyz and $x'y'z'$ coordinate

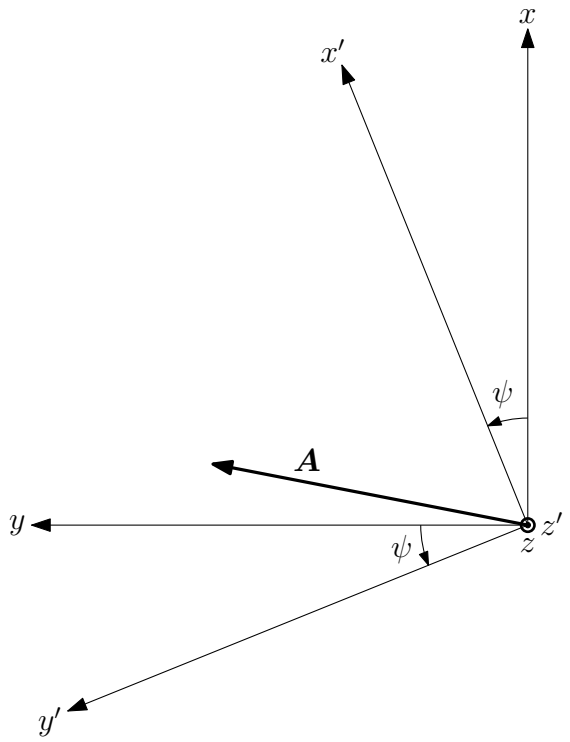

Figure A.1. Two coordinate frames and a vector in two dimensions

frames as the following:

$$\boldsymbol{A} = A_x\boldsymbol{i} + A_y\boldsymbol{j} + A_z\boldsymbol{k} \tag{A.1a}$$

$$= \begin{bmatrix} A_x \\ A_y \\ A_z \end{bmatrix}_{ijk} \tag{A.1b}$$

$$= A_{x'}\boldsymbol{i'} + A_{y'}\boldsymbol{j'} + A_{z'}\boldsymbol{k'} \tag{A.1c}$$

$$= \begin{bmatrix} A_{x'} \\ A_{y'} \\ A_{z'} \end{bmatrix}_{i'j'k'} \tag{A.1d}$$

Using trigonometric relations, the following equations are written easily. These

equations provide the correlation between the components of vector $\boldsymbol{A}$.

$$A_x = A_{x'} \cos\psi - A_{y'} \sin\psi \tag{A.2}$$

$$A_y = A_{x'} \sin\psi + A_{y'} \cos\psi \tag{A.3}$$

$$A_z = A_{z'} \tag{A.4}$$

$$A_{x'} = A_x \cos\psi + A_y \sin\psi \tag{A.5}$$

$$A_{y'} = -A_x \sin\psi + A_y \cos\psi \tag{A.6}$$

$$A_{z'} = A_z \tag{A.7}$$

The above equation sets can also be written in the matrix form. Here, the three by three matrices are called "transformation matrices". This type of matrices are used throughout the text.

$$\begin{bmatrix} A_x \\ A_y \\ A_z \end{bmatrix} = \begin{bmatrix} \cos\psi & -\sin\psi & 0 \\ \sin\psi & \cos\psi & 0 \\ 0 & 0 & 1 \end{bmatrix} \begin{bmatrix} A_{x'} \\ A_{y'} \\ A_{z'} \end{bmatrix} \tag{A.8}$$

$$\begin{bmatrix} A_{x'} \\ A_{y'} \\ A_{z'} \end{bmatrix} = \begin{bmatrix} \cos\psi & \sin\psi & 0 \\ -\sin\psi & \cos\psi & 0 \\ 0 & 0 & 1 \end{bmatrix} \begin{bmatrix} A_x \\ A_y \\ A_z \end{bmatrix} \tag{A.9}$$

It should also be noted that

$$T^{-1} = T^T \tag{A.10}$$

where T is a transformation matrix [23].

A.2. Time Derivative with Respect to Different Coordinate Frames

Here, a time dependent vector $\boldsymbol{Q}(\boldsymbol{t})$ is considered. Also, two coordinate frames are defined. The first coordinate frame is the XYZ coordinate frame. The second one is the xyz coordinate frame. The xyz coordinate frame rotates with the angular velocity $\boldsymbol{\Omega}$ with respect to the fixed coordinate frame XYZ.

First, the time dependent vector is written in the component form as

$$\boldsymbol{Q} = Q_x\boldsymbol{i} + Q_y\boldsymbol{j} + Q_z\boldsymbol{k}. \tag{A.11}$$

Now, the time derivative of this vector with respect to the xyz coordinate frame is calculated. Since the derivative taken is with respect to the xyz coordinate frame, $\boldsymbol{i}$, $\boldsymbol{j}$ and $\boldsymbol{k}$ are considered to be constant. The yielding equation is

$$\left(\dot{\boldsymbol{Q}}\right)_{xyz} = \dot{Q}_x\boldsymbol{i} + \dot{Q}_y\boldsymbol{j} + \dot{Q}_z\boldsymbol{k}. \tag{A.12}$$

Next, the time derivative of this vector with respect to the XYZ coordinate frame is calculated. Since the derivative taken is with respect to the XYZ coordinate frame, $\boldsymbol{i}$, $\boldsymbol{j}$ and $\boldsymbol{k}$ are no longer considered to be constant. The yielding equation is

$$\left(\dot{\boldsymbol{Q}}\right)_{XYZ} = \dot{Q}_x\boldsymbol{i} + \dot{Q}_y\boldsymbol{j} + \dot{Q}_z\boldsymbol{k} + Q_x\dot{\boldsymbol{i}} + Q_y\dot{\boldsymbol{j}} + Q_z\dot{\boldsymbol{k}}. \tag{A.13}$$

In the above equation, it is easily seen that the first three terms on the right side are equal to the time derivative of vector $\boldsymbol{Q}$ with respect to the xyz coordinate frame. In addition, the last three terms on the right side of the equation can be written as $\boldsymbol{\Omega} \times \boldsymbol{Q}$ [23]. Details of this are not covered in this text. After the replacements, the

equation becomes to

$$\left(\dot{\boldsymbol{Q}}\right)_{XYZ} = \left(\dot{\boldsymbol{Q}}\right)_{xyz} + \boldsymbol{\Omega} \times \boldsymbol{Q}. \tag{A.14}$$

The use of time derivative of a vector is very common. The result changes if the derivative is taken with respect to different coordinate frames. Therefore, care should be taken while taking the time derivative of a vector.

A.3. Relations between Position, Velocity and Acceleration of a Point

First, a fixed coordinate frame (reference coordinate frame) is defined. This is the XYZ coordinate frame which neither translates nor rotates. Then, a moving point A is considered. Finally, another point named K is defined; this point is stationary. This is the reference point which is used while defining the position, velocity and acceleration of point A.

The relation between the position and the velocity of point A is written as the following. Here, it should be noted that position and velocity of point A are defined with respect to point K as stated before.

$$\left(\dot{\boldsymbol{p}}_{\boldsymbol{A/K}}\right)_{XYZ} = \boldsymbol{v}_{\boldsymbol{A/K}} \tag{A.15}$$

The relation between the velocity and the acceleration of point A is written as the following. Here, it should be noted that velocity and acceleration of point A are defined with respect to point K as stated before.

$$\left(\dot{\boldsymbol{v}}_{\boldsymbol{A/K}}\right)_{XYZ} = \boldsymbol{a}_{\boldsymbol{A/K}} \tag{A.16}$$

A.4. Rigid Bodies

In this section, rigid bodies are studied briefly. It is especially important to note that only the properties and concepts, which are used in the text, are discussed here. In the first part, properties of rigid bodies, which are independent of motion, are studied. In the second part, motion of a rigid body in three dimensions is studied.

A.4.1. Mass and Inertia of a Rigid Body

A.4.1.1. Inertia Definitions. To be able to make definitions, a coordinate frame has to be defined first. The xyz coordinate frame is attached to the rigid body and its origin is coincident with the center of gravity of the rigid body. All inertias are defined with respect to this coordinate frame.

The moments of inertia of the rigid body with respect to the xyz coordinate frame are defined as the following [24]:

$$I_x = \int \left(y^2 + z^2\right) dm \tag{A.17}$$

$$I_y = \int \left(x^2 + z^2\right) dm \tag{A.18}$$

$$I_z = \int \left(x^2 + y^2\right) dm \tag{A.19}$$

The products of inertia of the rigid body with respect to the xyz coordinate frame are defined as the following [24]:

$$I_{xy} = \int (xy)\, dm \tag{A.20}$$

$$I_{xz} = \int (xz)\, dm \tag{A.21}$$

$$I_{yz} = \int (yz)\, dm \tag{A.22}$$

It should also be noted that

$$I_{xy} = I_{yx}, \tag{A.23}$$

$$I_{xz} = I_{zx}, \tag{A.24}$$

$$I_{yz} = I_{zy} \tag{A.25}$$

according to [24].

If a rigid body is assumed to be massless, then the dm term in Equations (A.17) - (A.22) becomes zero. This makes the moments and products of inertia equal to zero.

A.4.1.2. Parallel Axis Theorem. The moments and products of inertia of a rigid body with respect to different coordinate frames are not the same. Parallel Axis Theorem defines relations between these different values.

Point G represents the center of gravity of the rigid body. The $Gxyz$ coordinate frame is attached to the rigid body and its origin is coincident with the center of gravity of the rigid body.

Point S is an arbitrary point which can be inside or outside of the rigid body. The origin of the coordinate frame $Sx'y'z'$ is coincident with point S. The axes of the $Sx'y'z'$ coordinate frame are parallel to the axes of the $Gxyz$ coordinate frame and the corresponding axes of each coordinate frame point the same direction.

Position of point G with respect to point S is shown as $\boldsymbol{p_{G/S}}$. $\bar{x}$, $\bar{y}$ and $\bar{z}$ are the components of $\boldsymbol{p_{G/S}}$ defined according to any of the two coordinate frames.

The definitions made so far are seen in Figure A.2 on page 138.

As the last definition, m stands for the mass of the rigid body.

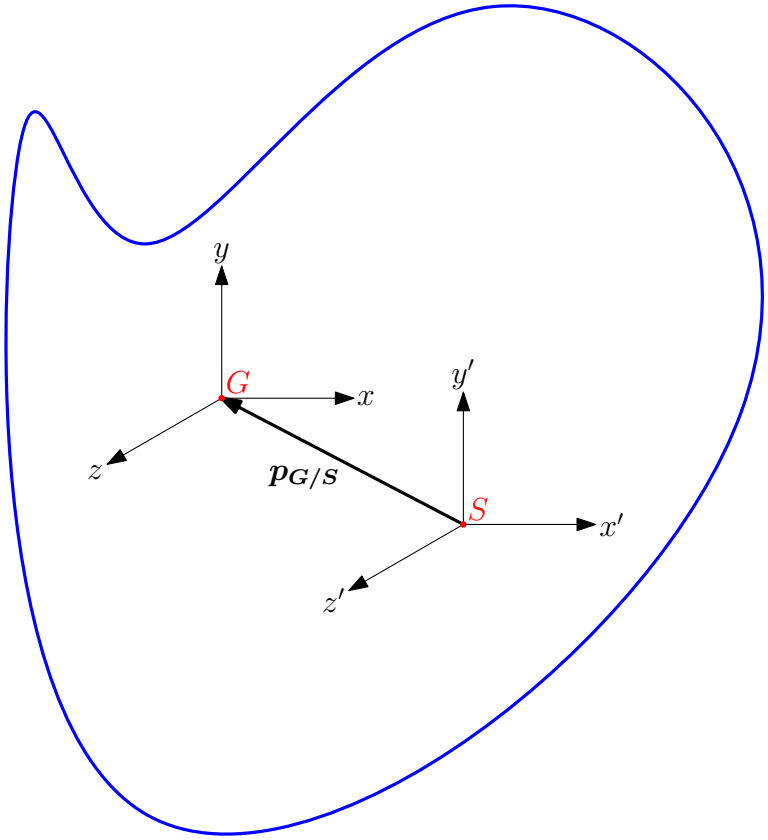

Figure A.2. Definitions for the Parallel Axis Theorem

The moments of inertia of the rigid body with respect to the $Sx'y'z'$ coordinate frame are written as the following [25]:

$$I_{x'} = I_x + m\left(\bar{y}^2 + \bar{z}^2\right) \tag{A.26}$$

$$I_{y'} = I_y + m\left(\bar{x}^2 + \bar{z}^2\right) \tag{A.27}$$

$$I_{z'} = I_z + m\left(\bar{x}^2 + \bar{y}^2\right) \tag{A.28}$$

The products of inertia of the rigid body with respect to the $Sx'y'z'$ coordinate frame are written as the following [25]:

$$I_{x'y'} = I_{xy} + m\bar{x}\bar{y} \tag{A.29}$$

$$I_{x'z'} = I_{xz} + m\bar{x}\bar{z} \tag{A.30}$$

$$I_{y'z'} = I_{yz} + m\bar{y}\bar{z} \tag{A.31}$$

A.4.1.3. Differently Oriented Coordinate Frames. Parallel Axis Theorem considers two coordinate frames with the same orientation; but their origins are attached to different points. Here, effort is spent to analyze the relations between the inertias of the rigid body when the orientations of the coordinate frames are different; but their origins coincide. The derivations are made by using the definitions in Section A.4.1.1.

Two coordinate frames are defined, namely the xyz and $x'y'z'$ coordinate frames. These two coordinate frames are attached to the same arbitrarily selected point, which is either inside or outside of the rigid body. Here, one case is selected: The x and x' axes are parallel but they point opposite directions; the same is also valid for the y and y' axes. The z and z' axes are parallel and point the same direction, they are coincident in other words. These coordinate frames are seen in Figure A.3.

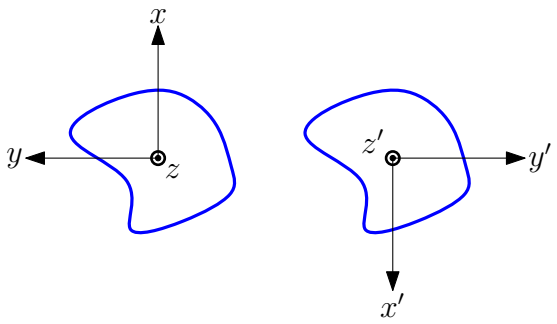

Figure A.3. Two coordinate frames with different orientations

Using Equations (A.17) - (A.22), the following equalities are written:

$$I_x = I_{x'} \tag{A.32}$$

$$I_y = I_{y'} \tag{A.33}$$

$$I_z = I_{z'} \tag{A.34}$$

$$I_{xy} = I_{x'y'} \tag{A.35}$$

$$I_{xz} = -I_{x'z'} \tag{A.36}$$

$$I_{yz} = -I_{y'z'} \tag{A.37}$$

A.4.2. Motion of a Rigid Body in Three Dimensions

A.4.2.1. Relations between Different Points in a Rigid Body. When a rigid body is moving, every point on the rigid body moves in a different manner. This fact makes it obvious that there are relations between points in a rigid body. Here, these relations are studied.

The rigid body translates and rotates freely in the three dimensional space. $\boldsymbol{\omega}$ stands for the angular velocity of the rigid body, whereas $\boldsymbol{\alpha}$ stands for the angular acceleration of the rigid body.

Two points are chosen in the rigid body; namely point A and point B. Also a stationary point is chosen in the three dimensional space, this is point K. This is the reference point which is used while defining positions, velocities and accelerations. The XYZ coordinate frame is considered to be fixed. These are seen in Figure A.4. In addition, the xyz coordinate frame is attached to the rigid body.

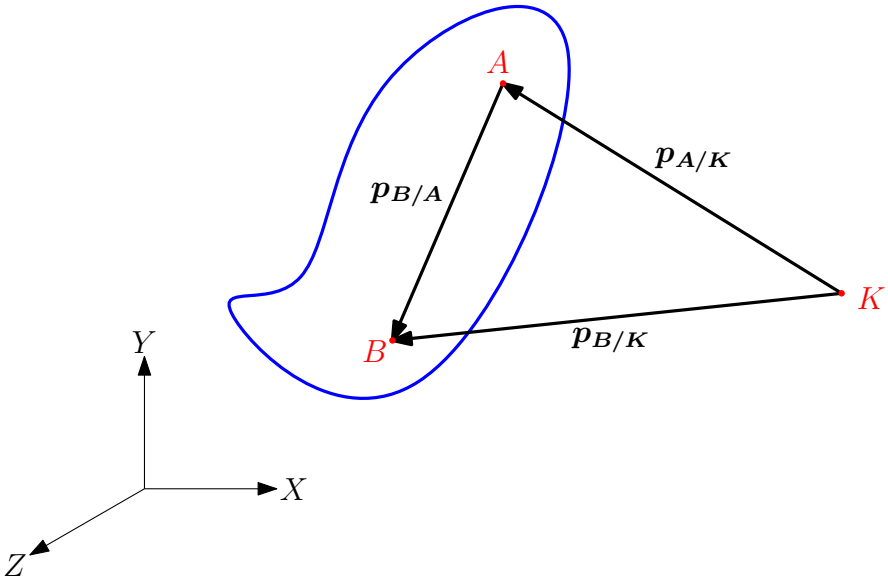

Figure A.4. A rigid body with points and positions

Looking at Figure A.4, it is clearly seen that

$$\boldsymbol{p_{B/K}} = \boldsymbol{p_{A/K}} + \boldsymbol{p_{B/A}}. \tag{A.38}$$

This equation is about the relation between the positions of the points.

Taking the derivative of the above equation with respect to the XYZ coordinate frame, the relation between the velocities of the points is found as the following:

$$\left(\dot{\boldsymbol{p}}_{\boldsymbol{B/K}}\right)_{XYZ} = \left(\dot{\boldsymbol{p}}_{\boldsymbol{A/K}}\right)_{XYZ} + \left(\dot{\boldsymbol{p}}_{\boldsymbol{B/A}}\right)_{XYZ} \tag{A.39}$$

$$\boldsymbol{v}_{\boldsymbol{B/K}} = \boldsymbol{v}_{\boldsymbol{A/K}} + \underbrace{\left(\dot{\boldsymbol{p}}_{\boldsymbol{B/A}}\right)_{xyz}}_{0} + \boldsymbol{\omega} \times \boldsymbol{p}_{\boldsymbol{B/A}} \tag{A.40}$$

$$\boldsymbol{v}_{\boldsymbol{B/K}} = \boldsymbol{v}_{\boldsymbol{A/K}} + \boldsymbol{\omega} \times \boldsymbol{p}_{\boldsymbol{B/A}} \tag{A.41}$$

Taking the derivative of the above equation with respect to the XYZ coordinate frame, the relation between the accelerations of the points is found as the following:

$$\left(\dot{\boldsymbol{v}}_{\boldsymbol{B/K}}\right)_{XYZ} = \left(\dot{\boldsymbol{v}}_{\boldsymbol{A/K}}\right)_{XYZ} + (\dot{\boldsymbol{\omega}})_{XYZ} \times \boldsymbol{p}_{\boldsymbol{B/A}} + \boldsymbol{\omega} \times \left(\dot{\boldsymbol{p}}_{\boldsymbol{B/A}}\right)_{XYZ} \tag{A.42}$$

$$\boldsymbol{a}_{\boldsymbol{B/K}} = \boldsymbol{a}_{\boldsymbol{A/K}} + \boldsymbol{\alpha} \times \boldsymbol{p}_{\boldsymbol{B/A}} + \boldsymbol{\omega} \times \left[\underbrace{\left(\dot{\boldsymbol{p}}_{\boldsymbol{B/A}}\right)_{xyz}}_{0} + \boldsymbol{\omega} \times \boldsymbol{p}_{\boldsymbol{B/A}}\right] \tag{A.43}$$

$$\boldsymbol{a}_{\boldsymbol{B/K}} = \boldsymbol{a}_{\boldsymbol{A/K}} + \boldsymbol{\alpha} \times \boldsymbol{p}_{\boldsymbol{B/A}} + \boldsymbol{\omega} \times \left(\boldsymbol{\omega} \times \boldsymbol{p}_{\boldsymbol{B/A}}\right) \tag{A.44}$$

A.4.2.2. Angular Velocity of a Rigid Body. In this section, angular velocity of a rigid body is studied. The method used is basically rotating the reference coordinate frame until the orientation of the body-fixed coordinate frame is obtained.

The reference and body-fixed coordinate frames are defined first. The $OXYZ$ coordinate frame is the reference or fixed coordinate frame. The origin of this coordinate frame is called point O. The $Gxyz$ coordinate frame is attached to the rigid body. The origin of the $Gxyz$ coordinate frame is coincident with the center of gravity of the rigid body, which is point G. These two coordinate frames are seen in Figure A.5 on page 142 as well.

As the first step, the reference coordinate frame $OXYZ$ is rotated ψ radians

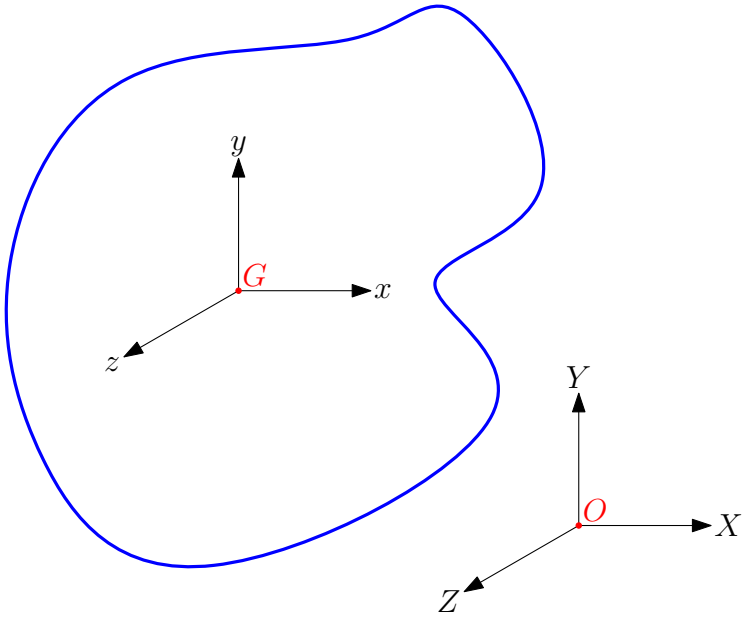

Figure A.5. The reference and body-fixed coordinate frames

about its Z axis. This rotation is called "yaw". The representation of this rotation is seen in Figure A.6.

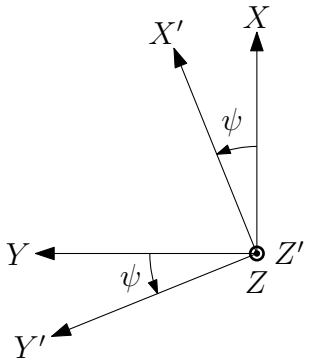

Figure A.6. Representation of the rotation about the Z axis

Next, the obtained coordinate frame $X'Y'Z'$ is rotated θ radians about its Y' axis. This rotation is called "pitch". The representation of this rotation is seen in Figure A.7 on page 143.

Finally as the third step, the obtained coordinate frame $X''Y''Z''$ is rotated ϕ radians about its X'' axis. This rotation is called "roll". The representation of this rotation is seen in Figure A.8 on page 143.

Since all of the possible rotations, that a rigid body can make, are included on the

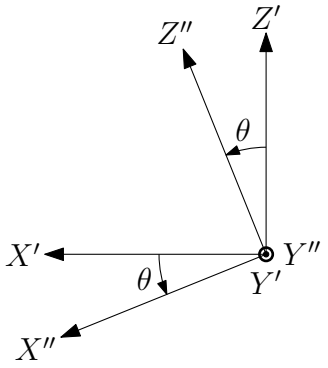

Figure A.7. Representation of the rotation about the Y' axis

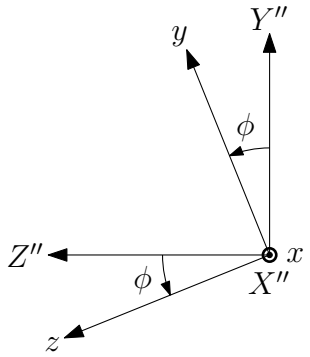

Figure A.8. Representation of the rotation about the X'' axis

previous three steps, it is concluded that the finally obtained coordinate frame is the body-fixed coordinate frame $Gxyz$. This actually means that the rotational relation between the reference and the body-fixed coordinate frames is defined completely by means of rotation angles and rotation rates (rates of rotation angles).

Using the rotation rates, the angular velocity of the rigid body is found. The rotation rates of the rigid body in the previous three steps are represented as $\dot{\psi}\boldsymbol{K}$, $\dot{\theta}\boldsymbol{J'}$ and $\dot{\phi}\boldsymbol{I''}$, respectively. Therefore, the angular velocity of the rigid body is written as

$$\boldsymbol{\omega} = \dot{\phi}\boldsymbol{I''} + \dot{\theta}\boldsymbol{J'} + \dot{\psi}\boldsymbol{K}. \tag{A.45}$$

Applying vector transformations in two dimensions to the above equation yields

$$\boldsymbol{\omega} = \dot{\phi}\boldsymbol{I''} + \dot{\theta}\boldsymbol{J'} + \dot{\psi}\boldsymbol{K'} \tag{A.46a}$$

$$= \left(\dot{\phi} - \dot{\psi}\sin\theta\right)\boldsymbol{I''} + \dot{\theta}\boldsymbol{J''} + \dot{\psi}\cos\theta\boldsymbol{K''} \tag{A.46b}$$

$$= \left(\dot{\phi} - \dot{\psi}\sin\theta\right)\boldsymbol{i} + \left(\dot{\psi}\cos\theta\sin\phi + \dot{\theta}\cos\phi\right)\boldsymbol{j} + \left(\dot{\psi}\cos\theta\cos\phi - \dot{\theta}\sin\phi\right)\boldsymbol{k}. \tag{A.46c}$$

Defining the rotation rates in terms of rotation angles and the body-fixed coordinate frame components of the angular velocity is very useful in some applications. This is done as the following [23] but the details of the derivation are not covered here.

$$\dot{\phi} = \omega_x + \frac{(\omega_y\sin\phi + \omega_z\cos\phi)\sin\theta}{\cos\theta} \tag{A.47}$$

$$\dot{\theta} = \omega_y\cos\phi - \omega_z\sin\phi \tag{A.48}$$

$$\dot{\psi} = \frac{\omega_y\sin\phi + \omega_z\cos\phi}{\cos\theta} \tag{A.49}$$

A.4.2.3. Transformations in Three Dimensions. The definitions made in Section A.4.2.2 are also valid here. This means that the coordinate frames and the angles, which are used here, are the same with the ones used in Section A.4.2.2. Here, $\boldsymbol{A}$ is an arbitrary vector.

The transformation from the reference coordinate frame components to the body-fixed coordinate frame components is found first. To do this, the two dimensional

transformations for each rotation made in Section A.4.2.2 are obtained as the following:

$$\begin{bmatrix} A_{X'} \\ A_{Y'} \\ A_{Z'} \end{bmatrix} = \begin{bmatrix} \cos\psi & \sin\psi & 0 \\ -\sin\psi & \cos\psi & 0 \\ 0 & 0 & 1 \end{bmatrix} \begin{bmatrix} A_X \\ A_Y \\ A_Z \end{bmatrix} \tag{A.50}$$

$$\begin{bmatrix} A_{X''} \\ A_{Y''} \\ A_{Z''} \end{bmatrix} = \begin{bmatrix} \cos\theta & 0 & -\sin\theta \\ 0 & 1 & 0 \\ \sin\theta & 0 & \cos\theta \end{bmatrix} \begin{bmatrix} A_{X'} \\ A_{Y'} \\ A_{Z'} \end{bmatrix} \tag{A.51}$$

$$\begin{bmatrix} A_x \\ A_y \\ A_z \end{bmatrix} = \begin{bmatrix} 1 & 0 & 0 \\ 0 & \cos\phi & \sin\phi \\ 0 & -\sin\phi & \cos\phi \end{bmatrix} \begin{bmatrix} A_{X''} \\ A_{Y''} \\ A_{Z''} \end{bmatrix} \tag{A.52}$$

Using the above three matrix equations, the following result is found:

$$\begin{bmatrix} A_x \\ A_y \\ A_z \end{bmatrix} = \begin{bmatrix} 1 & 0 & 0 \\ 0 & \cos\phi & \sin\phi \\ 0 & -\sin\phi & \cos\phi \end{bmatrix} \begin{bmatrix} \cos\theta & 0 & -\sin\theta \\ 0 & 1 & 0 \\ \sin\theta & 0 & \cos\theta \end{bmatrix} \begin{bmatrix} \cos\psi & \sin\psi & 0 \\ -\sin\psi & \cos\psi & 0 \\ 0 & 0 & 1 \end{bmatrix} \begin{bmatrix} A_X \\ A_Y \\ A_Z \end{bmatrix} \tag{A.53}$$

Next, the transformation from the body-fixed coordinate frame components to the reference coordinate frame components is found. To do this, the two dimensional transformations for each rotation made in Section A.4.2.2 are obtained as the following:

$$\begin{bmatrix} A_X \\ A_Y \\ A_Z \end{bmatrix} = \begin{bmatrix} \cos\psi & -\sin\psi & 0 \\ \sin\psi & \cos\psi & 0 \\ 0 & 0 & 1 \end{bmatrix} \begin{bmatrix} A_{X'} \\ A_{Y'} \\ A_{Z'} \end{bmatrix} \tag{A.54}$$

$$\begin{bmatrix} A_{X'} \\ A_{Y'} \\ A_{Z'} \end{bmatrix} = \begin{bmatrix} \cos\theta & 0 & \sin\theta \\ 0 & 1 & 0 \\ -\sin\theta & 0 & \cos\theta \end{bmatrix} \begin{bmatrix} A_{X''} \\ A_{Y''} \\ A_{Z''} \end{bmatrix} \tag{A.55}$$

$$\begin{bmatrix} A_{X''} \\ A_{Y''} \\ A_{Z''} \end{bmatrix} = \begin{bmatrix} 1 & 0 & 0 \\ 0 & \cos\phi & -\sin\phi \\ 0 & \sin\phi & \cos\phi \end{bmatrix} \begin{bmatrix} A_x \\ A_y \\ A_z \end{bmatrix} \tag{A.56}$$

Using the above three matrix equations, the following result is found:

$$\begin{bmatrix} A_X \\ A_Y \\ A_Z \end{bmatrix} = \begin{bmatrix} \cos\psi & -\sin\psi & 0 \\ \sin\psi & \cos\psi & 0 \\ 0 & 0 & 1 \end{bmatrix} \begin{bmatrix} \cos\theta & 0 & \sin\theta \\ 0 & 1 & 0 \\ -\sin\theta & 0 & \cos\theta \end{bmatrix} \begin{bmatrix} 1 & 0 & 0 \\ 0 & \cos\phi & -\sin\phi \\ 0 & \sin\phi & \cos\phi \end{bmatrix} \begin{bmatrix} A_x \\ A_y \\ A_z \end{bmatrix} \tag{A.57}$$

Here, it is necessary to rewrite Equation (A.10) which states that

$$T^{-1} = T^T \tag{A.58}$$

where T is a transformation matrix [23].

A.4.2.4. Force Balance Equation of a Rigid Body. Points O and G, and the coordinate frames $OXYZ$ and $Gxyz$ are defined in Section A.4.2.2. These definitions also comply here. These points and coordinate frames are seen in Figure A.5 on page 142 as well.

$\boldsymbol{F}$ stands for the total force applied on the rigid body. m and $\boldsymbol{\omega}$ stand for the mass and angular velocity of the rigid body respectively. $\boldsymbol{v_G}$ and $\boldsymbol{a_G}$ stand for the velocity and acceleration of point G with respect to point O which is fixed.

The total force applied on the rigid body is written as

$$\boldsymbol{F} = m\boldsymbol{a_G} \tag{A.59a}$$

$$= m(\dot{\boldsymbol{v}}_{\boldsymbol{G}})_{OXYZ} \tag{A.59b}$$

$$= m\left[(\dot{\boldsymbol{v}}_{\boldsymbol{G}})_{Gxyz} + \boldsymbol{\omega} \times \boldsymbol{v_G}\right] \tag{A.59c}$$

$$= m\left(\begin{bmatrix} \dot{v}_{G_x} \\ \dot{v}_{G_y} \\ \dot{v}_{G_z} \end{bmatrix}_{ijk} + \begin{bmatrix} \omega_x \\ \omega_y \\ \omega_z \end{bmatrix}_{ijk} \times \begin{bmatrix} v_{G_x} \\ v_{G_y} \\ v_{G_z} \end{bmatrix}_{ijk}\right). \tag{A.59d}$$

If the left-hand side of the equation is also written in the component form, the equation becomes to

$$\begin{bmatrix} F_x \\ F_y \\ F_z \end{bmatrix}_{ijk} = m \left(\begin{bmatrix} \dot{v}_{G_x} \\ \dot{v}_{G_y} \\ \dot{v}_{G_z} \end{bmatrix}_{ijk} + \begin{bmatrix} \omega_x \\ \omega_y \\ \omega_z \end{bmatrix}_{ijk} \times \begin{bmatrix} v_{G_x} \\ v_{G_y} \\ v_{G_z} \end{bmatrix}_{ijk} \right). \tag{A.60}$$

Here, the subscripts ijk stand to emphasize that the results are in the body-fixed coordinate frame components. Since both sides of the equation are in the same form, the subscripts are dropped down, yielding

$$\begin{bmatrix} F_x \\ F_y \\ F_z \end{bmatrix} = m \left(\begin{bmatrix} \dot{v}_{G_x} \\ \dot{v}_{G_y} \\ \dot{v}_{G_z} \end{bmatrix} + \begin{bmatrix} \omega_x \\ \omega_y \\ \omega_z \end{bmatrix} \times \begin{bmatrix} v_{G_x} \\ v_{G_y} \\ v_{G_z} \end{bmatrix} \right). \tag{A.61}$$

If the rigid body is assumed to be massless, the force balance equation simplifies to

$$\boldsymbol{F} = 0. \tag{A.62}$$

A.4.2.5. Moment Balance Equation of a Rigid Body. Points O and G, and the coordinate frames $OXYZ$ and $Gxyz$ are defined in Section A.4.2.2. These definitions also comply here. These points and coordinate frames are seen in Figure A.5 on page 142 as well.

$\boldsymbol{\omega}$ stands for the angular velocity of the rigid body. I stands for the inertia tensor of the rigid body with respect to the body-fixed coordinate frame. $\boldsymbol{H_{(G)}}$ stands for the angular momentum of the rigid body with respect to the fixed coordinate frame about the center of gravity G. $\boldsymbol{M_{(G)}}$ stands for the total moment applied on the rigid body about the center of gravity G.

The angular momentum of the rigid body with respect to the fixed coordinate frame about the center of gravity G is written as the following [24]:

$$\boldsymbol{H_{(G)}} = \begin{bmatrix} H_{(G)_x} \\ H_{(G)_y} \\ H_{(G)_z} \end{bmatrix}_{ijk} \tag{A.63a}$$

$$= \begin{bmatrix} I_x\omega_x - I_{xy}\omega_y - I_{xz}\omega_z \\ -I_{xy}\omega_x + I_y\omega_y - I_{yz}\omega_z \\ -I_{xz}\omega_x - I_{yz}\omega_y + I_z\omega_z \end{bmatrix}_{ijk} \tag{A.63b}$$

$$= \left(\begin{bmatrix} I_x & -I_{xy} & -I_{xz} \\ -I_{xy} & I_y & -I_{yz} \\ -I_{xz} & -I_{yz} & I_z \end{bmatrix} \begin{bmatrix} \omega_x \\ \omega_y \\ \omega_z \end{bmatrix} \right)_{ijk} \tag{A.63c}$$

$$= \left(I \begin{bmatrix} \omega_x \\ \omega_y \\ \omega_z \end{bmatrix} \right)_{ijk} \tag{A.63d}$$

The total moment applied on the rigid body about the center of gravity G is written as the following:

$$\boldsymbol{M_{(G)}} = \left(\dot{\boldsymbol{H}}_{\boldsymbol{(G)}}\right)_{OXYZ} \tag{A.64a}$$

$$= \left(\dot{\boldsymbol{H}}_{\boldsymbol{(G)}}\right)_{Gxyz} + \boldsymbol{\omega} \times \boldsymbol{H_{(G)}} \tag{A.64b}$$

$$= \left(I \begin{bmatrix} \dot{\omega}_x \\ \dot{\omega}_y \\ \dot{\omega}_z \end{bmatrix} \right)_{ijk} + \begin{bmatrix} \omega_x \\ \omega_y \\ \omega_z \end{bmatrix}_{ijk} \times \left(I \begin{bmatrix} \omega_x \\ \omega_y \\ \omega_z \end{bmatrix} \right)_{ijk} \tag{A.64c}$$

$$= \left(I \begin{bmatrix} \dot{\omega}_x \\ \dot{\omega}_y \\ \dot{\omega}_z \end{bmatrix} + \begin{bmatrix} \omega_x \\ \omega_y \\ \omega_z \end{bmatrix} \times I \begin{bmatrix} \omega_x \\ \omega_y \\ \omega_z \end{bmatrix} \right)_{ijk} \tag{A.64d}$$

If the left-hand side of the equation is also written in the component form, the equation

becomes to

$$\begin{bmatrix} M_{(G)_x} \\ M_{(G)_y} \\ M_{(G)_z} \end{bmatrix}_{ijk} = \left(I \begin{bmatrix} \dot{\omega}_x \\ \dot{\omega}_y \\ \dot{\omega}_z \end{bmatrix} + \begin{bmatrix} \omega_x \\ \omega_y \\ \omega_z \end{bmatrix} \times I \begin{bmatrix} \omega_x \\ \omega_y \\ \omega_z \end{bmatrix} \right)_{ijk} . \tag{A.65}$$

Here, the subscripts ijk stand to emphasize that the results are in the body-fixed coordinate frame components. Since both sides of the equation are in the same form, the subscripts are dropped down, yielding

$$\begin{bmatrix} M_{(G)_x} \\ M_{(G)_y} \\ M_{(G)_z} \end{bmatrix} = I \begin{bmatrix} \dot{\omega}_x \\ \dot{\omega}_y \\ \dot{\omega}_z \end{bmatrix} + \begin{bmatrix} \omega_x \\ \omega_y \\ \omega_z \end{bmatrix} \times I \begin{bmatrix} \omega_x \\ \omega_y \\ \omega_z \end{bmatrix} . \tag{A.66}$$

If all of the components of the inertia tensor I are equal to zero, the moment balance equation simplifies to

$$\boldsymbol{M_{(G)}} = 0. \tag{A.67}$$

An axisymmetrical rigid body, which spins about its axis of symmetry, is considered as a special case. Obviously, a coordinate frame attached to the rigid body also spins about the axis of symmetry. Therefore, obtaining the total moment applied on the rigid body in the body-fixed coordinate frame components is meaningless because the values change as the rigid body spins. It is more applicable to use another coordinate frame which does not spin but makes all the other rotations. Also, this new coordinate frame is selected so that the moments and products of inertia of the rigid body with respect to the new coordinate frame remain constant during the motion.

Figure A.9 on page 150 shows the new coordinate frame $Gx'y'z'$ as well as the other coordinate frames which are already defined. As stated before, the new coordinate

frame $Gx'y'z'$ does not spin. In the case of Figure A.9, it does not rotate about the y or y' axes. Here, it should be noted that the y axis is chosen as the axis of symmetry. Therefore, all of the calculations hereafter are done according to the coordinate frames represented in Figure A.9.

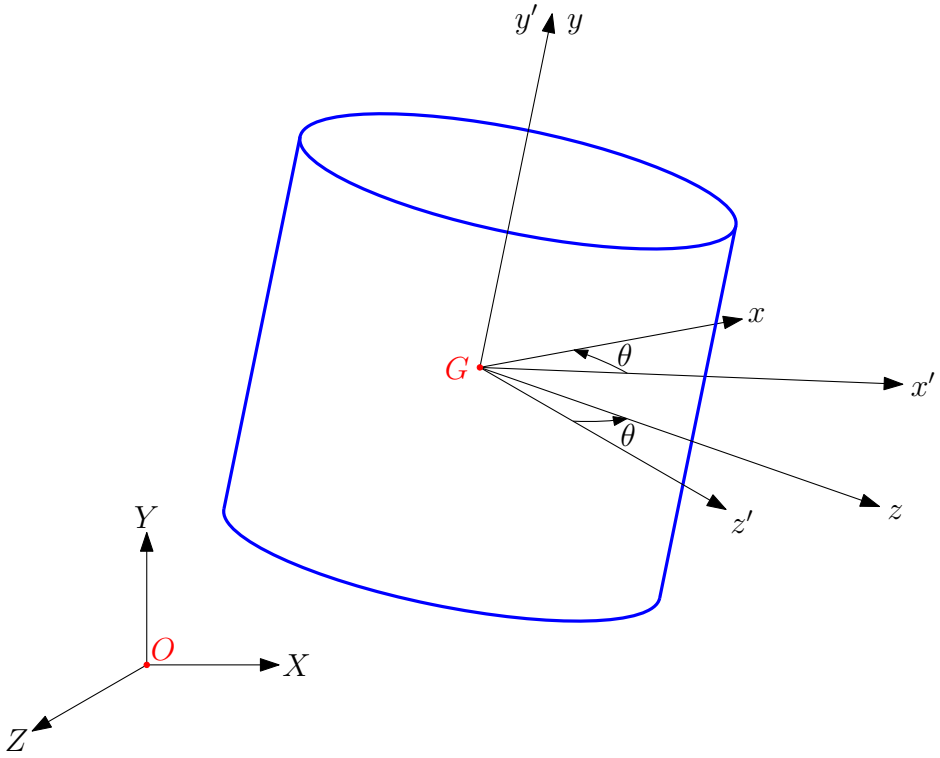

Figure A.9. An axisymmetrical rigid body with coordinate frames

The x', y' and z' axes are principal axes of inertia because the rigid body in concern is axisymmetrical. Using the definitions in Section A.4.1.1, it is seen that the products of inertia with respect to the $Gx'y'z'$ coordinate frame ($I_{x'y'}$, $I_{x'z'}$ and $I_{y'z'}$) are equal to zero. Therefore, the angular momentum of the rigid body with respect to the fixed coordinate frame about the center of gravity G is written as the following where $I_{x'}$, $I_{y'}$ and $I_{z'}$ stand for the moments of inertia with respect to the $Gx'y'z'$

coordinate frame [24]:

$$\boldsymbol{H_{(G)}} = \begin{bmatrix} H_{(G)_{x'}} \\ H_{(G)_{y'}} \\ H_{(G)_{z'}} \end{bmatrix}_{i'j'k'} \tag{A.68a}$$

$$= \begin{bmatrix} I_{x'}\omega_{x'} \\ I_{y'}\omega_{y'} \\ I_{z'}\omega_{z'} \end{bmatrix}_{i'j'k'} \tag{A.68b}$$

The total moment applied on the rigid body about the center of gravity G is written as the following where $\boldsymbol{\Omega}$ stands for the angular velocity of the $Gx'y'z'$ coordinate frame with respect to the $OXYZ$ coordinate frame:

$$\boldsymbol{M_{(G)}} = \left(\dot{\boldsymbol{H}}_{\boldsymbol{(G)}}\right)_{OXYZ} \tag{A.69a}$$

$$= \left(\dot{\boldsymbol{H}}_{\boldsymbol{(G)}}\right)_{Gx'y'z'} + \boldsymbol{\Omega} \times \boldsymbol{H_{(G)}} \tag{A.69b}$$

$$= \left(\dot{\boldsymbol{H}}_{\boldsymbol{(G)}}\right)_{Gx'y'z'} + \left(\boldsymbol{\omega} - \dot{\theta}\boldsymbol{j'}\right) \times \boldsymbol{H_{(G)}} \tag{A.69c}$$

$$= \begin{bmatrix} I_{x'}\dot{\omega}_{x'} \\ I_{y'}\dot{\omega}_{y'} \\ I_{z'}\dot{\omega}_{z'} \end{bmatrix}_{i'j'k'} + \begin{bmatrix} \omega_{x'} \\ \omega_{y'} - \dot{\theta} \\ \omega_{z'} \end{bmatrix}_{i'j'k'} \times \begin{bmatrix} I_{x'}\omega_{x'} \\ I_{y'}\omega_{y'} \\ I_{z'}\omega_{z'} \end{bmatrix}_{i'j'k'} \tag{A.69d}$$

$$= \begin{bmatrix} I_{x'}\dot{\omega}_{x'} + \left(I_{z'} - I_{y'}\right)\omega_{y'}\omega_{z'} - I_{z'}\omega_{z'}\dot{\theta} \\ I_{y'}\dot{\omega}_{y'} + \left(I_{x'} - I_{z'}\right)\omega_{x'}\omega_{z'} \\ I_{z'}\dot{\omega}_{z'} + \left(I_{y'} - I_{x'}\right)\omega_{x'}\omega_{y'} + I_{x'}\omega_{x'}\dot{\theta} \end{bmatrix}_{i'j'k'} \tag{A.69e}$$

If the left-hand side of the equation is also written in the component form, the equation becomes to

$$\begin{bmatrix} M_{(G)_{x'}} \\ M_{(G)_{y'}} \\ M_{(G)_{z'}} \end{bmatrix}_{i'j'k'} = \begin{bmatrix} I_{x'}\dot{\omega}_{x'} + \left(I_{z'} - I_{y'}\right)\omega_{y'}\omega_{z'} - I_{z'}\omega_{z'}\dot{\theta} \\ I_{y'}\dot{\omega}_{y'} + \left(I_{x'} - I_{z'}\right)\omega_{x'}\omega_{z'} \\ I_{z'}\dot{\omega}_{z'} + \left(I_{y'} - I_{x'}\right)\omega_{x'}\omega_{y'} + I_{x'}\omega_{x'}\dot{\theta} \end{bmatrix}_{i'j'k'} . \tag{A.70}$$

Here, the subscripts $i'j'k'$ stand to emphasize that the results are in the $Gx'y'z'$ coordinate frame components. Since both sides of the equation are in the same form, the subscripts are dropped down, yielding

$$\begin{bmatrix} M_{(G)_{x'}} \\ M_{(G)_{y'}} \\ M_{(G)_{z'}} \end{bmatrix} = \begin{bmatrix} I_{x'}\dot{\omega}_{x'} + (I_{z'} - I_{y'})\,\omega_{y'}\omega_{z'} - I_{z'}\omega_{z'}\dot{\theta} \\ I_{y'}\dot{\omega}_{y'} + (I_{x'} - I_{z'})\,\omega_{x'}\omega_{z'} \\ I_{z'}\dot{\omega}_{z'} + (I_{y'} - I_{x'})\,\omega_{x'}\omega_{y'} + I_{x'}\omega_{x'}\dot{\theta} \end{bmatrix}. \tag{A.71}$$

If $I_{x'}$, $I_{y'}$ and $I_{z'}$ are equal to zero, the moment balance equation simplifies to

$$\boldsymbol{M_{(G)}} = 0. \tag{A.72}$$

APPENDIX B: SIMPLIFIED MAGIC FORMULA EQUATIONS

As stated in Section 3.3.4.1, Magic Formula equations in [20] are simplified using Assumptions 3.11, 3.19, 3.20 and 3.21. These simplified equations are represented here. The starting equations are as the following:

$$V_c = \sqrt{{V_{cx}}^2 + {V_{cy}}^2} \tag{B.1}$$

$$V_{sy} = V_{cy} \tag{B.2}$$

$$V_s = |V_{sy}| \tag{B.3}$$

$$V_r = V_{cx} \tag{B.4}$$

$$F'_{zo} = \lambda_{F_{zo}} F_{zo} \tag{B.5}$$

$$df_z = \left(F_z - F'_{zo}\right) / F'_{zo} \tag{B.6}$$

$$\alpha^* = -V_{cy} / \left(|V_{cx}| + \varepsilon\right) \tag{B.7}$$

$$\cos' \alpha = V_{cx} / V_c \tag{B.8}$$

$$\zeta_2 = 1 \tag{B.9}$$

$$\zeta_3 = 1 \tag{B.10}$$

$$\zeta_5 = 1 \tag{B.11}$$

$$\lambda^*_{\mu y} = \lambda_{\mu y} / \left(1 + \lambda_{\mu V} V_s / V_o\right) \tag{B.12}$$

The equations, which are related with the lateral force, are as the following:

$$K_{y\alpha} = p_{Ky1} F'_{zo} \sin\left(p_{Ky4} \arctan\left(F_z / \left(p_{Ky2} F'_{zo}\right)\right)\right) \zeta_3 \lambda_{Ky\alpha} \tag{B.13}$$

$$C_y = p_{Cy1} \lambda_{Cy} \tag{B.14}$$

$$\mu_y = \left(p_{Dy1} + p_{Dy2} df_z\right) \lambda^*_{\mu y} \tag{B.15}$$

$$D_y = \mu_y F_z \zeta_2 \tag{B.16}$$

$$B_y = K_{y\alpha} / \left(C_y D_y + \varepsilon_y\right) \tag{B.17}$$

$$\alpha_y = \alpha^* \tag{B.18}$$

$$E_y = \left(p_{Ey1} + p_{Ey2} df_z\right) \left(1 - p_{Ey3} \mathrm{sgn}\left(\alpha_y\right)\right) \lambda_{Ey} \tag{B.19}$$

$$F_{yo} = D_y \sin\left(C_y \arctan\left(B_y \alpha_y - E_y \left(B_y \alpha_y - \arctan\left(B_y \alpha_y\right)\right)\right)\right) \tag{B.20}$$

$$F_y = F_{yo} \tag{B.21}$$

The overturning couple is obtained as

$$M_x = F_z R_o \left(q_{sx1} + q_{sx3} F_y / F'_{zo}\right) \lambda_{Mx}. \tag{B.22}$$

The rolling resistance moment is found as

$$M_y = -F_z R_o \left(q_{sy1} \arctan\left(V_r / V_o\right)\right) \lambda_{My}. \tag{B.23}$$

The equations for the aligning torque are as the following:

$$D_{to} = F_z \left(R_o / F'_{zo}\right) \left(q_{Dz1} + q_{Dz2} df_z\right) \lambda_t \mathrm{sgn}\left(V_{cx}\right) \tag{B.24}$$

$$D_t = D_{to} \zeta_5 \tag{B.25}$$

$$C_t = q_{Cz1} \tag{B.26}$$

$$B_t = \left(q_{Bz1} + q_{Bz2} df_z + q_{Bz3} {df_z}^2\right) \lambda_{Ky\alpha} / \lambda^*_{\mu y} \tag{B.27}$$

$$S_{Ht} = q_{Hz1} + q_{Hz2} df_z \tag{B.28}$$

$$\alpha_t = \alpha^* + S_{Ht} \tag{B.29}$$

$$E_t = \left(q_{Ez1} + q_{Ez2} df_z + q_{Ez3} {df_z}^2\right) \left(1 + q_{Ez4} \left(2/\pi\right) \arctan\left(B_t C_t \alpha_t\right)\right) \tag{B.30}$$

$$t_o = D_t \cos\left(C_t \arctan\left(B_t \alpha_t - E_t \left(B_t \alpha_t - \arctan\left(B_t \alpha_t\right)\right)\right)\right) \cos' \alpha \tag{B.31}$$

$$M'_{zo} = -t_o F_{yo} \tag{B.32}$$

$$M_{zo} = M'_{zo} \tag{B.33}$$

$$M_z = M_{zo} \tag{B.34}$$

APPENDIX C: EQUATIONS OF THE SINGLE TRACK MODEL

The equations of motion of the Single Track Model are derived in a few steps. First, starting equations are written; they are the force balance equation, moment balance equation, road and wheel interactions and kinematic relations. Then, the derivations are done in four steps. Finally, the resulting equations are obtained. The motion is completely defined by the resulting equations. The method, which is followed here, is similar to the one in [26].

It should be noted that the definitions made in Section 4 are valid in this section too.

C.1. Starting Equations

C.1.1. Force Balance Equation

Assumption 4.3 declares that there is no drag force applied on the vehicle. Hence, the only remaining forces are the ones applied on the wheels from the road and the weight of the vehicle. Rewriting Equation (A.59a) with these forces yields

$$\boldsymbol{F_F} + \boldsymbol{F_R} + \boldsymbol{W} = m\boldsymbol{a_G}. \tag{C.1}$$

C.1.2. Moment Balance Equation

Applying Assumptions 4.3, 4.4, 4.5, 4.6 and 4.7 onto Equation (A.65) yields

$$(l_F \boldsymbol{i} \times \boldsymbol{F_F}) + (-l_R \boldsymbol{i} \times \boldsymbol{F_R}) = I_z \ddot{\psi} \boldsymbol{k}. \tag{C.2}$$

C.1.3. Road and Wheel Interactions

Using Assumptions 4.4, 4.8 and 4.9, the equations, which give information about the forces applied on the wheels from the road, are obtained as

$$F_{F_{x_F}} = 0, \tag{C.3}$$

$$F_{F_{y_F}} = c_F \alpha_F, \tag{C.4}$$

$$F_{R_{x_R}} = 0, \tag{C.5}$$

$$F_{R_{y_R}} = c_R \alpha_R. \tag{C.6}$$

C.1.4. Kinematic Relations

Transforming Equation (A.41) and using Assumptions 4.5 and 4.6, the velocity of the contact point of the front wheel with the road is written as

$$\boldsymbol{v_F} = \boldsymbol{v_G} + \boldsymbol{\omega} \times (l_F \boldsymbol{i}) \tag{C.7a}$$

$$= \boldsymbol{v_G} + \dot{\psi} l_F \boldsymbol{j} \tag{C.7b}$$

$$= v_{G_x} \boldsymbol{i} + \left(v_{G_y} + \dot{\psi} l_F \right) \boldsymbol{j}. \tag{C.7c}$$

Similarly, the velocity of the contact point of the rear wheel with the road is written as

$$\boldsymbol{v_R} = \boldsymbol{v_G} + \boldsymbol{\omega} \times (-l_R \boldsymbol{i}) \tag{C.8a}$$

$$= \boldsymbol{v_G} - \dot{\psi} l_R \boldsymbol{j} \tag{C.8b}$$

$$= v_{G_x} \boldsymbol{i} + \left(v_{G_y} - \dot{\psi} l_R \right) \boldsymbol{j}. \tag{C.8c}$$

By the definition of the side-slip angle, it is easy to conclude that

$$\tan\beta = \frac{v_{G_y}}{v_{G_x}} \tag{C.9}$$

which is rewritten as

$$\beta \approx \frac{v_{G_y}}{v_{G_x}} \tag{C.10}$$

by making and using Assumption 4.10.

C.2. Derivations

C.2.1. Step 1

By using trigonometric relations, the vehicle longitudinal axis component of $\boldsymbol{v_F}$ is written as

$$v_{F_x} = v_F \cos\left(\delta_F - \alpha_F\right). \tag{C.11}$$

This equation is then written as

$$v_{G_x} = v_F \cos\left(\delta_F - \alpha_F\right) \tag{C.12}$$

by using the fact that

$$v_{F_x} = v_{G_x} \tag{C.13}$$

which is obtained from Equation (C.7c).

By using trigonometric relations, the vehicle lateral axis component of $\boldsymbol{v_F}$ is

written as

$$v_{F_y} = v_F \sin(\delta_F - \alpha_F). \tag{C.14}$$

This equation is then written as

$$v_{G_y} + \dot{\psi} l_F = v_F \sin(\delta_F - \alpha_F) \tag{C.15}$$

by using the fact that

$$v_{F_y} = v_{G_y} + \dot{\psi} l_F \tag{C.16}$$

which is obtained from Equation (C.7c).

Dividing Equation (C.15) by Equation (C.12), it is found that

$$\tan(\delta_F - \alpha_F) = \frac{v_{G_y} + \dot{\psi} l_F}{v_{G_x}}. \tag{C.17}$$

This equation is rewritten as

$$\delta_F - \alpha_F = \frac{v_{G_y} + \dot{\psi} l_F}{v_{G_x}} \tag{C.18}$$

by making and using Assumptions 4.11 and 4.13. Using Equation (C.10) yields

$$\delta_F - \alpha_F = \frac{\beta v_{G_x} + \dot{\psi} l_F}{v_{G_x}} \tag{C.19a}$$

$$= \beta + \frac{\dot{\psi} l_F}{v_{G_x}}. \tag{C.19b}$$

Rearranging to obtain α_F leads to

$$\alpha_F = -\beta - \frac{\dot{\psi} l_F}{v_{G_x}} + \delta_F. \tag{C.20}$$

By using trigonometric relations, the vehicle longitudinal axis component of $\boldsymbol{v_R}$ is written as

$$v_{R_x} = v_R \cos\left(\delta_R - \alpha_R\right). \tag{C.21}$$

This equation is then written as

$$v_{G_x} = v_R \cos\left(\delta_R - \alpha_R\right) \tag{C.22}$$

by using the fact that

$$v_{R_x} = v_{G_x} \tag{C.23}$$

which is obtained from Equation (C.8c).

By using trigonometric relations, the vehicle lateral axis component of $\boldsymbol{v_R}$ is written as

$$v_{R_y} = v_R \sin\left(\delta_R - \alpha_R\right). \tag{C.24}$$

This equation is then written as

$$v_{G_y} - \dot{\psi} l_R = v_R \sin\left(\delta_R - \alpha_R\right) \tag{C.25}$$

by using the fact that

$$v_{R_y} = v_{G_y} - \dot{\psi} l_R \tag{C.26}$$

which is obtained from Equation (C.8c).

Dividing Equation (C.25) by Equation (C.22), it is found that

$$\tan\left(\delta_R - \alpha_R\right) = \frac{v_{G_y} - \dot{\psi} l_R}{v_{G_x}}. \tag{C.27}$$

This equation is rewritten as

$$\delta_R - \alpha_R = \frac{v_{G_y} - \dot{\psi} l_R}{v_{G_x}} \tag{C.28}$$

by making and using Assumptions 4.12 and 4.14. Using Equation (C.10) yields

$$\delta_R - \alpha_R = \frac{\beta v_{G_x} - \dot{\psi} l_R}{v_{G_x}} \tag{C.29a}$$

$$= \beta - \frac{\dot{\psi} l_R}{v_{G_x}}. \tag{C.29b}$$

Rearranging to obtain α_R leads to

$$\alpha_R = -\beta + \frac{\dot{\psi} l_R}{v_{G_x}} + \delta_R. \tag{C.30}$$

C.2.2. Step 2

Using Equation (A.16), $\boldsymbol{a_G}$ is written as

$$\boldsymbol{a_G} = (\dot{\boldsymbol{v}}_{\boldsymbol{G}})_{OXYZ}. \tag{C.31}$$

This equation is then rewritten as

$$\boldsymbol{a_G} = (\dot{\boldsymbol{v}}_{\boldsymbol{G}})_{Gxyz} + \boldsymbol{\omega} \times \boldsymbol{v_G} \tag{C.32}$$

according to Equation (A.14). Using Assumption 4.6 yields

$$\boldsymbol{a_G} = \begin{bmatrix} \dot{v}_{G_x} \\ \dot{v}_{G_y} \\ \dot{v}_{G_z} \end{bmatrix}_{ijk} + \begin{bmatrix} 0 \\ 0 \\ \dot{\psi} \end{bmatrix}_{ijk} \times \begin{bmatrix} v_{G_x} \\ v_{G_y} \\ v_{G_z} \end{bmatrix}_{ijk} . \tag{C.33}$$

Making and using Assumptions 4.15 and 4.16; and using Equation (C.10) yield

$$\boldsymbol{a_G} = \begin{bmatrix} 0 \\ (\beta \dot{v}_{G_x}) \\ 0 \end{bmatrix}_{ijk} + \begin{bmatrix} 0 \\ 0 \\ \dot{\psi} \end{bmatrix}_{ijk} \times \begin{bmatrix} v_{G_x} \\ \beta v_{G_x} \\ 0 \end{bmatrix}_{ijk} \tag{C.34a}$$

$$= \begin{bmatrix} -\dot{\psi}\beta v_{G_x} \\ \dot{\beta} v_{G_x} + \dot{\psi} v_{G_x} \\ 0 \end{bmatrix}_{ijk} \tag{C.34b}$$

$$= v_{G_x} \begin{bmatrix} -\dot{\psi}\beta \\ \dot{\beta} + \dot{\psi} \\ 0 \end{bmatrix}_{ijk} . \tag{C.34c}$$

C.2.3. Step 3

Rewriting Equation (C.1) in z components and using Assumption 4.16 lead to

$$F_{F_z} + F_{R_z} - mg = ma_{G_z} \tag{C.35a}$$

$$= 0. \tag{C.35b}$$

Rewriting Equation (C.1) in x and y components leads to

$$F_{F_x} + F_{R_x} = ma_{G_x}, \tag{C.36}$$

$$F_{F_y} + F_{R_y} = ma_{G_y}. \tag{C.37}$$

Transforming these two equations so that they are written in x_F, y_F, x_R, y_R components and including Assumptions 4.13 and 4.14 yield

$$F_{F_{x_F}} - F_{F_{y_F}}\delta_F + F_{R_{x_R}} - F_{R_{y_R}}\delta_R = ma_{G_x}, \tag{C.38}$$

$$F_{F_{x_F}}\delta_F + F_{F_{y_F}} + F_{R_{x_R}}\delta_R + F_{R_{y_R}} = ma_{G_y}. \tag{C.39}$$

Using Equations (C.3), (C.4), (C.5) and (C.6) with these two equations yields

$$-c_F\alpha_F\delta_F - c_R\alpha_R\delta_R = ma_{G_x}, \tag{C.40}$$

$$c_F\alpha_F + c_R\alpha_R = ma_{G_y}. \tag{C.41}$$

Using Equations (C.20), (C.30) and (C.34c) with these two equations yields

$$-c_F\delta_F\left(-\beta - \frac{\dot{\psi}l_F}{v_{G_x}} + \delta_F\right) - c_R\delta_R\left(-\beta + \frac{\dot{\psi}l_R}{v_{G_x}} + \delta_R\right) = -mv_{G_x}\dot{\psi}\beta, \tag{C.42}$$

$$c_F\left(-\beta - \frac{\dot{\psi}l_F}{v_{G_x}} + \delta_F\right) + c_R\left(-\beta + \frac{\dot{\psi}l_R}{v_{G_x}} + \delta_R\right) = mv_{G_x}\left(\dot{\beta} + \dot{\psi}\right). \tag{C.43}$$

C.2.4. Step 4

Equation (C.2) is written in the expanded form as

$$l_F F_{F_y}\boldsymbol{k} - l_F F_{F_z}\boldsymbol{j} - l_R F_{R_y}\boldsymbol{k} + l_R F_{R_z}\boldsymbol{j} = I_z\ddot{\psi}\boldsymbol{k}. \tag{C.44}$$

Equation (C.44) is written in y components as

$$-l_F F_{F_z} + l_R F_{R_z} = 0. \tag{C.45}$$

Equation (C.44) is written in z components as

$$l_F F_{F_y} - l_R F_{R_y} = I_z \ddot{\psi}. \tag{C.46}$$

Transforming this equation so that it is written in x_F, y_F, x_R, y_R components and including Assumptions 4.13 and 4.14 yield

$$l_F \left(F_{F_{x_F}} \delta_F + F_{F_{y_F}} \right) - l_R \left(F_{R_{x_R}} \delta_R + F_{R_{y_R}} \right) = I_z \ddot{\psi}. \tag{C.47}$$

Using Equations (C.3), (C.4), (C.5) and (C.6) with this equation yields

$$l_F c_F \alpha_F - l_R c_R \alpha_R = I_z \ddot{\psi}. \tag{C.48}$$

Using Equations (C.20) and (C.30) with this equation yields

$$l_F c_F \left(-\beta - \frac{\dot{\psi} l_F}{v_{G_x}} + \delta_F \right) - l_R c_R \left(-\beta + \frac{\dot{\psi} l_R}{v_{G_x}} + \delta_R \right) = I_z \ddot{\psi}. \tag{C.49}$$

C.3. Resulting Equations

Equations (C.35b), (C.42), (C.43), (C.45) and (C.49) are the resulting equations, which are obtained in Section C.2. It is beneficial to rewrite them as the following:

$$F_{F_z} + F_{R_z} - mg = 0 \tag{C.50}$$

$$-c_F \delta_F \left(-\beta - \frac{\dot{\psi} l_F}{v_{G_x}} + \delta_F \right) - c_R \delta_R \left(-\beta + \frac{\dot{\psi} l_R}{v_{G_x}} + \delta_R \right) = -m v_{G_x} \dot{\psi} \beta \tag{C.51}$$

$$c_F \left(-\beta - \frac{\dot{\psi} l_F}{v_{G_x}} + \delta_F \right) + c_R \left(-\beta + \frac{\dot{\psi} l_R}{v_{G_x}} + \delta_R \right) = m v_{G_x} \left(\dot{\beta} + \dot{\psi} \right) \tag{C.52}$$

$$-l_F F_{F_z} + l_R F_{R_z} = 0 \tag{C.53}$$

$$l_F c_F \left(-\beta - \frac{\dot{\psi} l_F}{v_{G_x}} + \delta_F \right) - l_R c_R \left(-\beta + \frac{\dot{\psi} l_R}{v_{G_x}} + \delta_R \right) = I_z \ddot{\psi} \tag{C.54}$$

This section is divided into three parts. In the first part, vertical forces are obtained. In the second part, state-space description with β and $\dot{\psi}$ as state variables is obtained. Finally in the third part, state-space description with v_{G_y} and $\dot{\psi}$ as state variables is obtained.

C.3.1. Vertical Forces

Solving Equations (C.50) and (C.53) together, vertical forces are found as

$$F_{F_z} = \frac{l_R mg}{l_F + l_R}, \tag{C.55}$$

$$F_{R_z} = \frac{l_F mg}{l_F + l_R}. \tag{C.56}$$

C.3.2. State-Space Description with β and $\dot{\psi}$ as State Variables

Rewriting Equations (C.52) and (C.54) in expanded form yields

$$-c_F\beta - c_F\frac{\dot{\psi}l_F}{v_{G_x}} + c_F\delta_F - c_R\beta + c_R\frac{\dot{\psi}l_R}{v_{G_x}} + c_R\delta_R = mv_{G_x}\dot{\beta} + mv_{G_x}\dot{\psi}, \tag{C.57}$$

$$-l_Fc_F\beta - l_Fc_F\frac{\dot{\psi}l_F}{v_{G_x}} + l_Fc_F\delta_F + l_Rc_R\beta - l_Rc_R\frac{\dot{\psi}l_R}{v_{G_x}} - l_Rc_R\delta_R = I_z\ddot{\psi}. \tag{C.58}$$

By looking at these equations, the state vector is chosen as

$$x = \begin{bmatrix} \beta \\ \dot{\psi} \end{bmatrix}. \tag{C.59}$$

The state-space form for the front and rear steered case is written as

$$\dot{x} = \begin{bmatrix} -\frac{c_F+c_R}{mv_{G_x}} & \frac{c_Rl_R-c_Fl_F}{mv_{G_x}{}^2} - 1 \\ \frac{c_Rl_R-c_Fl_F}{I_z} & -\frac{c_Rl_R{}^2+c_Fl_F{}^2}{I_zv_{G_x}} \end{bmatrix} x + \begin{bmatrix} \frac{c_F}{mv_{G_x}} & \frac{c_R}{mv_{G_x}} \\ \frac{c_Fl_F}{I_z} & -\frac{c_Rl_R}{I_z} \end{bmatrix} u \tag{C.60}$$

where

$$u = \begin{bmatrix} \delta_F \\ \delta_R \end{bmatrix}. \tag{C.61}$$

The state-space form for the front steered case is written as

$$\dot{x} = \begin{bmatrix} -\frac{c_F+c_R}{mv_{G_x}} & \frac{c_R l_R - c_F l_F}{mv_{G_x}{}^2} - 1 \\ \frac{c_R l_R - c_F l_F}{I_z} & -\frac{c_R l_R{}^2 + c_F l_F{}^2}{I_z v_{G_x}} \end{bmatrix} x + \begin{bmatrix} \frac{c_F}{mv_{G_x}} \\ \frac{c_F l_F}{I_z} \end{bmatrix} u \tag{C.62}$$

where

$$u = \delta_F. \tag{C.63}$$

The state-space form for the rear steered case is written as

$$\dot{x} = \begin{bmatrix} -\frac{c_F+c_R}{mv_{G_x}} & \frac{c_R l_R - c_F l_F}{mv_{G_x}{}^2} - 1 \\ \frac{c_R l_R - c_F l_F}{I_z} & -\frac{c_R l_R{}^2 + c_F l_F{}^2}{I_z v_{G_x}} \end{bmatrix} x + \begin{bmatrix} \frac{c_R}{mv_{G_x}} \\ -\frac{c_R l_R}{I_z} \end{bmatrix} u \tag{C.64}$$

where

$$u = \delta_R. \tag{C.65}$$

If the output is selected as the side-slip angle β, it is represented with the equation

$$y = \begin{bmatrix} 1 & 0 \end{bmatrix} x. \tag{C.66}$$

If it is selected as the yaw rate $\dot{\psi}$, it is represented with the equation

$$y = \begin{bmatrix} 0 & 1 \end{bmatrix} x. \tag{C.67}$$

C.3.3. State-Space Description with v_{G_y} and $\dot{\psi}$ as State Variables

Using Equations (C.10) and (C.60) together, the state-space form for the front and rear steered case is found to be

$$\dot{x} = \begin{bmatrix} -\frac{c_F+c_R}{mv_{G_x}} & \frac{c_Rl_R-c_Fl_F}{mv_{G_x}} - v_{G_x} \\ \frac{c_Rl_R-c_Fl_F}{I_zv_{G_x}} & -\frac{c_Rl_R{}^2+c_Fl_F{}^2}{I_zv_{G_x}} \end{bmatrix} x + \begin{bmatrix} \frac{c_F}{m} & \frac{c_R}{m} \\ \frac{c_Fl_F}{I_z} & -\frac{c_Rl_R}{I_z} \end{bmatrix} u \tag{C.68}$$

where

$$x = \begin{bmatrix} v_{G_y} \\ \dot{\psi} \end{bmatrix} \tag{C.69}$$

and

$$u = \begin{bmatrix} \delta_F \\ \delta_R \end{bmatrix}. \tag{C.70}$$

The state-space form for the front steered case is written as

$$\dot{x} = \begin{bmatrix} -\frac{c_F+c_R}{mv_{G_x}} & \frac{c_Rl_R-c_Fl_F}{mv_{G_x}} - v_{G_x} \\ \frac{c_Rl_R-c_Fl_F}{I_zv_{G_x}} & -\frac{c_Rl_R{}^2+c_Fl_F{}^2}{I_zv_{G_x}} \end{bmatrix} x + \begin{bmatrix} \frac{c_F}{m} \\ \frac{c_Fl_F}{I_z} \end{bmatrix} u \tag{C.71}$$

where

$$u = \delta_F. \tag{C.72}$$

The state-space form for the rear steered case is written as

$$\dot{x} = \begin{bmatrix} -\frac{c_F+c_R}{mv_{G_x}} & \frac{c_Rl_R-c_Fl_F}{mv_{G_x}} - v_{G_x} \\ \frac{c_Rl_R-c_Fl_F}{I_zv_{G_x}} & -\frac{c_Rl_R{}^2+c_Fl_F{}^2}{I_zv_{G_x}} \end{bmatrix} x + \begin{bmatrix} \frac{c_R}{m} \\ -\frac{c_Rl_R}{I_z} \end{bmatrix} u \tag{C.73}$$

where

$$u = \delta_R. \tag{C.74}$$

If the output is selected as the vehicle lateral axis component of the velocity, which is v_{G_y}, it is represented with the equation

$$y = \begin{bmatrix} 1 & 0 \end{bmatrix} x. \tag{C.75}$$

If it is selected as the yaw rate $\dot{\psi}$, it is represented with the equation

$$y = \begin{bmatrix} 0 & 1 \end{bmatrix} x. \tag{C.76}$$

APPENDIX D: RELATED COMPUTER SOFTWARE

Computer software developed for this study is included in a separate DVD. Contents of the DVD are grouped according to the sections of the text. In other words, directory paths in the DVD are similar to sections in the text. Software belonging to a section is easily found by exploring the directories in the DVD.

REFERENCES

1. Peters, G. A. and B. J. Peters, *Automotive Vehicle Safety*, Taylor & Francis, Great Britain, 2002.

2. Shino, M., P. Raksincharoensak, M. Kamata and M. Nagai, "Side Slip Control of Small-Scale Electric Vehicle by DYC", *Vehicle System Dynamics Supplement*, Vol. 41, pp. 487–496, 2004.

3. Tsunashima, H., M. Murakami and J. Miyata, "Vehicle and Road State Estimation Using Interacting Multiple Model Approach", *Vehicle System Dynamics*, Vol. 44, No. 1, pp. 750–758, 2006.

4. Satria, M. and M. C. Best, "State Estimation of Vehicle Handling Dynamics Using Non-Linear Robust Extended Adaptive Kalman Filter", *Vehicle System Dynamics Supplement*, Vol. 41, pp. 103–112, 2004.

5. Grip, H. F., L. Imsland, T. A. Johansen, T. I. Fossen, J. C. Kalkkuhl and A. Suissa, "Nonlinear Vehicle Side-Slip Estimation with Friction Adaptation", *Automatica*, Vol. 44, pp. 611–622, 2008.

6. Fukada, Y., "Slip-Angle Estimation for Vehicle Stability Control", *Vehicle System Dynamics*, Vol. 32, No. 4, pp. 375–388, 1999.

7. Imsland, L., T. A. Johansen, T. I. Fossen, H. F. Grip, J. C. Kalkkuhl and A. Suissa, "Vehicle Velocity Estimation Using Nonlinear Observers", *Automatica*, Vol. 42, pp. 2091–2103, 2006.

8. Imsland, L., T. A. Johansen, H. F. Grip and T. I. Fossen, "On Non-Linear Unknown Input Observers - Applied to Lateral Vehicle Velocity Estimation on Banked Roads", *International Journal of Control*, Vol. 80, No. 11, pp. 1741–1750, 2007.

9. Grip, H. F., L. Imsland, T. A. Johansen, T. I. Fossen, J. C. Kalkkuhl and A. Suissa, "Nonlinear Vehicle Velocity Observer with Road-Tire Friction Adaptation", *Proceedings of the 45th IEEE Conference on Decision & Control*, San Diego, 13–15 December 2006, pp. 3603–3608, 2006.

10. Grip, H. F., L. Imsland, T. A. Johansen, J. C. Kalkkuhl and A. Suissa, "Estimation of Road Inclination and Bank Angle in Automotive Vehicles", *Proceedings of the 2009 American Control Conference*, St. Louis, 10–12 June 2009, pp. 426–432, 2009.

11. Cherouat, H., M. Braci and S. Diop, "Vehicle Velocity, Side Slip Angles and Yaw Rate Estimation", *Proceedings of the IEEE International Symposium on Industrial Electronics 2005*, Dubrovnik, 20–23 June 2005, pp. 349–354, 2005.

12. Imsland, L., T. A. Johansen, T. I. Fossen, J. C. Kalkkuhl and A. Suissa, "Vehicle Velocity Estimation Using Modular Nonlinear Observers", *Proceedings of the 44th IEEE Conference on Decision and Control, and the European Control Conference 2005*, Seville, 12–15 December 2005, pp. 6728–6733, 2005.

13. Hodgson, G. and M. C. Best, "A Parameter Identifying a Kalman Filter Observer for Vehicle Handling Dynamics", *Proceedings of the Institution of Mechanical Engineers*, Vol. 220, pp. 1063–1072, 2006.

14. Zhu, T. and H. Zheng, "Application of Unscented Kalman Filter to Vehicle State Estimation", *Proceedings of the 2008 ISECS International Colloquium on Computing, Communication, Control, and Management*, pp. 135–139, 2008.

15. Zhu, T. and H. Zheng, "Vehicle State Estimation Based on Unscented Kalman State Estimation", *Proceedings of the 2008 International Symposium on Computational Intelligence and Design*, pp. 42–46, 2008.

16. Scherer, C. W. and İ. E. Köse, "Robustness with Dynamic IQCs: An Exact State-Space Characterization of Nominal Stability with Applications to Robust Estimation", *Automatica*, Vol. 44, pp. 1666–1675, 2008.

17. Chumsamutr, R., T. Fujioka and M. Abe, "Sensitivity Analysis of Side-Slip Angle Observer Based on a Tire Model", *Vehicle System Dynamics*, Vol. 44, No. 7, pp. 513–527, July 2006.

18. Blundell, M. and D. Harty, *The Multibody Systems Approach to Vehicle Dynamics*, Elsevier Butterworth-Heinemann, Great Britain, 2004.

19. Bayliss, M., "A Simplified Vehicle and Driver Model for Vehicle Systems Development", *Proceedings of the Driving Simulation Conference 2005 North America*, Orlando, 30 November–2 December 2005, pp. 10–20, 2005.

20. Pacejka, H. B., *Tyre and Vehicle Dynamics*, Elsevier Butterworth-Heinemann, United Kingdom, 2006.

21. Löfberg, J., "YALMIP: A Toolbox for Modeling and Optimization in MATLAB", *Proceedings of the CACSD Conference*, Taipei, 2004.

22. Sturm, J. F., "Using SeDuMi 1.02, a MATLAB Toolbox for Optimization Over Symmetric Cones", *Optimization Methods and Software*, Vol. 11–12, pp. 625–653, 1999.

23. Baruh, H., *Analytical Dynamics*, McGraw-Hill, Singapore, 1999.

24. Beer, F. P. and E. R. Johnston, *Vector Mechanics for Engineers: Dynamics*, McGraw-Hill, United States of America, 1997.

25. Zatsiorsky, V. M., *Kinetics of Human Motion*, Human Kinetics, United States of America, 2002.

26. Kiencke, U. and L. Nielsen, *Automotive Control Systems*, Springer, Germany, 2000.